TRANSPORTATION RESEARCH RECORD 679

Roadside Safety Appurtenances

TRANSPORTATION RESEARCH BOARD

COMMISSION ON SOCIOTECHNICAL SYSTEMS
NATIONAL RESEARCH COUNCIL

NATIONAL ACADEMY OF SCIENCES
WASHINGTON, D.C. 1978

Transportation Research Record 679
Price $3.00

mode
1 highway transportation

subject areas
21 facilities design
25 structures design and performance
51 transportation safety

Notice

The papers in this Record have been reviewed by and accepted for publication by knowledgeable persons other than the authors according to procedures approved by a Report Review Committee consisting of members of the National Academy of Sciences, the National Academy of Engineering, and the Institute of Medicine.

The views expressed in these papers are those of the authors and do not necessarily reflect those of the sponsoring committee, the Transportation Research Board, the National Academy of Sciences or the sponsors of TRB activities.

To eliminate a backlog of publications and to make possible earlier, more timely publication of reports given at its meetings, the Transportation Research Board has, for a trial period, adopted less stringent editorial standards for certain classes of published material. The new standards apply only to papers and reports that are clearly attributed to specific authors and that have been accepted for publication after committee review for technical content. Within broad limits, the syntax and style of the published version of these reports are those of the author(s).

The papers in this Record were treated according to the new standards.

Library of Congress Cataloging in Publication Data
National Research Council. Transportation Research Board.
Roadside safety appurtenances.

(Transportation research record; 679)
Twelve reports prepared for the 57th annual meeting of the Transportation Research Board.
1. Roads–Safety measures–Congresses. Roads–Accessories–Congresses. I. Title. II. Series.
TE7.H5 no. 679 [TE228] 380.5'08s [625.7'95] 79-12623
ISBN 0-309-02824-8

Sponsorship of the Papers in This Transportation Research Record

GROUP 2–DESIGN AND CONSTRUCTION OF TRANSPORTATION FACILITIES
Eldon J. Yoder, Purdue University, chairman

General Design Section
Lester A. Herr, Federal Highway Administration, chairman

Committee on Safety Appurtenances
Jarvis D. Michie, Southwest Research Institute, chairman
Gordon A. Alison, William E. Behm, William C. Burnett, Harold D. Cooner, Arthur M. Dinitz, Malcolm D. Graham, James H. Hatton, Jr., Roger W. Hove, William W. Hunter, Edwin C. Lokken, Roy J. Mohler, Eric F. Nordlin, Robert M. Olson, William L. Raymond, Jr., F. G. Schlosser, Richard A. Strizki, Flory J. Tamanini, John G. Viner, Charles Y. Warner, Earl C. Williams, Jr.

Lawrence F. Spaine, Transportation Research Board staff

The organizational units and officers and members are as of December 31, 1977.

Contents

TRANSPORTATION RESEARCH BOARD
National Research Council
ERRATA 1979

Special Report 175
page 67, column 2, line 36
Change "because it has a larger size aggregate" to "if it had had a larger-size aggregate"

Special Report 176
page 3, caption for Figure 1.3
Change "Segeto" to "Shigeto"
page 13, column 2, line 4
Change "Figure 2.6" to "Figure 2.5"
page 15, Figure 2.10, Zone A
Change heading "E" to "C"
page 17, column 2, line 37
Change "fluids, as shown in Figure 2.1p5." to "fluids."
page 18, column 1, line 11 from bottom
Change "site" to "side"
page 18, caption for Figure 2.17
Change "(7 to 6 ft)" to "(7 to 16 ft)"
pages 92 and 93, Figures 4.8 and 4.9
Reverse captions for figures
page 231, column 3, line 18
Change "13, 17" to "17"

Transportation Research Record 667
page 41, column 1, line 9 from bottom
Change "versus" to "per unit of"
page 41, column 2, line 3 from bottom
Change "versus" to "and"
page 42, column 2, line 17 from bottom
After "All scenarios" insert "chosen"
page 43, column 1, lines 24-26
Change no. 4 to read: "4. A table of fuel consumption versus emission rates is accessed each second for each vehicle by using the vehicle's speed-acceleration couplet (8)."
page 43, column 1, line 31
Change "fuel consumption" to "fuel efficiency"
page 43, column 2, last line
Change Equation 6 to read: "FE = 0.695 + 0.182*(average speed) - 0.0023*(average speed)^2"
page 44, Figure 3, caption and vertical axis
Change "fuel consumption" to "fuel efficiency"
page 45, Figure 8, caption and vertical axis
Change "fuel consumption" to "fuel efficiency"
page 47, column 1, line 1
Change "fuel consumption" to "fuel efficiency"
page 47, column 1, line 3
Change Equation 7 to read: "HC = 8.342 - 0.240*(average speed) + 0.007 25*(average speed)^2"
page 47, column 1, line 6
Change Equation 8 to read: "HC = 1.36 + 34.522 ÷ (average speed)"
page 47, column 1, line 8
Change Equation 9 to read: "CO = 171.71 - 9.222*(average speed) + 0.164*(average speed)^2"
page 47, column 1, line 11
Change Equation 10 to read: "CO = 16.03 + 766.0 ÷ (average speed)"
page 47, column 1, lines 16-17
Change "the cycle length, which minimizes delay at an isolated intersection, also" to "a cycle length that minimizes delay at an isolated intersection also"
page 47, column 1, line 4 from bottom
After "is not considered" insert "in these other papers."

Transportation Research Record 673
page 52, column 2, line 12 from bottom
Change "90 and 100" to "90 and 10"

Transportation Research Record 675
page 19, column 1
Insert the following before the last paragraph:

Hydrated Portland Cement Pastes

Hydrated portland cement pastes were used to test the hypothesis discussed above. The second-intrusion method was applied to hydrated portland cement pastes, which were mixed in vacuum with a water-cement ratio of 0.4 and cured for 3 and 60 days in saturated calcium hydroxide solution at 20°C. The pastes were oven dried at the end of curing periods, and duplicate specimens (1-3 g each) were tested. The specimens were taken out of the sample cell at the end of the first pressurizing-depressurizing cycle and placed and tested in the porosimeter again as a new specimen. The surface tension of mercury was taken as 484 dyne/cm^2 and the contact angle as 117° for all cycles. Thus, the Washburn equation becomes

$$P = 127.500/D(\mu m) \quad (3)$$

where P is in pounds force per square inch.

Winslow and Diamond (3) determined the contact angle of mercury on oven-dried hydrated portland cement pastes by observing the penetration pressure of mercury into small boreholes of known diameters. The assumption of equal contact angle in first and second intrusions is supported by Winslow and Diamond's procedure, since they intruded and extruded mercury into the small holes in cycles and observed no change in penetration pressure.

Conventional and uniform pore-size distributions of hydrated portland cement pastes are shown in Figures 6 and 7. The first-intrusion curves are similar to those reported in early investigations (3). There is practically no intrusion up to the threshold diameter D_t, and a major fraction of the total pore volume is within a small range of sizes smaller than D_t; finally, the slope tends to become smaller and smaller as smaller diameters are intruded. Thirty-six percent of the total mercury intruded is retained in the paste hydrated for 3 days and 40 percent in the paste hydrated for 60 days at end of depressurizing.

Transportation Research Record 679
page 1, column 2, line 13
Change "4895 N/s (1100 lb/s)" to "4895 N·s (1100 lbf·s)"
page 16, column 2, line 20 from bottom
Change "10.05 kN" to "1025 kg" and "62.27-kN" to "6350-kg"

page 16, column 2, line 15 from bottom and lines 10-11 from bottom
Change "19.93 kN" to "2032 kg"
page 16, column 2, lines 5-6 from bottom
Change "19.88 kN" to "2028 kg"
page 18, column 1, lines 6 and 12
Change "10.05-kN" to "1025-kg" and "1.913-kN" to "195-kg"
page 18, column 1, line 20, and column 2, lines 20 and 23
Change "62.27-kN" to "6350-kg"
page 26, column 1, lines 13-15
Change each "nt·s" to "N·s" and each "lb-s" to "lbf·s"
page 26, column 2, lines 4-6
Change each "nt" to "N" and each "lb" to "lbf"
page 27, column 1, lines 1-2 and following table
Change to "production lot (1 kN = 225 lbf):

Test Piece	Axial Load (kN)
CT 7-11-1	136.3
CT 7-11-2	115.6
CT 7-11-3	116.1
CT 7-12-3	119.7
CT 7-12-4	122.1
Average	121.9"

page 27, column 1, lines 9-11 from bottom and following table
Change to "table (1 kN = 225 lbf):

Test Piece	Shear Load (kN/coupling)
CT 7-11-4	28.0
CT 7-11-5	17.3
CT 7-11-6	23.6
CT 7-12-1	17.3
CT 7-12-2	19.6
Average	21.2"

page 27, column 2, line 13
Change "227 kg (500 lb) and 4536 kg (10 000 lb)" to "2.2 kN (500 lbf) and 44.5 kN (10 000 lbf)"
page 28, column 1, lines 3, 14-15, 18, and 22
Change each "nt·s" to N·s" and each "lb·s" to "lbf·s"
page 29, Abstract, line 15
Change "362 kg·s" to "3.6 kN·s"
page 30, column 2, line 21
Change "1145, 1105, and 1060 kg·s" to "11.2, 10.8, and 10.4 kN·s"
page 30, column 2, line 17 from bottom
Change "492, 487, 500, and 464 kg·s" to "4.93, 4.89, 5.02, and 4.65 kN·s"
page 31, column 1, line 11
Change "350, 360, 350, and 357 kg·s" to "3.43, 3.53, 3.43, and 3.50 kN·s"
page 31, column 1, line 39
Change "338, 349, and 388 kg·s" to "3.31, 3.43, and 3.80 kN·s"
page 31, column 2, line 35
Change "91 kg·s" to "0.89 kN·s"
page 31, column 2, line 44
Change "Tunnel momentum change, kg·s 504 351 338 452" to "Tunnel momentum change, kN·s 4.93 3.43 3.31 4.43"
page 31, Table 3
Change the momentum change values from kg·s to kN·s for each category: "Speed Trap Measurement: NM, 4.75, 3.51,–,4.96"; "Integration of Tunnel Acceleration: 11.17, 4.93, 3.42, 3.31, 4.50"; "Integration of Rear-Deck Acceleration: 10.8, 4.89, 3.53, 3.43, 4.10"; "High-Speed Film Analysis: 10.4, 4.89, 3.43, 3.80, 4.48"
page 32, column 1, lines 7 and 10
Change "91 kg·s" to "0.89 kN·s" and "457, 418, 457, and 506 kg·s" to "4.43, 4.11, 4.25, and 4.97 kN·s"
page 33, column 1, lines 7-8
Change "500 kg·s" to "4.89 kN·s" and "350 kg·s" to "3.34 kN·s"
page 33, column 1, text table
Change the momentum change values from kg·s to kN·s for each test: "Test 1:–, 11.22, 10.83, 10.39"; "Test 2: 4.75, 4.94, 4.89, 5.02"; "Test 3: 3.51, 3.44, 3.53, 3.43"; Test 4:–, 3.31, 3.42, 3.80"; "Test 5: 4.96, 4.48, 4.10, 4.48"
page 33, column 1, line 31
Change "350 kg·s" to "3.34 kN·s"
page 33, column 2, lines 5 and 7
Change "500 kg·s" to "4.89 kN·s" and "91 kg·s" to "0.89 kN·s"

Transportation Research Record 681
page 19, column 2, line 22
Change "frequently" to "infrequently"

Transportation Research Record 720
page ii, Library of Congress data
Change "[666'.89]" to "[66';893]"

Transportation Research Record 721
page ii, Library of Congress data
Add "National Research Council. Transportation Research Board.
Rail and motor carrier reports.
(Transportation research record; 721)
1. Railroads—Addresses, essays, lectures. 2. Railroads—United States—Addresses, essays, lectures. 3. Transportation, Automotive—Freight—Addresses, essays, lectures. 4. Transportation—Law and legislation—United States—Addresses, essays, lectures. I. Title. II. Series.
TE7.H5 no. 721 [HE1031] 380.5s [385]
ISBN 0-309-02971-6 79-607922

Transportation Research Record 734
page ii, column 1
Change publication data to
Transportation Research Record 734
Price $3.40
Edited for TRB by Mary McLaughlin

mode
1 highway transportation

subject areas
24 pavement design and performance
31 bituminous materials and mixes
34 general materials
35 mineral aggregates
62 soil foundations

Change Library of Congress data to
Library of Congress Cataloging in Publication Data
National Research Council. Transportation Research Board.
Copper mill tailings, incinerator residue, low-quality aggregate characteristics and energy savings in construction.

(Transportation research record; 734)

Performance of Highway Safety Devices

Robert D. Carlson, Joseph R. Allison, and James E. Bryden,
New York State Department of Transportation

Accident records were compiled over a 5-year period (1971-1975) to evaluate performance of light-post guiderail and median barrier, slip-base sign posts, frangible-base luminaire supports, and impact attenuation devices. Guiderail and median barrier injury rates were very low, with only eight serious injuries and no fatalities recorded in 392 accidents. Penetration of the barrier occurred in only 4 percent of mid-section accidents. Based on only 10 accidents, slip-base sign supports appear to be performing satisfactorily. Based on 78 accidents, performance of aluminum frangible-base luminaire supports is excellent. Of 393 impacts recorded on four types of attenuators, only six severe injuries and one fatality occurred; most serious accidents were related to specific problems with individual attenuators or with secondary collisions.

In the 1960s New York State research on highway safety devices resulted in development of improved guiderail to protect errant vehicles by safely redirecting them back onto the roadway. For situations where use of guiderail is impractical, such as elevated gores, impact attenuation devices were developed to stop cars at safe deceleration levels. Breakaway supports were designed to lessen impact severities with highway sign and luminaire supports.

Although these new or improved devices were developed through carefully controlled testing programs, satisfactory performance in controlled tests does not assure that actual in-service performance will be without problems (1). The objective of the additional research reported here was to document field performance of New York's traffic barriers, as well as that of impact attenuators, slip-base sign supports, and frangible-base luminaire supports.

SAFETY DEVICES STUDIED

Guiderail and Median Barrier

New York's standard guiderails and median barriers use lightweight posts (S3x5.7) that yield on impact, allowing the rail element to deflect gradually and absorb the vehicle's lateral energy. This system was developed when early crash tests showed that heavy posts could produce high decelerations (2). Rail elements now used include cable, corrugated W-beam, and structural tubing (box-beams). Rail type and post spacing for a given installation, either guiderail or median barrier, are selected on the basis of available deflection space behind the rail. By installing the most flexible system possible for the available deflection distance, decelerations on the impacting vehicle are held as low as possible. Details of New York's light-post barriers are shown in Figure 1. In addition, concrete median barriers and heavy-post barriers are used (on rare occasions) for special situations.

Sign and Luminaire Supports

Collisions with fixed sign supports or luminaire poles may produce extremely high decelerations, resulting in severe injuries or death to vehicle occupants. Thus, bases were designed that release at ground level upon impact. Sign supports used in New York (see Figure 2), patterned after those developed in Texas (3, 4), employ a slip connection at the base consisting of two horizontal plates—one attached to the foundation near ground level and the other welded to the support leg. These plates are bolted together through slots that allow the plates to slip apart on impact, releasing the support leg. A hinge in the support's upper portion allows the leg to swing free of the vehicle, while remaining attached to the sign so it will not be thrown into the highway.

Luminaire supports having a frangible cast aluminum base (see Figure 3) were designed to fracture with a maximum change in the impacting vehicle's momentum of 4895 N/s (1100 lb/s), according to Federal Highway Administration (FHWA) standards in effect in the late 1960s (5). Upon impact, the cast aluminum base shatters, releasing the aluminum lamp pole, which passes over the vehicle and usually falls off the roadway. The luminaires evaluated included a 9.1-m (30-ft) pole, a 20.3-cm (8-in) base diameter, and a 4.6-m (15-ft) mast arm.

Impact Attenuators

Where fixed objects cannot be removed or converted to a safe design and adequate space is not available to install guiderail, the vehicle must come to a complete stop while keeping decelerations to a tolerable level. New York's designs allow a maximum average deceleration of 6 *g*.

Sand-Filled Plastic Barrels

Sand-filled plastic barrels (see Figure 4a) are frangible polyethelene barrels 91.4 cm (36-in) deep and 91.4 cm (36 in) in diameter. Upon impact, the barrels shatter and the sand is accelerated, transferring energy from the vehicle to the sand. The amount of sand in the barrels varies from 181 kg (400 lb) in the front to 952.6 kg (2100 lb) in rear units to achieve uniform deceleration as the vehicle penetrates the array.

Water-Filled Vinyl Tubes

This attenuator employs water-filled flexible vinyl tubes having orifices in the top. The tubes are compressed on impact, transferring energy from the vehicle to the liquid, which is forced through the orifice into the air.

These tubes are arranged in two configurations—one for high speeds [above 64.4 km/h (40 mph)] and the other for lower speeds. The high-speed devices (see Figure 4b), termed "cell-sandwich units," have plywood panels between groups of tubes to distribute impact force across the full width of tubes. Panels mounted along the sides of the unit provide redirection capability for side impacts. The low-speed units (Figure 4c), called "cluster units," consist of individual vinyl tubes bolted together in rows. The entire unit is attached to a backup wall or to the object being shielded. No interior or side panels are used.

Figure 1. Design details of light-post barriers.

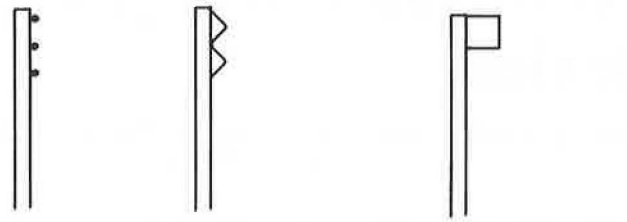

Barrier Type	Cable Guiderail	W-Beam Guiderail	Box-Beam Guiderail
Post Size	← S3x5.7 with 8"x24"x¼" soil plate →		
Post Length	63" min	63" min	63" min
Rail Element	Three 3/4" ϕ steel cables	10- or 12-gage, 12" deep steel W-beam	6"x6"x3/16" steel structural tube
Post-to-Rail Connection	5/16" ϕ hookbolt	Hex-head, 4000-lb min tensile strength, 1/16" ϕ 1½" long bolt, with support bolt at bottom	5"x3½"x3/8" long angle with 3/8" ϕ bolt through tube, ½" ϕ bolt through post
Mounting Height To Top of Rail	30" (center of top cable)	33"	30"

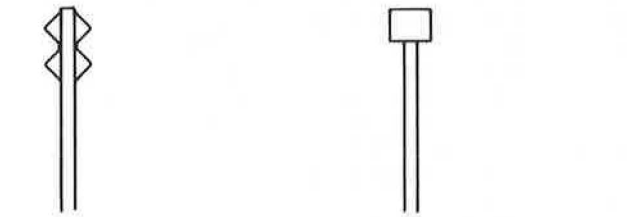

Barrier Type	W-Beam Median Barrier	Box-Beam Median Barrier
Post Size	← S3x5.7 with 8"x24"x¼" soil plate →	
Post Length	63" min	53-3/4" min
Rail Element	Two 10- or 12-gage 12" deep steel W-beams	6"x8"x¼" steel structural tube
Post-to-Rail Connection	Hex-head, 4000-lb min tensile strength, 1/16" ϕ 1½" long bolt, with support bolt at bottom	¼" thick special steel rail support plate, with two 3/4" bolts through post
Mounting Height To Top of Rail	33"	30"

Figure 2. Typical sign support details, showing slip base (left) and upper hinge (right).

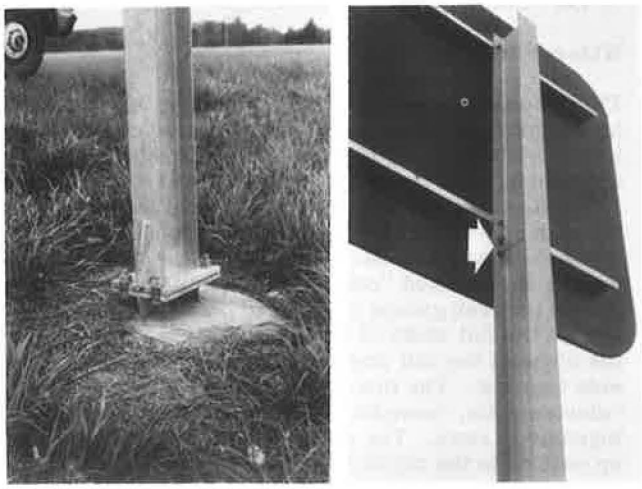

Figure 3. Typical aluminum frangible-base luminaire support.

Figure 4. Typical impact attenuation devices.

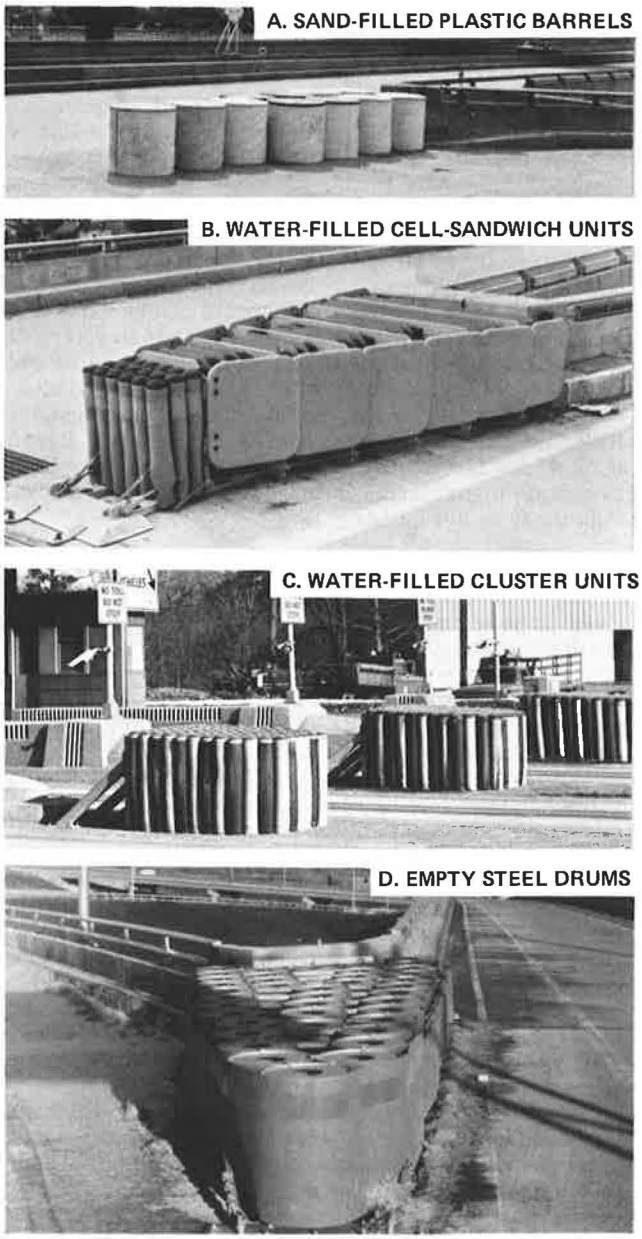

Empty Steel Drums

Consisting of 20-gage, 208-L (55-gal) steel drums with 20.3-cm (8-in) holes cut in the top and bottom, this device is commonly referred to as the "Texas Barrel" system (see Figure 4d). The drums are tack-welded or clipped together at the rims and anchored to a back-up wall. The energy of the impacting vehicle is absorbed in crushing the drums.

Data Collection Methods

This evaluation of highway safety hardware is based on accident experience on New York State highways. Data sources were as follows:

1. Guiderail and median barrier. The guiderail and median barrier sample consists of 47 construction contracts in the eastern half of New York State (except New York City) on which the guiderail installation was completed by 1971. These contracts cover 367 km (228 miles) of highway and include 145 839 m (478 473 ft) of barrier. In addition to locations monitored on the state highway system, guiderail and median barriers on 314 km (195 miles) of the New York State Thruway were monitored from April 1 to October 1, 1973.

The department's highway maintenance subdivision handled data collection on the state system. When an installation was struck at one of the selected sites, the maintenance foreman responsible for repair completed and forwarded a special accident form. Cost data were transmitted when they became available. Research personnel also checked for accident locations on departmental printouts, and obtained actual police reports from the Department of Motor Vehicles when available. On the Thruway, data collection was coordinated by the N. Y. State Thruway Authority's traffic and safety engineer. State police completed a special report form at the time of an accident, and attached a copy of the police accident report. These reports, along with guiderail repair data, were then forwarded.

2. Impact attenuators. Since only a limited number of attenuators were in service at the beginning of the study, all sites across the state were monitored. New installations put in service during 1971 to 1975 were added to the study. When data collection ended, 70 units were being monitored, including 21 water-filled cell-sandwich units, 11 water-filled cluster units, 35 sand-filled plastic barrel units, and 3 empty steel drum units. On the state system, data collection was conducted in the same manner as for guiderail and median barrier. In New York City, data collection was coordinated through the New York City Department of Highways, the maintenance supervisor for impact attenuators, and the manager of the Traffic Engineering Division of the Port Authority of New York and New Jersey.

3. Sign and luminaire supports. State highways where guiderail and median barrier data were also being collected were monitored, but only a few reports were received on breakaway sign supports and none on frangible-base luminaire supports. Performance of these sign and luminaire supports thus was also monitored along the Thruway. From April 1 to October 1, 1973, slip-base supports were monitored on the Thruway's entire 900-km (559-mile) length, while luminaire support observations were restricted to the Niagara and New England sections, totaling 58 km (36 miles).

In addition, a 20-km (12½-mile) section of I-90 in Albany was selected for the monitoring of luminaire supports, where a total of 392 poles were in service. On both state roads and the Thruway, data collection procedures and forms were identical to those used for guiderail and median barrier. For I-90, researchers obtained a listing of all impacts on luminaire supports directly from the utility company, including the accident date and pole number. These data were then used to search Albany police records for accident reports.

Study Variables and Evaluation Criteria

The safety devices studied include a number of design and construction variables that could be expected to affect performance. Several other variables also must be known to describe each accident. The major ones included were as follows:

1. Barrier or impact attenuator type. Five types of guiderail and median barrier, 4 impact attenuators, 1 slip-base sign support, and 1 frangible-base luminaire support were included.

2. Impact location on barrier. Location of impact on the barrier was recorded.

3. Impact conditions. Vehicle speed and trajectory before impact and secondary impacts with other objects were recorded when available.

4. Vehicle size. Only passenger car accidents are included; in most cases, specific vehicle weight and size were unavailable, because of the large number of hit-and-run accidents, and because police accident reports do not indicate vehicle model.

5. Barrier mounting height. An earlier study of performance of New York barriers (1) indicated that mounting height of the rail element plays an important role in a barrier's performance; in 1969, the specified mounting height to the center of the rail was increased to 68.6 cm (27 in) for all rail types, and actual field measurements were made in this study to determine rail height on each of the 47 contracts and on the Thruway. (These measurements characterize the range of heights on each contract, but do not define actual heights at individual accident sites.)

Several parameters were used to evaluate performance of safety appurtenances:

1. Severity of injury. Injuries were categorized as none, minor, severe, or fatal. Hit-and-run accidents were classified as no injuries, because it is reasonable to assume that most included no injuries, or at worst injuries of a very minor nature.

2. Vehicle reaction. A vehicle's reaction on impact is a primary indicator of the performance of a safety device. Data collected include barrier penetration and post-impact vehicle trajectories for guiderail and median barrier, when known. For attenuators, the final position of the vehicle was noted when available. For sign and luminaire support bases, vehicle trajectory and whether the vehicle stopped at the support were noted when possible.

3. Maintenance requirements. Accident damage repairs were reported in this study in terms of equipment, materials, and labor costs necessary to restore the device to operation. Routine maintenance activities such as winterizing were reported for attenuators.

GUIDERAIL AND MEDIAN BARRIER PERFORMANCE

In all, 392 impacts on guiderail and median barrier were recorded during the study period (90 percent occurred during 1972 and 1973). Police reports were included for all Thruway accidents, but for only 31 on state roads.

Severity of Injury

Injury data for all barrier accidents are given in Table 1. W-beam guiderail accidents are reported separately for the Thruway and state highways. Because police reports were generated by all Thruway accidents and by accidents on only a few state roads, the level of injuries reported may have been different. Accidents for the other barrier types were not separated, because accidents for each barrier type occurred almost exclusively on one system or the other.

The low number of severe injuries and the lack of fatalities indicate good performance by these barriers. The number of injuries recorded is too small to permit meaningful comparisons among guiderail types. However, by combining minor and severe injuries, a comparison between all guiderail and all median barrier and between the two types of median barrier was made using the χ^2 analysis technique. While the small difference between guiderail and median barrier injury rates was not statistically significant, the difference between W-beam and box-beam median barrier is significant at the 95 percent confidence level. Two factors may partially explain this difference. First, nearly all W-beam median barrier accidents were recorded on the Thruway, but box-beam median barrier accidents occurred predominantly on state roads. Because of the differences in police reporting, injury data possibly were more complete for the Thruway, with some very minor injuries going unreported on state roads. Second, warrants for use of the two types of median barrier are different, and as a result different types of impacts can be expected on each. Box-beam, the stiffer of the two barriers, is normally used in narrow medians up to 3 m (10 ft) wide; as a result, it is exposed to relatively low-angle hits. W-beam median barrier, on the other hand, is used in wider medians—generally 3 m (10 ft) or more. Because it is placed farther from the roadway, it is more likely to sustain higher-angle impacts—generally more severe than those at low angles.

Barrier Penetration and Rail Height

Barrier penetrations are given in Table 2. An "unrecorded" category accounts for hit-and-run accidents and police reports with incomplete data. However, nearly all these vehicles were probably contained. End-section accidents are not included, since end sections are not designed to prevent penetration.

With the exception of cable guiderail, penetration rates are very low. Because of the small sample for midsection cable accidents, little significance can be attached to this penetration rate. All these penetration rates, with the exception of cable guiderail, are below those recorded in an earlier New York study of traffic barriers (1). The small number of penetrations recorded precludes statistical comparison between barrier types, or with data from the earlier study for individual barrier types. However, the overall penetration rate is significantly lower in this study.

That earlier study identified rail mounting height as a possible contributing factor to barrier penetration, and mounting heights were increased in 1969. Because rail heights could not be obtained at individual accident sites, height was measured at 161-m (1/10-mile) increments on all contracts included in this study on state roads, and randomly along the Thruway (see Table 2).

Because considerable variability was observed within each contract, rail heights could not be determined at specific accident sites to identify relationships with barrier penetration. Such analysis is further frustrated by the small number of penetrations recorded. However, it can be concluded that overall penetration rates are significantly lower than in the previous study, and average barrier heights are higher than the previous standard.

Results of End-Section Accidents

Some 29 accidents involving barrier end sections were recorded in this study as follows: 11 cable guiderail, 2 W-beam guiderail, 6 box-beam guiderail, and 10 box-beam median barrier, and 1 impact involved a barrier transition. No injuries were recorded on the 11 end-section impacts on cable guiderail.

The proportion of end-section accidents on cable guiderail was greater than on other barrier types. This is attributed to greater flexibility, which enables a vehicle to deflect the cable barrier outward and remain in contact with it. In three of the accidents involving de-

Table 1. Severity of injuries for barrier accidents.

Barrier Type	No Injuries No.	No Injuries Percent of Total	Minor Injuries No.	Minor Injuries Percent of Total	Severe Injuries No.	Severe Injuries Percent of Total	Total Accidents
Cable guiderail	21	91.3	2	8.7	0	0.0	23
W-beam guiderail (state)	9	81.8	2	18.2	0	0.0	11
W-beam guiderail (thruway)	33	80.5	6	14.6	2	4.9	41
Box-beam guiderail	33	89.2	4	10.8	0	0.0	37
All guiderail	96	85.7	14	12.5	2	1.8	112
W-beam median barrier	73	82.0	14	15.7	2	2.2	89
Box-beam median barrier	177	92.7	10	5.2	4	2.1	191
All median barrier	250	89.3	24	8.6	6	2.1	280
All barriers	346	88.3	38	9.7	8	2.0	392

Table 2. Barrier penetration in midsection accidents.

Barrier Type	Penetrated No.	Penetrated Percent of Total	Contained No.	Contained Percent of Total	Unrecorded No.	Unrecorded Percent of Total	Total	Mean Mounting Height (cm)
Cable guiderail	4	33.3	5	41.6	3	25.0	12	71.9
W-beam guiderail	4	8.0	40	80.0	6	12.0	50	79.7
Box-beam guiderail	0	0.0	7	22.6	24	77.4	31	75.9
W-beam median barrier	5	5.6	81	91.0	3	3.3	89	74.2
Box-beam median barrier	2	1.1	19	10.5	160	88.4	181	75.4
All barriers	15	4.1	152	41.9	196	54.0	363	

Note: 1 cm = 0.39 in.

parture ends, the vehicle impacted the barrier at distances from the end of 27.4, 30.5, and 83.8 m (90, 100, and 275 ft), and followed along the barrier to the end anchor.

Only two impacts were recorded on W-beam guiderail end sections, both hit-and-run, but no problems were identified from these accidents. Six accidents involving box-beam guiderail end sections were recorded; one resulted in a minor injury, but the barrier performed satisfactorily in all six. Reports provided by maintenance personnel indicated that the vehicles were redirected parallel to the barrier in every case.

Ten box-beam median barrier end-section impacts were recorded, all hit-and-run. As with other barrier types, maintenance reports indicated satisfactory performance, with vehicles redirected along the barrier. No end-section impacts were recorded on W-beam median barrier.

Accident Damage and Repair Costs

Data on accident damage and repair costs provided by maintenance personnel are given in Table 3, including the rail length and number of posts damaged, as well as replacement quantities. Lack of normal distributions somewhat complicates analysis of these data, but differences between barrier types can be tested by means of the Mann-Whitney U test (6).

Average barrier damage tended to decrease as rail stiffness increased. Cable guiderail, the most flexible, had the highest average length of barrier damaged per accident—31.9 m (104.7 ft). Conversely, box-beam, the stiffest guiderail, had only 7.7 m (25.4 ft) damaged per accident. The same trend is apparent for median barriers. Grouping the state and Thruway W-beam guiderail for this analysis, all differences in barrier damage between guiderail types and between median barrier types are statistically significant at the 95 percent confidence level. Post damage is also related to barrier stiffness. With the exception of box-beam guiderail, most damaged posts had to be replaced.

Table 3 also summarizes accident repair costs for each barrier type. The Mann-Whitney U test was again applied to test differences among the three guiderail types and between the two median barriers. Grouping all W-beam guiderail together, the differences among the three guiderail types are not significant. However, W-beam median barrier was significantly more expensive than box-beam median barrier, although the absolute difference is not great. Although box-beam median barrier had the lowest average repair cost of all barriers, it also had the greatest range, with several very expensive accidents recorded.

Based on the limited sample reported here and considering differences in repair criteria and methods between the state and Thruway maintenance forces, differences in repair costs between barrier types appear to be minor—certainly insufficient to dictate the choice of barrier type to be used.

Summary

The 392 accidents recorded in this study indicate good performance by these barrier types. In nearly 90 percent of the accidents on the state system, the vehicle was able to leave the scene unassisted, indicating successful barrier performance. No fatalities were recorded, and most injuries were minor. Barrier penetration rates were lower overall than those recorded in an earlier New York study. Although few end-section accidents were recorded, performance was generally satisfactory. Accident damage was generally less for the stiffer barriers. Differences in total repair costs between barrier types were small, and do not appear sufficient to affect choice of barrier type.

SIGN AND LUMINAIRE SUPPORT PERFORMANCE

Slip-base sign supports produced the fewest accident reports—only ten. Three resulted in injuries—two minor and one serious; in all three, a secondary collision was involved. In all ten accidents, the base mechanism was reported to have released properly. In one, the slip-base was mounted 30.5 cm (12 in) above ground rather than the specified maximum 10 cm (4 in), which

Table 3. Barrier damage in accidents.

Barrier Type	Total Reports	Posts (mean)		Rail (mean length in m)		Repair Cost ($)	
		Damaged	Replaced	Damaged	Replaced	Mean	Range
Cable guiderail	23	8.0	6.0	31.9	0.0	243	40-1014
W-beam guiderail (state)	11	5.8	3.3	28.3	4.7	183	58-382
W-beam guiderail (thruway)	41	4.2	3.2	14.0	9.4	227	36-626
All W-beam guiderail	52	4.6	3.2	16.8	8.4	219	36-626
Box-beam guiderail	36	5.7	1.8	7.7	2.1	224	60-878
W-beam median barrier	89	4.8	4.0	16.5	11.7	250	64-1079
Box-beam median barrier	191	3.9	3.3	10.6	0.7	207	15-1329

Note: 1 m = 3.28 ft.

Table 4. Accident performance of frangible-base luminaire supports.

Accidents	Thruway	I-90	Total
Total accidents	24	54	78
Police reports	24	35	59
Hit-and-run	0	19	19
Injuries			
None	15	48	63
Minor	8	4	12
Severe	1	2	3
Fatal	0	0	0

Table 5. Accidents involving impact attenuators.

Accidents	Sand Barrels	Sandwich Units	Cluster Units	Steel Drums
Total impacts	242	63	84	4
Police reports	9	6	30	0
Hit-and-run	233	57	54	4
Injuries				
None, unknown	238	59	68	4
Minor	3	0	14	0
Severe	1	3	2	0
Fatal	0	1	0	0
Units in service	35	21	11	3

resulted in snagging the vehicle undercarriage and an abrupt stop, with the sign falling on it. Each support leg is designed to hold the sign erect if the other is impacted. However, this sign structure was previously struck on the opposite leg, and when the leg support hinge was bent back into position, it was apparently weakened so that it alone could not support the sign. As a result of this failure, damaged supports are no longer simply bent back into position. Rather, the supporting flange is cut through, and a steel plate the same thickness as the flange is welded into position.

Most accidents involving sign supports also involved other highway appurtenances such as guiderail and fencing, with cost data lumped into a single amount. Thus, cost data could not be obtained for sign supports alone.

In all, 59 police-investigated accidents involving luminaire supports were recorded, plus an additional 19 hit-and-run accidents, as summarized in Table 4. On the Thruway, nine injury accidents were recorded—eight minor and one severe. On I-90, four accidents resulted in minor injuries and two in severe injuries. Several injuries reported may have been caused by secondary impacts with other vehicles or with other fixed objects such as retaining walls, bridge rails, guiderail, or rock cuts, either before or after striking the luminaire base. Accident repair cost data (1973 costs) were received for 19 Thruway accidents. For six accidents where the poles could be reused, repair costs ranged from $257 to $392, with an average of $362. For the remaining 13 accidents where poles were replaced, repair costs ranged from $583 to $796, averaging $715. No cost data were available on the I-90 accidents.

Although the number of impacts recorded in this study on sign supports and luminaire bases is small, excellent performance by these safety devices is indicated. Collision with a rigid sign support or luminaire base would normally result in a very severe impact. Therefore, the small number of injuries recorded here, more than half of which involved secondary impacts with other objects, indicated a substantial reduction in injuries over what would be expected for similar supports with rigid bases.

IMPACT ATTENUATOR PERFORMANCE

Table 5 summarizes 393 collisions with impact attenuators reported during the years 1971 through 1976.

Severity of Accidents

Sand-Filled Plastic Barrels

Some 242 impacts were recorded by maintenance personnel. Police investigated nine, of which four resulted in injuries—three minor and one severe.

Water-Filled Cell-Sandwich Units

A total of 63 impacts on cell-sandwich units were recorded by maintenance personnel. All but six were hit-and-run. Three serious injuries and one fatality were reported. The former all occurred at the same location, which also sustained one hit that produced no injuries. This high injury rate at a single attenuator may be related to an installation problem involving the restraining cables, which was subsequently corrected. A fifth impact was recorded after the modifications, with no injuries.

In the single fatal accident involving a cell-sandwich unit, a subcompact vehicle skidded into the device sideways. The vehicle compressed the unit about 50 percent, and then rotated and made contact with the right side panels. The vehicle was then deflected across the ramp and struck a concrete bridge parapet. It is not known at what point during the accident the fatal injury occurred.

Water-Filled Clusters

Some 84 impacts were reported at 11 locations by maintenance personnel, with police reports for 30. Twenty-nine of the police reports were received for three sites on the George Washington Bridge where frequent police patrols resulted in reports for accidents that might go unreported elsewhere. In one serious injury impact, impact speed was reported at 80 km/h (50 mph). The other serious injury included a collision with another

Table 6. Repair costs for impact attenuators.

Attenuation Device	Total Impacts	Repair Costs ($)					
		Labor	Materials	Equipment	Total	Low	High
Sand-filled barrels							
All accidents	242	102	391	34	527	18	2523
Multiple-barrel damage	140	136	584	46	766	118	2523
Single-barrel damage	85	50	105	17	171	28	374
Modified arrays	17	80	228	23	331	18	716
Cell-sandwich units							
All accidents	63	92	72	31	195	34	1890
Modified site excluded	59	83	63	29	176	34	1890
Cluster units (New York City)							
All accidents	25	92	263	32	388	36	2718
Less replaced units	21	64	18	25	107	36	250
Cluster units (Port Authority)	59	123	128	—[a]	251	0	NA
Steel drums, all accidents	4	289	2	58	349[b]	112	623[b]

[a] Included as 25 percent overhead on labor costs.
[b] Damage from two accidents on one unit was repaired at one time.

Table 7. Summary of nonimpact maintenance on New York City impact attenuators.

Year	Sand Barrels	Sandwich Units	Cluster Units
1974			
Units in service	19	16	7
Total repairs	22	21	8
Total average cost, $	99	107	114
Average materials cost, $	46	26	29
1975 (through September)			
Units in service	21	17	8
Total repairs	25	6	6
Total average cost, $	103	228	253
Average materials cost, $	33	101	124

vehicle after first striking the cluster unit. Of 14 minor injury accidents, seven involved secondary impacts with other vehicles, or with the bridge parapet either before or after striking the cluster unit.

Empty Steel Drums

Attenuators made from empty steel drums were installed at three locations. Four impacts were reported, all hit-and-run accidents with no police reports filed. Because of the minor damage to the devices, it is apparent that all were relatively minor. Therefore, the performance of this device in more severe collisions remains unknown.

Maintenance Requirements

Accident repair costs for attenuators are given in Table 6. These costs were highly variable, depending upon impact severity. Cell-sandwich units had the lowest overall average repair cost and sand barrels the highest. However, for a more complete picture, several considerations must be noted in analyzing these costs.

Repairs on the cluster units were very easy. The unit was simply straightened as necessary, and the cells refilled with antifreeze solution. A total of 25 impacts were recorded on all cluster units maintained by New York City. However, four resulted in damage much more severe than the other 21, which required major reconditioning or replacements. The average repair cost on the New York City cluster units, excluding these extraordinary expenses, was $102, with a maximum of $250. Repair costs for 59 recorded impacts on cluster units maintained by the Port Authority averaged $251.

Not considering the four major repairs noted before, repair costs on the cell-sandwich units were more variable than on the cluster units. Because they are installed at higher-speed locations, the potential for variability in impact severity is greater. As discussed in the section on accident severity, one unit required rebuilding after four impacts because of a construction deficiency. In addition, two hits on this unit before rebuilding resulted in damages of $431 and $1143. Because of this extraordinary damage, these impacts are not considered typical. Maintenance costs without them averaged $176 for 59 reported impacts.

While minor impacts on cell-sandwich units and cluster units may often go undetected, except for obvious scrapes and scuff marks, nearly all impacts on sand-barrel units result in broken barrels that generate a maintenance report. These minor impacts, termed "nuisance hits", may often be caused by the presence of the attenuator itself, since less recovery room is available in the gore area. To reduce damage to the entire array by minor impacts, the three leading barrels were positioned 2.7 m (9 ft) in front of the main array of four units. Seventeen minor hits on the three leading barrels of these modified arrays, and 85 single-barrel hits on the standard arrays, are reported separately in Table 6. The average cost for 140 multiple-barrel hits was $766, and this is the figure that can most properly be compared with repair costs on cell-sandwich and cluster units, where nuisance hits did not normally generate repair cost reports.

Only three repairs were made for four impacts on the steel drum units, at an average cost of $349. Because used paint drums were used as replacements, material costs were very low. However, labor costs were very high for these repairs. Maintenance personnel reported difficulty in disassembling the damaged drums from the unit and replacing new drums in the proper positions. More experience in repairing these devices may achieve some reductions in labor costs.

In addition to impact repairs, routine maintenance is also required on these devices. This includes winterizing, repair of minor damage from vandalism and other deterioration, and removal of debris that collects in the units. Repair cost data for nonimpact maintenance for all units maintained by New York City for 1974 and for the first 9 months of 1975 are summarized in Table 7.

DISCUSSION

All four types of attenuators performed very well in preventing serious injuries to occupants of impacting vehicles. Except for several injuries on the cluster units attributed to secondary collisions and high-speed impacts, no large differences are apparent between any of the attenuator types in terms of injury severity. Although large differences in maintenance costs are apparent among systems, total cost also depends on initial

cost of the installation and the number of impacts it can withstand before replacement is required.

The study's principal findings are that

1. Guiderail and median barrier performed well in 392 accidents recorded in this study.
2. The barrier penetration rate recorded was significantly lower than in an earlier New York study of barriers.
3. Twenty-eight barrier end-section accidents resulted in no injuries.
4. No large differences in barrier accident repair costs were recorded.
5. Only ten impacts were recorded on slip-base sign supports. Although two resulted in minor injuries and a third in a hospitalization injury, secondary impacts were involved in all three.
6. Seventy-eight impacts on frangible-base luminaire supports resulted in minor injuries in 12 cases, and hospitalization injuries in three more. Several of these injuries probably resulted from secondary collisions with other fixed objects or vehicles.
7. Of 393 impacts recorded on impact attenuators, only 17 minor injuries, 6 hospitalization injuries, and 1 fatality were recorded.
8. Accident repair costs were highest for the sand-barrel units and lowest for the cell-sandwich units, but this may be offset by the higher initial cost of both types of water-filled cells, and the possible need for major reconstruction or replacement after a limited number of impacts.

REFERENCES

1. J. Van Zweden and J. E. Bryden. In-Service Performance of Highway Barriers. Engineering Research and Development Bureau, New York State Department of Transportation, Res. Rept. 51, 1977.
2. G. W. McAlpin and others. Development of an Analytical Procedure for Prediction of Highway Barrier Performance. HRB, Highway Research Record 83, 1965, pp. 189-200.
3. N. J. Rowan and others. Impact Behavior of Sign Supports: 2. A Staff Progress Report. Texas Transportation Institute, Res. Rept. 68-2, 1965.
4. R. M. Olson and others. Breakaway Components Produce Safer Roadside Signs. HRB, Highway Research Record 174, 1967, pp. 1-29.
5. Application of Highway Safety Measures: Breakaway Luminaire Supports. Federal Highway Administration, Circular Memorandum, 1968.
6. A. J. Duncan. Quality Control and Industrial Statistics, 3rd Ed. Richard D. Irwin, Inc., Homewood, IL, 1965, pp. 533-39.

Abridgment

Cost-Effectiveness Model for Guardrail Selection

L. R. Calcote, Southwest Research Institute, San Antonio, Texas

In view of the problems of ever-increasing highway construction costs and the limited funding available, it is critical to guardrail selection and installation that a cost-effectiveness formulation be included as an aid in the decision-making policy. This is particularly true for the rural, low-volume highway. For such roads, strict adherence to the conventional guardrail warranting and selection procedures could lead to the installation of guardrails of maximum effectiveness at some sites and no installations at other sites because of the lack of available funds. Thus, a need exists for effective criteria for the selection of guardrail types based on a cost-effectiveness analysis. A typical cost-effective procedure can be used to evaluate the options of (a) removing or reducing the hazard so that the guardrail is no longer warranted, (b) installing the most cost-effective guardrail systems that funds permit, or (c) leaving hazards unshielded at sites where guardrail installation is not cost-effective. This report focuses principally on the second of these options; the guardrail is assumed to be warranted. However, the third option (c) can also be exercised for the included hazard types of fixed objects or embankments. Of course, the value of such a cost-effectiveness decision-making policy need not be limited to low-volume roads and could result in more efficient use of available funds for all types of highway systems.

The objective of this program was to develop a cost-effectiveness model for guardrail selection that would include cost parameters for various guardrail configurations as well as criteria for analysis of system effectiveness under various dynamic impact conditions. Eleven guardrail types were selected for inclusion in the program. Five of the designs (G1, G2, G3, G4S, G4W) were included in NCHRP Report 118 (1). The remaining six systems were arbitrarily selected from commonly used designs and some of the newer designs coming into use. Most of the systems have now been included in the 1977 American Association of State Highway and Transportation Officials (AASHTO) Guide (2). The corresponding system notations follow (1 m = 3.3 ft):

System in This Report	Notation in AASHTO Guide
A	GR2, except for post size
B	G4(1W), except for round rather than square posts
C	Not included (W-beam on 0.2 x 0.2-m wood posts with blockouts at 3.8-m spacing)
D	G4(2W)
E	G4(2S)
G1	G1
G2	G2
G3	G3
G4S	G4(1S)
G4W	G4(1W)
Thrie	G9

Selected impact category values used in the study for vehicle sizes, vehicle speeds, and angles of impact are

shown in the following table (1 kg = 2.2 lb; 1 km/h = 0.6 mph):

Category	Value
Vehicle weight (kg)	
Intermediate and standard-size vehicles	2041
Subcompacts and compacts	1021
Vehicle speed (km/h)	
Less than 64.4	48.3
64.4 to 96.5	80.5
Over 96.5	112.7
Angle of impact (°)	
Less than 10°	7
10 to 20°	15
20 to 30°	25
Over 30°	30

A present-worth probabilistic formulation was used in the development of the cost-effectiveness model. This method combines the guardrail installation cost and all annual maintenance and accident costs into a single equivalent sum at zero time. Of the alternatives compared, the one with the lowest present worth is the most economical. With this approach, the total government or state cost, converted to present dollars, is given by C_G = cost of installation + cost of maintenance and repair - salvage value, and the total societal cost by C_S = severity costs per accident (fatalities, injuries, guardrail and vehicle damage, and traffic delay) × probable number of accidents.

To apply this formulation in developing the computer algorithm, it was necessary to estimate the following items:

1. Traffic mix [fractions of total traffic by 1021-kg (2250-lb) and 2041-kg (4500-lb) vehicles];
2. Number of encroachments;
3. Probabilities of out-of-control vehicles traversing the offset distance to the guardrail or obstacle;
4. Distribution of vehicle speeds;
5. Distribution of impact angles;
6. Accident severities in terms of guardrail damage, number of occupant injuries or fatalities, and vehicle damage for each combination of the category vehicle speeds and impact angles;
7. Travel delay time for accident blockage and guardrail repair;
8. Costs of injuries, fatalities, vehicle damage, travel delay, and guardrail installation, repair, maintenance, and salvage value; and
9. Service life of the guardrail and rate of interest.

For the most part, these parameters were quantified from available historical data. Exceptions included estimates of traffic mix and unit construction costs, which were obtained from the states, and impact angle distributions, which were obtained analytically from geometric and vehicle properties with limited supportive field data. Also, in the most radical departure from usual practice, accident severity estimates were based on full-scale test results rather than analysis of accident data. Available test results were first carefully correlated with the BARRIER VII computer simulation. Once satisfactory correlation was achieved, the program was used to obtain extrapolation predictions for the 24 category impact combinations from the second table and each of the 11 guardrail types. For illustrative purposes, a guardrail service life of 15 years and a current interest rate of 8 percent were used.

A COCOST program for comparative cost-effectiveness values and ranking of the 11 included guardrail types with given roadway conditions was developed in the program. The following definitions were used with regard to the cost-effectiveness values:

1. State cost—money spent by the state in installing and maintaining the guardrail;
2. Societal cost—costs associated with accidents, including costs of injuries and fatalities, costs of guardrail and vehicle damage, and cost of traffic delay;
3. Total cost—the sum of state and societal costs;
4. Benefit—the difference between societal cost with no guardrail installation and societal cost with the guardrail installed (hazard types include fixed objects or embankments); and
5. Benefit-to-cost ratio—the ratio of the benefit to the state cost (to effect a savings in societal costs greater than the state cost of the guardrail installation, a benefit-to-cost ratio greater than unity must be realized).

The COCOST user's manual includes the basis and limitations of the program, computer program descriptions and listings, a series of site selection tables based on the representative costs and input values, and sample problems for applying the computer program for the following: (a) selection at a particular site of the most cost-effective guardrail system of the 11 included types, (b) guardrail placement at a site for the optimum location and guardrail type, and (c) priority ranking of several site selections for appropriation of available funds.

COCOST was prepared with a view to producing a product that has the desired flexibility but is as simple to use and as easy to implement as possible within the limitations imposed by the specified scope of the study. Program inputs are simple to prepare with familiar engineering terms and format. If preselected representative inputs are acceptable to the user, only four COCOST cards per set are required, the second of which

Figure 1. A sample COCOST output sheet.

SUMMARY OF RESULTS EXAMPLE GUARDRAIL PLACEMENT CASE - 6-FT SHOULDER

PAVEMENT-TO-GUARDRAIL DISTANCE = 6 FT GUARDRAIL-TO-OBSTACLE DISTANCE = 9 FT

PAVEMENT-TO-OBSTACLE DISTANCE = 15 FT SOCIETAL COST WITH NO GUARDRAIL = $ 3561.28

AADT = 5000 GUARDRAIL LENGTH = 276 FT OBSTACLE LENGTH = 200 FT

DEGREE OF CURVE	PREFERRED GUARDRAIL ORDER BY INDICATED CRITERIA										
	1	2	3	4	5	6	7	8	9	10	11
0 STATE COST	G1	G2	A	C	B	E	D	G4W	G4S	THRIE	G3
VALUES	768.59	1113.59	1154.99	1292.99	1568.99	1596.59	1637.99	1706.99	1706.99	1982.99	3638.99
SOCIETAL COST	G2	G4S	G1	D	THRIE	A	E	G3	C	B	G4W
VALUES	754.82	1669.59	1740.45	1759.36	1815.26	1834.07	1877.61	2017.82	2087.30	2407.57	2412.90
TOTAL COST	G2	G1	A	G4S	C	D	E	THRIE	B	G4W	G3
VALUES	1868.92	2509.05	2989.06	3376.59	3380.29	3397.35	3479.21	3798.26	3976.57	4119.89	5656.81
BENEFIT/COST	G2	G1	A	C	G4S	D	E	THRIE	B	G4W	G3
VALUES	2.52	2.37	1.50	1.19	1.11	1.10	1.05	.88	.79	.67	.42

is a blank card. Card sets are simply stacked so that as many cases can be run as desired. To facilitate adaptation to a particular computer, both CBC and IBM operational versions of the programs have been prepared. The computer programs are small, and run times are minimal.

Interpretation of the computer output results is not difficult. For example, Figure 1 shows a typical COCOST output sheet, in which it can be seen that the guardrail types are ranked by state cost, societal cost, total cost, and benefit-to-cost ratio in the order of decreasing preference (the best is number 1 and the worst is number 11), along with the corresponding values. Thus, the G2 system is the preferable guardrail for this site from the standpoints of either societal cost, total cost, or benefit-to-cost ratio. The analyst can select the cost-effectiveness measure desired and can extract the indicated values, along with the corresponding state cost, for subsequent analyses to establish priorities for appropriation of funds or for other uses.

ACKNOWLEDGMENTS

The work described herein was conducted by the Division of Structural Research and Ocean Engineering, Southwest Research Institute (SwRI), for the Federal Highway Administration (FHWA). The opinions, findings, and conclusions expressed are mine and not necessarily those of the sponsor. For FHWA technical support of the program, special appreciation is expressed to Michael J. McDanold. SwRI personnel who made significant contributions to the program development include M. E. Bronstad, V. B. Parr, T. H. Swiercinsky, R. E. Kirksey, G. W. Deel, C. E. Kimball, and Jane E. Baker.

REFERENCES

1. J. D. Michie and M. E. Bronstad. Location, Selection, and Maintenance of Highway Traffic Barriers. NCHRP, Rept. 118, 1971.
2. Guide for Selecting, Locating, and Designing Traffic Barriers. AASHTO, 1977.

Abridgment

Computerized Inventory and Priority Analysis for Roadside Obstacles

Richard A. Cunard, Traffic Engineering Services, Traffic Improvement Association of Oakland County, Michigan
David D. Perkins, Goodell-Grivas, Incorporated, Southfield, Michigan
Tapan K. Datta, Wayne State University

Highway safety is significantly influenced by the design and maintenance of the roadside environment. During 1976, over 26 percent of all fatal accidents in Michigan involved collisions with fixed objects in or adjacent to the roadway. Recent highway safety programs emphasize hazard-free roadway facilities and have resulted in reduced accident severity associated with single-vehicle collisions with roadside obstacles. Such programs generally involve the removal, relocation, or protection of roadside obstacles. Even though the potential safety benefits derived from roadside improvement programs are substantial, the traffic engineer is faced with the high cost of removal or relocation of roadside obstacles and the need for a practical program for the identification and prioritization of hazardous roadside obstacles.

In order to make informed decisions regarding the allocation of safety funds for roadside hazard removal, the traffic engineer must first establish a comprehensive data base of the type and location of all potential hazards as they exist along the highway and the relative hazardousness of each. With this information, a systematic roadside safety program may be developed to eliminate or protect those obstacles that present the greatest hazard to the motorist.

This paper describes a computerized information system consisting of a comprehensive inventory of all roadside obstacles in the city of Livonia, Michigan. Livonia is located in the northwestern part of the Detroit metropolitan area and covers 92.9 km^2 (36 $miles^2$) with a population of 110 000 persons. The highway system consists of approximately 483 km (300 miles) of roadway.

In 1976, Livonia experienced a total of 3889 accidents, of which 6 percent were collisions with fixed objects. However, these fixed-object accidents accounted for over 33 percent of all 1976 fatal accidents in the city.

The inventory system incorporates a prioritization mechanism that provides the traffic engineer with a measure of the relative hazard potential associated with each type of roadside obstacle and with the priority to be given to eliminating or protecting that obstacle.

INVENTORY OF ROADSIDE OBSTACLES

Data Collection

The data source from which information on roadside obstacles' type and location was extracted for the development of a computerized inventory of roadside obstacles was 35-mm color photologs. Photologging is a photographic data-collection technique that records a pictorial representation of the roadway and its environs. An instrumented vehicle equipped with a 35-mm color movie camera, distance-measuring instrument (DMI), and a camera actuation device were used for the photologging process. Camera actuation was set at 62 frames/km (100 frames/mile) or every 16.1 m (52.8 ft). The distance traveled by the vehicle from predetermined benchmarks was recorded by the DMI and superimposed

on the photolog along with the street name, date, time of day, and direction of travel.

Data Extraction

Data extraction involved viewing the photologs using photoviewing equipment on a frame-by-frame basis. The criteria for identifying an object as a roadside obstacle included the following factors:

1. Type of object,
2. Lateral distance of the object from the edge of the roadway,
3. Physical dimension of the object, and
4. Existence of curbs along the roadway.

During discussions with city officials, the following conventions were established for the determination of what objects would be recorded in the inventory. On curbed roadway sections, obstacles were recorded if they were located within 1.22 m (4 ft) of the curb. For uncurbed roadways, 3.05 m (10 ft) was used as the lateral distance criterion.

Data extraction was performed by trained photoviewing analysts using photolog viewing devices. Roadside obstacles were located longitudinally with respect to the nearest cross street by using the DMI reading on each photolog and adding to that the distance to the obstacle from the photologging vehicle. This distance was determined by the use of a calibrated grid placed on the viewing screen. The grid was also used to determine the lateral distance of the obstacle from the curb or edge of the roadway.

Other information including the direction of travel, main street and cross street names, and obstacle type was recorded and added to the roadside obstacle inventory program. A total of 2342 roadside obstacles were recorded during the data extraction process for Livonia.

Figure 1 shows a typical printout of the roadside obstacle inventory.

SEVERITY RANKING PROCEDURE

A practical priority-ranking scheme that can be easily used and understood at the local level is necessary, if limited roadside improvement funds are to be optimally allocated. The procedure for developing the replacement indices contained in this roadside obstacle inventory was developed to meet this need. Other research (1, 2) conducted to date has resulted in prioritization techniques that have made a significant contribution to the state of the art. However, they are somewhat complicated and often prove to be impractical for use in large-scale applications such as a comprehensive inventory of all roadside obstacles for a community. The priority-ranking procedure used in the determination of the replacement indices is based on the following basic assumptions:

1. For curbed roadway sections, obstacles located within 1.22 m (4 ft) of the edge of the curb constitute a potential hazard in a single-vehicle collision.
2. For uncurbed roadway sections, obstacles located within 3.05 m (10 ft) of the edge of the roadway constitute a similar hazard.
3. The probability of an obstacle being involved in a

Figure 1. A typical printout of a roadside obstacle inventory.

CITY OF LIVONIA, ROADSIDE OBSTACLE REPORT AS OF : 07-28-77 PAGE 001
DEPARTMENT OF PUBLIC WORKS

OBSTACLE NUMBER	MAIN STREET	CROSS STREET	DIST FROM INTERSEC	& DIREC	SIDE OF STREET	OBSTACLE TYPE	CURB	DATE	CURB DIST	SEVER RANK	REPL INDEX
01020000100	ANGLING	SEVEN MILE	1148	NORTH	EAST	TREE(S)	NOCB	110976	9	12	24
01020000200	ANGLING	FLORAL	100	NORTH	EAST	TREE(S)	NOCB	110976	5	12	72
01020000300	ANGLING	FLORAL	186	NORTH	EAST	TREE(S)	NOCB	110976	3	12	96
01020000400	ANGLING	FARGO	196	NORTH	EAST	ROCK(S)	NOCB	110976	3	4	32
01020000500	ANGLING	FARGO	330	NORTH	EAST	ROCK(S)	NOCB	110976	4	4	28
01020000600	ANGLING	FARGO	317	NORTH	WEST	WOOD UTILITY	NOCB	110976	8	11	33
01020000700	ANTAGO	SEVEN MILE	50	NORTH	EAST	FIRE HYDRANT	NOCB	110976	7	5	20
01020000800	ANTAGO	VASSAR	45	SOUTH	EAST	FIRE HYDRANT	NOCB	110976	7	5	20
01020000900	ANTAGO	GRAND RIVER	246	SOUTH	WEST	ROCK(S)	NOCB	110976	7	4	16
01020001000	BRENTWOOD	SEVEN MILE	0		WEST	NO OBSTACLES	CURB	110976	0	0	0
01020001100	BRETTON	PARKVILLE	0		SOUTH	NO OBSTACLES	NOCB	110976	0	0	0
01020001200	BRETTON	MAPLEWOOD	0		SOUTH	NO OBSTACLES	CURB	111276	0	0	0
01020001300	BRIDGE	RENSELLOR	153	EAST	NORTH	TREE(S)	NOCB	111276	6	12	60
01020001400	BRIDGE	INKSTER	30	WEST	SOUTH	ROCK(S)	NOCB	111276	5	4	24
01020001500	DEERING	ST MARTINS	10	SOUTH	WEST	TREE(S)	NOCB	110976	6	12	60
01020001600	DEERING	PEMBROKE	50	NORTH	EAST	FIRE HYDRANT	NOCB	110976	7	5	20
01020001700	FARGO	DEERING	159	EAST	NORTH	HEAD WALL	NOCB	111276	8	7	21
01020001800	FARGO	DEERING	120	EAST	SOUTH	TREE(S)	NOCB	111276	9	12	24
01020001900	FARGO	WEYHER	153	EAST	SOUTH	POLE(S)	CURB	111276	4	6	6
01020002000	FARGO	BRENTWOOD	63	WEST	SOUTH	TREE(S)	CURB	111276	3	12	24
01020002100	FLORAL	PEMBROKE	0		WEST	NO OBSTACLES	NOCB	110976	0	0	0
01020002200	GILLMAN	NORFOLK	0		WEST	NO OBSTACLES	NOCB	110976	0	0	0
01020002300	LATHERS	DEAD END	414	SOUTH	WEST	TREE STUMP	NOCB	110976	5	12	72

single vehicle collision and, therefore, its relative hazardousness is a function of its distance from the curb or edge of the roadway.

4. The relative hazardousness of an obstacle is a function of its design and rigidity.

The type and rigidity are reflected in the severity-ranking index assigned to the 12 selected categories of roadside obstacles recorded in the inventory system. The severity-ranking values range from 1 to 12, based on the rigidity and type of the obstacle and its potential for causing harm to the occupants of a vehicle on impact. The highest severity ranking was assigned to trees, which had a value of 12, and the lowest severity-ranking value was shrubbery, which had a value of 1.

Two replacement index algorithms were developed for this application—one for obstacles located along curbed roadway sections $(RI)_c$ and others for uncurbed sections $(RI)_{nc}$.

For a curbed roadway, $(RI)_c$ = [(5 - lateral distance) × severity ranking]. For an uncurbed roadway, $(RI)_{nc}$ = [(11 - lateral distance) × severity ranking].

The possible values for the replacement index range from 1 for shrubbery (severity ranking = 1) located 1.22 and 3.05 m (4 and 10 ft) from the edge of a curbed and uncurbed roadway section respectively to 132 for a tree (severity ranking [SR] = 12) located at the edge of an uncurbed roadway section. In addition, the analysis of roadside obstacles gave higher priority (replacement index) to obstacles along uncurbed than along curbed roadway sections.

It was determined that the roadside obstacles that present the greatest hazard potential (trees, SR = 12; utility poles, SR = 11; mast arm supports, SR = 10; buildings, SR = 9; guardrails, SR = 8) constitute 48 percent of the total number of roadside obstacles recorded in the inventory. The treatment of hazardous roadside locations on the basis of obstacle type alone represents lengthy and costly roadside improvement program requirements if all high-severity obstacles are to be removed, relocated, or protected. However, the application of the priority procedure indicates that, based on the underlying assumptions that form the basis of the replacement index algorithms, a significantly lower number of obstacles require immediate treatment. In terms of the magnitude of the replacement indices (RI), which have been qualitatively stratified as low (RI = 0 through 45), medium (RI = 46 through 90), and high (RI = 91 through 132), approximately 3 percent (78) of all roadside obstacles have been identified as exhibiting a high replacement index. These obstacles should be given first priority in the roadside improvement program. Furthermore, the replacement indices for those obstacles in the high-priority range will provide the traffic engineer with a rank ordering of those obstacles requiring preferential treatment.

CONCLUSIONS

The computerized inventory and priority-ranking scheme for roadside obstacles provides a community with a practical tool for managing and improving the roadside environment. With it, an application may be made for federal funding for the planned removal, relocation, or protection of the most hazardous obstacles along the roadway, thereby maximizing the accident-reduction potential for each safety dollar spent. Once improvements have been made, the capabilities of the inventory system allow for continued updating to reflect the type of work that was done.

For Livonia, Michigan, 2342 roadside obstacles were recorded, of which almost 50 percent were high-severity potential obstacles—trees, utility poles, buildings, or guardrails. However, the application of the replacement index algorithm identified only approximately 3 percent (78) of all roadside obstacles as being in a high replacement category. Thus, the planned improvement of these sites may provide a substantial savings in accidents and accident severity in a cost-effective manner.

It is our intent to refine the existing system by correlating single-vehicle, fixed-object accidents in Livonia with the roadside obstacle inventory to obtain a better picture of the severity potential associated with various roadside obstacles and their characteristics. Also, future refinements can be made in the prioritization algorithm to account for traffic volumes, roadway geometrics, and other roadway information that can be obtained from photologs to further define the degree of hazard potential of roadside obstacles. However, a conscious effort will be made to maintain the simplicity and practicality of this system as a roadside management tool.

ACKNOWLEDGMENT

The opinions, findings, and conclusions expressed in this paper are ours and not necessarily those of the state of Michigan or the U.S. Department of Transportation, Federal Highway Administration.

REFERENCES

1. J. D. Glennon. Roadside Safety Improvement Programs on Freeways: A Cost-Effectiveness Priority Approach. NCHRP, Rept. 148, 1974.
2. J. W. Hall and others. Roadside Hazards on Non-Freeway Facilities. Transportation Studies, Jan. 1976.

Abridgment

Test Vehicle Kinematics by High-Speed Photography and Accelerometer Data

L. R. Calcote and R. E. Kirksey, Southwest Research Institute, San Antonio, Texas

Full-scale tests of vehicles influencing guardrail or median barrier systems involve complex dynamic mechanisms that are extremely difficult to characterize analytically. Thus, satisfactory theoretical values of the vehicle kinematics cannot be determined for correlating results obtained by experimental means. This abridgment concerns the results of a simple experimental test by which these theoretical quantities were established. Experimental data were collected by means of high-speed photography and accelerometers in the same manner as that used in the full-scale tests, and the results of the two techniques are compared with theoretical values.

EXPERIMENTAL PROGRAM

In the interest of maintaining a commonality of technique with the full-scale tests and the evaluation experiment, the simple two-target test apparatus shown in Figure 1 was devised. By rotating the apparatus at a constant angular speed $\dot{\theta}$, the theoretical nonzero kinematic quantities of Target 1 could be easily established by the relationships

$$x = r \cos \theta$$

$$y = r \sin \theta$$

$$v_{lat.} = r \dot{\theta}$$

$$a_{long.} = r \dot{\theta}^2$$

where r is the radius of rotation and θ is the heading angle. These quantities could then be used to evaluate the experimental values. In conducting the test, the procedures were identical to those used in the full-scale tests. For example, the initial position and velocities obtained from the high-speed film data were used as initial conditions for integration of the accelerometer data. The instantaneous heading angles required in the accelerometer data reduction were also taken from the film results.

Figure 1. Plan of test apparatus.

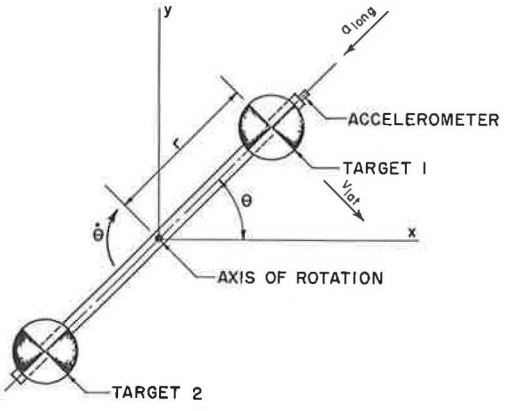

Figure 2 shows a comparison of longitudinal accelerations in which the accelerometers would be expected to give better results. Figure 3 is a comparison of x-coordinates in which the high-speed photography would be expected to be better. In the photography runs, the maximum degree of curve fit for the data points was specified at $k_{max} = 20°$, and film readings were taken at every frame. Film speeds were 196 and 168 frames per second for the two data cameras used in the experiment.

To check the sensitivity of the maximum degree of curve fit and the sampling rates with the high-speed photography, runs were made for every frame with $k_{max} = 10°$ and $k_{max} = 20°$, and for every second, fourth, and eighth frame with $k_{max} = 20°$. Figures 4 and 5 show plots of the results for longitudinal accelerations and lateral velocities, respectively. Also shown on the figures are the theoretical values and the 5 percent and 10 percent bands. Clearly indicated in both figures is the characteristic tendency for the curve-fitted quantities to blow up near the ends of the data. In these runs, data sampling was started at 0.087 second before the first location of interest and extended well past one revolution of the test apparatus. Results of the data reductions were computed at 0.01-second intervals from time t = 0 to time t = 1.00 second, the end of one revolution. This produced 101 pairs of data points for comparison purposes.

RESULTS

Figure 2, where the accelerometer data were expected to give better results, shows longitudinal acceleration values for slightly more than half a revolution of the test apparatus. Of the total of 101 pairs of data points for the full revolution, 69 of the photography points and 32 of the accelerometer points were closer to the theoretical value. Figure 3 shows that both techniques are close for the x-coordinate. Of the 101 data point pairs, the photography gave results closer to theoretical in 62 cases, accelerometer data were closer in 37 cases, and, to two decimal places, the results of the two methods were the same for two cases. From these and other figures, a preliminary conclusion can be drawn that the high-speed cine data are probably as accurate as the accelerometer data for all of the kinematic quantities. However, the cine data will not indicate the high-frequency peaks that are characteristic of accelerometer data in the full-scale tests. Much of this fluctuation is caused by vehicle ringing and is of such high frequency that it is not likely to be felt by the vehicle occupant.

As expected, Figures 4 and 5 show that the fluctuations of the results were of greater magnitude as the sampling rate was decreased. Changing the maximum

Figure 2. Comparison of longitudinal accelerations.

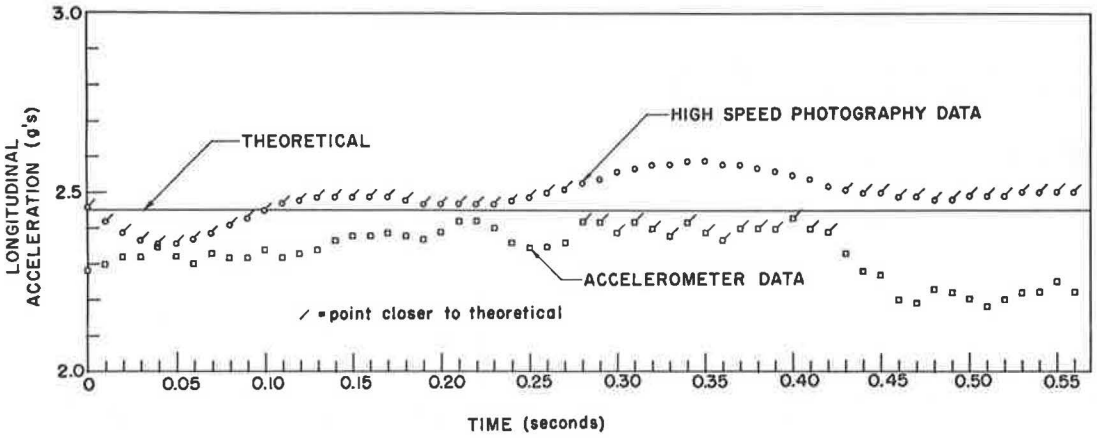

Figure 3. Comparison of x-coordinates.

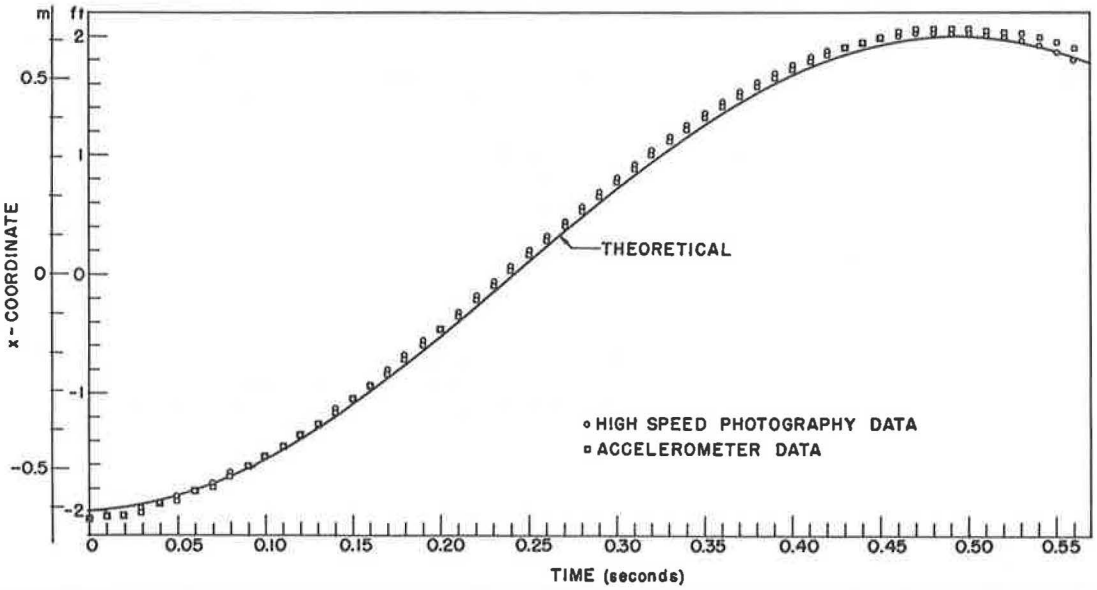

Figure 4. Longitudinal accelerations for various sampling rates.

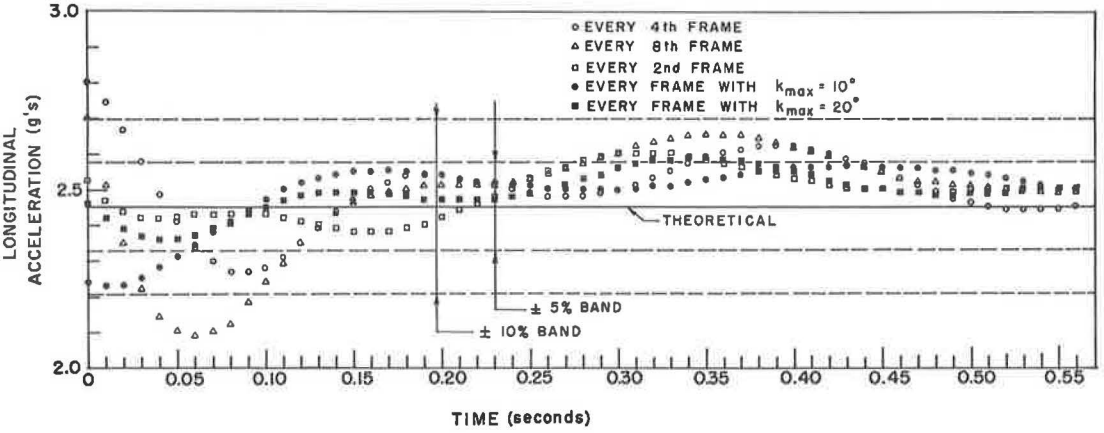

Figure 5. Lateral velocities for various sampling rates.

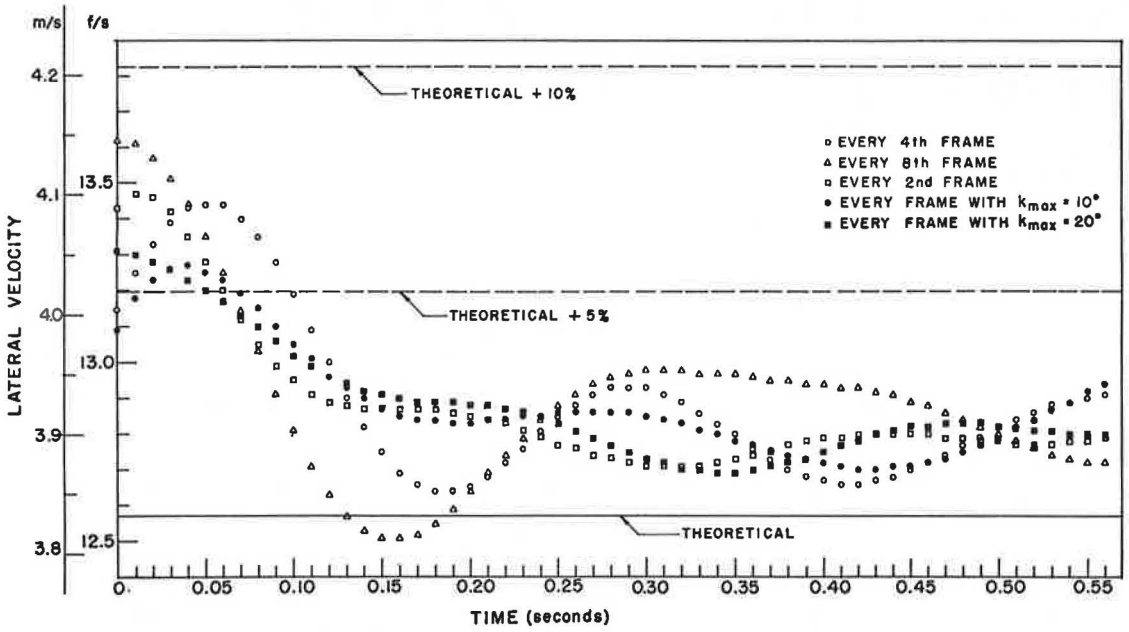

degree of curve from 10° to 20° did not appear to materially affect the results. To be reasonably confident of results with 5 percent accuracy, the figures indicate that at least every fourth frame should be read. With film speeds of approximately 200 frames per second in the evaluation experiment and 500 frames per second in the full-scale tests, a corresponding sampling rate for the full-scale tests would be 4 (500/200) or every tenth frame. Thus, it can be assumed that full-scale test runs with maximum 10° curve fits, data sampling at every sixth frame, and sampling that brackets the event by 0.10 second on each end will produce kinematic quantities within ±5 percent of the actual values.

CONCLUSIONS

It has been shown by means of a simple test how the data-acquisition techniques of high-speed photography and accelerometer readings compare with theoretical values. It had been assumed that the differentiation of cine data would not be as accurate as integration of accelerometer data for the desired kinematic quantities. However, this was not the case, and it can be concluded from this study that the cine data will yield results that are just as accurate as, and probably more accurate than, the accelerometer data. Of course, considerably more instrumentation is necessary for retrieval of the accelerometer data and can present undesirable sources of instrument error. Furthermore, initial conditions must be known in the integration process, and the instantaneous direction must be determined if the motion is curvilinear. The high-speed cine retrieval has the advantages of greater simplicity and the self-starting characteristic, but care must be exercised in the differentiation of the data. The errors caused by differentiation of curve fits near the ends of the sampled data can be made less significant if the period of interest can be bracketed on both ends by the data sampling.

ACKNOWLEDGMENTS

We wish to express appreciation to the Internal Research Panel of Southwest Research Institute for sponsoring the project in which this work was performed. Under the title, A Comparison of High-Speed Photography and Accelerometer Data-Reduction Techniques, the complete paper was previously published in Experimental Mechanics, Society for Experimental Stress Analysis, May 1977.

Abridgment

Experimental Evaluation of a Portable Energy-Absorbing System for Highway Service Vehicles

John F. Carney III, University of Connecticut, Storrs

This paper is concerned with the crash testing of a new portable energy-absorbing system attached to the rear of a highway service vehicle. The study objective was to design a system to provide protection for both the motoring public and the service personnel engaged in maintenance operations on our highways. Four full-scale crash tests were conducted to evaluate the performance of the system with respect to structural adequacy, impact severity, and vehicle trajectory. The details of the energy-absorbing systems design are presented in Carney and Sazinski (1). They show that the device must absorb 319 107 J (235 330 ft·lb) of energy and possess a collapsing stroke of 2.23 m (7.31 ft). Four 0.6-m (2-ft) diameter pipes connected in series are used as the unit energy-absorbing components. Because of vertical stability considerations, the depth of the pipe system was set at 0.86 m (34 in). Then a polymodular design was carried out. In the polymodular design, the wall thicknesses of the two pipes nearest the rear of the service vehicle were taken as 9.525 mm (0.375 in). The third pipe in the series was given a thickness of 6.756 mm (0.266 in). The fourth pipe, the one nearest the impact point, has a thickness of 6.756 mm (0.266 in) and 0.508-m (1.67-ft) long vertical slits, 180° apart, in its sides. With this setup, the pipe system exhibits increasing stiffness as the collapse length increases. Carney and Sazinski (1) show that this system can, when fully collapsed, just absorb the 319 107 J (235 330 ft·lb) of energy to be dissipated.

The system has been designed to possess the following two characteristics:

1. It is capable of absorbing most of the energy dissipated in a high-speed collision between an automobile and the highway service vehicle.
2. It absorbs this energy in such a way that the accelerations and acceleration rates to which the automobile and service vehicle are subjected are within the guidelines specified by the Federal Highway Administration.

The energy-absorbing system involves three components: (a) the service vehicle guidance frame, (b) the energy-absorbing pipes, and (c) the impacting plate assembly. The unit, as mounted on the service vehicle, is shown in Figure 1 (top). The impacting plate assembly shown in Figure 1 (bottom) is constructed of 6061-T6 aluminum. The remaining components of the energy-absorbing system are made of steel. It is interesting to note that the round aluminum tubing in the impacting plate assembly slides inside the structural tubing on collapse of the system.

Figure 1. Two views of the portable energy-absorbing system.

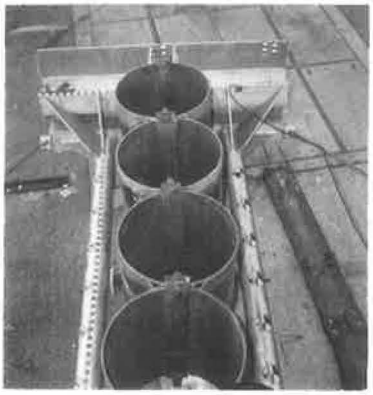

FULL-SCALE CRASH-TESTING PROGRAM

The crash-testing phase of the research was carried out under a subcontract by Calspan Corporation of Buffalo, New York. The testing program followed as closely as possible the procedures spelled out in Bronstad and Michie (2). Four full-scale crash tests were conducted to evaluate the performance of the energy-absorbing system under different impact conditions.

Test vehicle 1 was a 1971 Ford Maverick, weighing 10.05 kN (2260 lb), which impacted the 62.27-kN (14 000-lb) service truck equipped with the portable energy-absorbing system. The impact velocity was 73.69 km/h (45.8 mph). The impact angle was 0°, and impact occurred at the centerline of the truck.

Test vehicle 2 was a 1970 Pontiac, weighing 19.93 kN (4480 lb). The impact velocity was 74.90 km/h (46.55 mph). The impact angle was 0°, and impact occurred at the centerline of the truck.

Test vehicle 3 was a 1973 Plymouth, weighing 19.93 kN (4480 lb). The impact velocity was 73.18 km/h (45.48 mph). The impact angle was 0°, and impact occurred at a 0.762-m (2.5-ft) offset from the centerline of the truck.

Test vehicle 4 was a 1973 Plymouth, weighing 19.88 kN (4470 lb). The impact velocity was 7366 km/h (45.78 mph). The impact angle was 10°, and impact occurred at a 0.762-m (2.5-ft) offset from the centerline of the truck.

During the testing program, the four automobiles and the service truck were instrumented with accelerometer

Figure 2. Crash test 1.

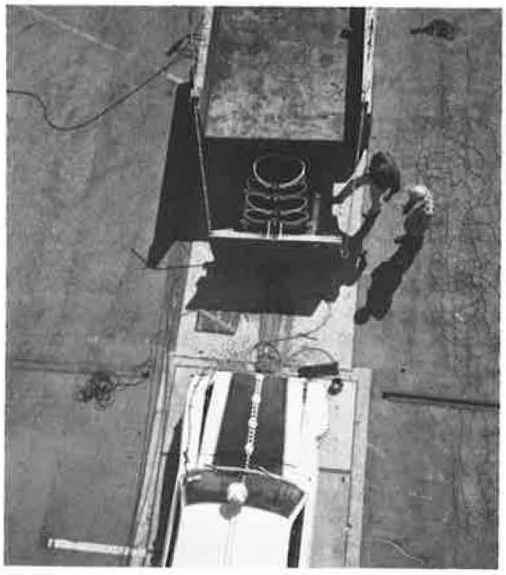

Figure 3. Crash test 2.

Figure 4. Crash test 3.

packages. The test results demonstrate the effectiveness of the energy-absorbing system. The four automobiles sustained—in view of their impact velocities—minimal damage; the service vehicle was undamaged by the four crashes. The same energy-absorbing system was employed for all four tests; the four collapsing pipes were the only system component to be replaced after each crash. Figures 2-5 show the results of the crashes on the impacting automobiles and the energy-absorbing unit.

The results of test 1 are presented in Figure 2, which shows the energy-absorbing system and the 1971 Ford Maverick after the collision. In this test, the average deceleration of the automobile was 9.8 *g*.

Figure 3 shows the results of test 2. The average deceleration of the automobile was 8.5 *g* in this crash test.

The collision mode and the postimpact configuration of test 3 are presented in Figure 4. In this test, the automobile's average deceleration was 7.7 *g*.

Figure 5. Crash test 4.

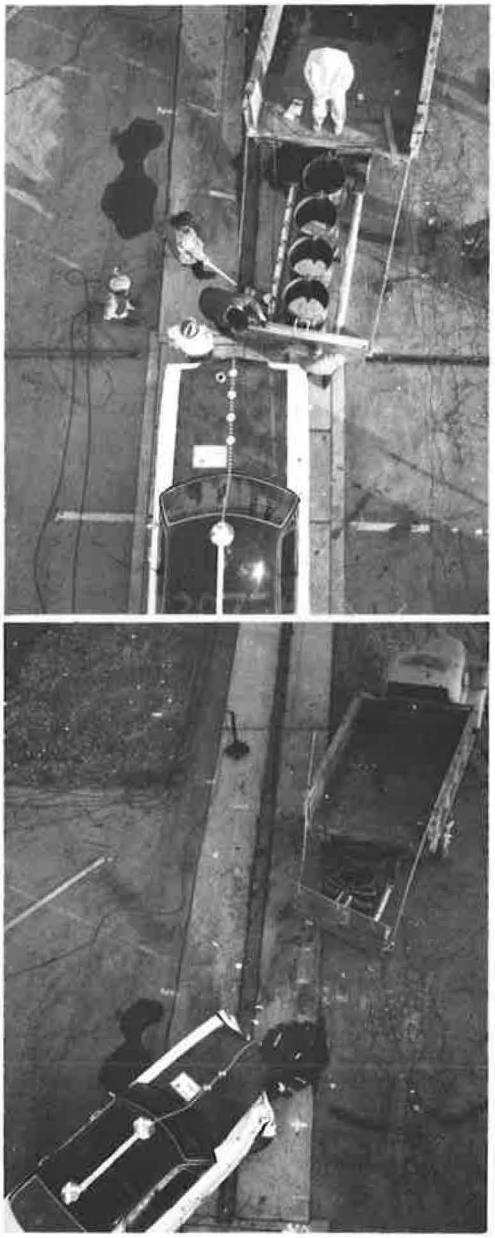

Figure 5 shows the collision mode and postimpact configuration of test 4. The average deceleration of the automobile was 7.8 *g* in this test.

The deceleration levels in the three "heavy" automobile crash tests were well within the guidelines set forth in Bronstad and Michie (2). In the 10.05-kN (2260-lb) automobile crash test, although the average deceleration was less than the limiting value of 12 *g* (2), there was an initial 80-*g* acceleration "spike" of approximately 10 ms duration after which the decelerations dropped to and remained at acceptable levels. This lightweight vehicle "spike" is caused by a 1.913-kN (430-lb) aluminum impacting plate assembly and can be reduced by decreasing the weight of this component, which must be moved to permit the collapse of the energy-absorbing system. Work in this area is continuing at the University of Connecticut.

SUMMARY AND CONCLUSIONS

A portable energy-absorbing system that is attached to the rear of a standard 62.27-kN (14 000-lb) highway service vehicle has been designed and constructed. Four full-scale crash tests were conducted to evaluate the system with respect to structural adequacy, impact severity, and vehicle trajectory.

The performance of the system has been demonstrated. Three of these units are now being used on department of transportation maintenance operations in Connecticut to provide protection for both the motoring public and service personnel engaged in maintenance operations. It offers effective protection for the equipment used in these maintenance and repair projects. Of particular value is its implementation during the highway line-striping operations. In addition, the energy-absorbing system provides immediate temporary protection during short-term repair or clean-up operations, i.e., the repairing of a Fitch sand-filled barrel installation.

The energy-absorbing system possesses the following favorable characteristics:

1. It absorbs most of the energy dissipated in a high-speed collision between an automobile and the highway service vehicle; it absorbs this energy in such a way that the accelerations and acceleration rates to which the automobile and service vehicle are subjected are within the guidelines specified by the Federal Highway Administration.
2. It is inexpensive to build. The total assembly can be constructed for less than $2000. This figure compares favorably with the $5500 cost of the hydro-cell unit that has been used during lane-striping operations in Connecticut.
3. It is very inexpensive to repair. Under most crash conditions, all that is required is to insert new 0.6-m (2-ft) diameter pipes into the system. These pipes are bolted together and cost about $100 each. The aluminum impacting plate and the steel frame under the dump truck body will not usually require repairs. In the case of a low-speed collision, the steel pipes can be jacked back to their original shape and reused.
4. There is no tendency for the impacting automobile to nose-dive under the energy-absorbing unit or catapult over the unit, and the system exhibits essentially no rebound characteristics.
5. In the event of an eccentric impact, the intrusion of the impacting automobile into the adjacent traffic lane is minimal.
6. The 62.27-kN (14 000-lb) service vehicle can be expected to suffer no damage during the crash, and adjacent lane intrusion by the truck is not a problem. The same 62.27-kN (14 000-lb) service vehicle was used for all four crash tests and suffered no damage.
7. It is compact and designed for use on curved and hilly roads.

ACKNOWLEDGMENT

This work was accomplished in cooperation with the Connecticut Department of Transportation and the U.S. Department of Transportation, Federal Highway Administration. The contents of this report reflect my views, and I am responsible for the facts and the accuracy of the data presented herein. The contents do not necessarily reflect the official views or policies of Connecticut or the Federal Highway Administration. This report does not constitute a standard, specification, or regulation.

REFERENCES

1. J. F. Carney III and R. J. Sazinski. A Portable Energy Absorbing System for Highway Service Vehicles. Transportation Engineering Journal, Vol. 104, No. TE4, July 1978.
2. M. E. Bronstad and J. D. Michie. Recommended Procedures for Vehicle Crash Testing of Highway Appurtenances. NCHRP, Rept. 153, 1974.

Abridgment

Crash Test Performance of a Guardrail Median Barrier and Temporary Construction-Zone Crash Cushion

Bruce O. Young, Energy Absorption Systems, Incorporated,
West Sacramento, California
Robert M. Davis, Aerojet Services Company, Sacramento, California

The viability of crash cushions for protecting errant motorists who hit roadside hazards is well established. An acceptable treatment for the narrow hazards created by recent widespread deployment of metal-beam guardrails and concrete median barriers (CMB) was not available prior to 1976. Southwest Research Institute of San Antonio, Texas, reported that "even at shallow angles of impact, vehicle stability is marginal..." with the long-ramp treatment of CMBs in New Jersey as recommended in Michie and Bronstad (3). The sloping transition sections—with ends buried beneath grade—eliminated impacting against blunt ends of CMBs or impalement by metal-beam guardrails but often caused ramping and subsequent rollover of errant vehicles. Existing crash cushion systems were too wide for narrow hazards; reducing their width left unit stability and side-angle redirection performance open to conjecture. In addition, rapidly expanding numbers of accidents in construction zones, created in part by temporary guardrail or CMB installations to detour traffic, dictated a need for temporary protection of work crews and motorists.

The GuardRail Energy Absorbing Terminal (G-R-E-A-T) and G-R-E-A-T Construction Zone (G-R-E-A-T_{oz}) are restorable attenuator systems developed to cushion both the narrow stationary and construction zone hazards. Both systems conform to the test standards for crash cusions outlined in Bronstat and Michie (4). Because the G-R-E-A-T is often used in bidirectional traffic, an additional test, for a wrong-way side-angle impact, was determined necessary to establish its performance suitability. This report describes the units, the test series, and the test results.

UNIT DESCRIPTION

The G-R-E-A-T crash cushion consists of crushable Hi-Dri Cartridges surrounded by steel thrie-beam guardrail. When hit head-on, thrie-beam fender panels telescope backward, permitting the impact energy to be dissipated in crushing the lightweight-concrete Hi-Dri cells. When impacted on the side, the side panels redirect the errant vehicle away at a shallow exit angle.

The nose section consists of a Hi-Dri Cartridge and a soft plastic nose wrap. This molds itself to the shape of the impacting vehicle. A G-R-E-A-T unit contains as many bays as is determined necessary to satisfy the allowable *g* loads on the impact vehicle. Each bay has a diaphragm, a Hi-Dri Cartridge, and two fender panels.

The Hi-Dri Cartridge contains many cylindrical lightweight concrete cells whose performance is documented by Walker and others (1). These cells are bonded to plywood retainer panels and encased in a moisture-resistant box. A thin plastic cover shrouds the cartridge and provides additional resistance to moisture penetration. The diaphragm consists of a short length of thrie-beam supported by two steel pipe legs.

Short sections of overlapping 10-gauge steel thrie-beam guardrail are fastened together through slotted holes that allow the panels to slide alongside one another in a telescoping manner when hit head-on. When hit on the side, the overlapping thrie-beam side panels form a truss that distributes the force of the impact along its entire length.

One end of the anchor chains is attached to a restraining chain rail that, in turn, is fastened to a concrete base. The other end of the chain attaches to a pin on the front side of the diaphragm support legs. The chains restrain the diaphragms when hit on the side but slip off the open-end leg pins when hit head on to allow the system to telescope.

When the G-R-E-A-T is used in a median barrier application where traffic is going the wrong way on the left side of the unit, deflector panels are attached to the back end of each fender panel and to the backup (see Figure 1) so that wrong-way traffic cannot snag on the backup or exposed ends of the fender panels.

This same crash cushion placed on a metal platform can quickly be bolted to a concrete surface; because of its transportability, it is ideally suited for providing the same effective protection at construction sites.

G-R-E-A-T_{oz}

Except for the addition of the portable steel platform (see Figure 2), the system is identical to a permanent G-R-E-A-T installation. Expansion-type anchor bolts secure the platform to a concrete base. For transportation the unit is separated at the splice in the base plates and lifted by using the tabs on the base plates. Each plate weighs approximately 635 kg (1400 lb), including the G-R-E-A-T unit.

No effective means has yet been found for attaching the G-R-E-A-T_{oz} platform to soil or to asphalt bases. Therefore, a concrete base of suitable size to prohibit movement during impact is necessary.

Restoration of the G-R-E-A-T and G-R-E-A-T_{oz} can be quickly achieved by pulling the unit out to its preimpact position and replacing the expended cartridges and shear pins. Refurbishment, in most cases, can be completed in approximately 30 min. Figure 3 shows the G-R-E-A-T system installed on the end of a guardrail.

TEST DESCRIPTION

The four tests conducted for Federal Highway Admin-

istration (FHWA) approval and the wrong-way side-angle impacts are reported herein. Test criteria conformed with requirements outlined in Bronstad and Michie (4).

The test unit was 0.76 m (30 in) wide and contained six bays and a nose section—total length equalled 6.4 m (21 ft). Data were acquired with longitudinal and transverse accelerometers mounted on the vehicle floorboard immediately behind the driver's seat. Acceleration data were fed through a hard line to a Dixson paper tape recorder located in a stationary vehicle. Two high-speed cameras, a Fastax filming at 1000 frames/s and a Photosonic filming at 500 frames/s, provided backup instrumentation. Standard targets were painted on the vehicles, and a high-speed timer was included in the photometric record.

Figure 1. G-R-E-A-T system median barrier protection.

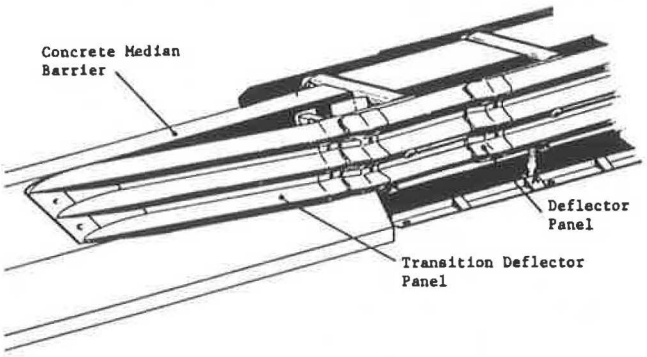

Test 1—Heavy Car, Centered on Unit Nose

The test vehicle was a 1960 Pontiac two-door sedan, weighing 1845 kg (4060 lb). Impact velocity was 101 km/h (63 mph), with impact occurring on the nose at a 0° angle to centerline and 0.46 m (18 in) to the right of the unit centerline.

During the impact, the test vehicle rotated counterclockwise 48°, rotating as the forward motion of the vehicle was virtually completed. The vehicle was permanently deformed approximately 0.36 m (14 in) on the front left side.

The accelerometer trace indicated the vehicle was subjected to an average deceleration of 8.0 g, with forces exceeding the 12-g level twice, once at 50 ms and again at 75 ms after initial impact, for 15 ms duration each. The peak load was 15 g. Except for the cartridges, the unit sustained no damage.

Test 2—Light Car, Centered on Unit Nose

In this test a 1971 Vega station wagon, weighing 1077 kg (2370 lb), impacted at 93.4 km/h (58 mph) on the center of the unit at a 0° angle to centerline. The vehicle rotated approximately 40°, but not until the forward motion neared completion. Vehicle deformation was approximately 0.25 m (10 in). Immediately after impact, the impact vehicle was started and driven for a short distance.

Average deceleration force was 7.8 g, exceeding 12 g for 20 ms duration beginning 50 ms after impact. Peak load was 13 g. Again, except for the cartridges, no unit damage was observed.

Figure 2. G-R-E-A-T system (portable) for construction zones.

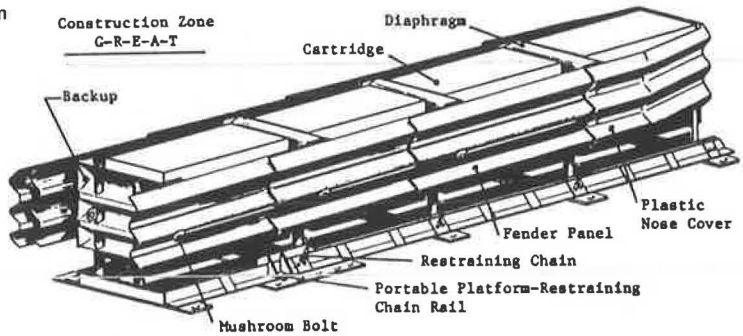

Figure 3. G-R-E-A-T system installed at end of guardrail.

Test 3—Heavy Car, 20° Side-Angle Impact at Midlength

The test vehicle was a 1968 four-door Buick LeSabre sedan, weighing 2054 kg (4520 lb), impacting at 101.4 km/h (63 mph) at midlength, at an angle of 20° as measured from unit centerline. The vehicle was gently redirected, exiting at an angle of 7°, and traveled approximately 274 m (900 ft) before drifting slightly to the left and stopping. The vehicle sustained significant sheet-metal damage on both front and rear fenders with only slight damage to the doors. The same vehicle was driven live the following day in a test series on a different unit.

Maximum transverse and longitudinal deceleration forces were 3 and 6 *g* respectively. No unit damage was discernible, nor were any cartridges expended. In normal service no maintenance would have been required.

Test 4—Heavy Car, 0-0.9m (0-3 ft) Offset From Unit Nose, 10-15° Impact Angle

The test vehicle was a 1968 Oldsmobile four-door hardtop, weighing 2050 kg (4510 lb). The impact point was on the center of the nose, but at a 10° angle with the unit's centerline. Impact velocity was 93.4 km/h (58 mph). The vehicle momentarily tended to rotate and follow the unit as it compressed, but then continued its approximate preimpact path until coming to a stop. Before stopping, the vehicle rotated to the left until it was oriented at a 30° angle to the unit centerline.

Compression of the G-R-E-A-T was normal until the final instant when the vehicle rotated left. One of the longitudinal slots on a right fender panel deformed, allowing a mushroom washer to pull out. Subsequently, the unit separated at that point and rotated clockwise through an arc of approximately 90°.

Damage to the vehicle was confined to a permanent centerline front-end deformation of approximately 0.36 m (14 in). Attenuator damage was limited to deformation of four fender panels, requiring either straightening or replacement, and expenditure of all frangible cartridges. Complete refurbishment was accomplished in approximately 1 h.

Average deceleration force for the event was 7.7 *g*. The force exceeded 12 *g* for a period of 15 ms, and the peak force was 13 *g*.

Tests 5 and 6—Wrong-Way Side-Angle Impacts

In the first wrong-way test, a 1967 1682-kg (3700-lb) Chevrolet was directed into the wrong-way thrie-beam transition panel, between the backup and concrete median barrier, at an angle of 20° and at 74 km/h (46 mph). Redirection was smooth, and the vehicle suffered only minor sheet-metal damage.

In the second wrong-way test, a 1966 Buick, weighing 1873 kg (4120 lb), impacted the side of the unit at approximately midlength of the unit at an 18° angle and at 88.5 to 96.6 km/h (55 to 60 mph). The vehicle was smoothly redirected at approximately a 6° exit angle with a minor change in velocity.

SUMMARY AND CONCLUSION

Live drivers involved in tests at speeds of up to about 80 km/h (50 mph) have reported no discomfort from restraining belts in both head-on and side-angle impacts. Southwest Research Institute has conducted one additional test on the G-R-E-A-T system, the results of which are described in Bronstad, Calcote, and Kimball (2).

The remainder of the functional tests conducted on the G-R-E-A-T system to date have displayed characteristics similar to those discussed above in performance, damage sustained, replacement parts required, and refurbishment considerations.

Test results proved that the G-R-E-A-T system satisfied the requirements established for serviceable impact attenuators. Actual in-service data obtained from the hundreds of units in use in the field nationwide have corroborated the results of the evaluation test series. These data prove that the G-R-E-A-T either safely stops or redirects errant vehicles, which might otherwise impact against narrow hazards.

The portable G-R-E-A-T system has had limited exposure due to its recent implementation in field service. However, initial feedback from several highway department construction projects has been favorable regarding ready transportability and installation. It is expected that additional data will continue to indicate utility and performance on a par with that of the permanent G-R-E-A-T system.

REFERENCES

1. G. W. Walker, B. O. Young, and C. Y. Warner. Crash Tests of an Articulalted Energy Absorbing Gore Barrier Employing Lightweight Concrete Cartridges. HRB, Highway Research Record 386, 1972, pp. 19-27.
2. M. E. Bronstad, L. R. Calcote, and C. E. Kimball, Jr.. Concrete Median Barrier Research, Volume 2. Federal Highway Administration, Rept. RD-77-4, March 1976, pp. 95, 99, 136, C.76, C.89-C.92, E.8-E.9.
3. J. D. Michie and M. E. Bronstad. Location, Selection, and Maintenance of Highway Traffic Barriers. NCHRP, Rept. 118, 1971, pp. 48-55.
4. M. E. Bronstad and J. D. Michie. Recommended Procedures for Vehicle Crash Testing of Highway Appurtenances. NCHRP, Rept. 153, 1974.

Properties of Guardrail Posts for Various Soil Types

L. R. Calcote and C. E. Kimball, Southwest Research Institute, San Antonio, Texas

Pendulum tests on two typical guardrail posts installed in five different soil types are discussed. The purpose of the tests was to determine post property variations as a function of soil conditions. Results of the tests were then used for post input properties in the BARRIER VII computer program to estimate the ultimate effect of soil conditions on guardrail performance. It is shown that guardrail installations less than the recommended minimum length of 45.7 m (150 ft) can be expected to fail with the more severe impacts when installed in the poorer soils. For vehicle containment and redirection with barrier lengths of 45.7 m or greater, the end posts should be sufficiently anchored to develop the full strength of the post in the lateral direction, as well as the usual longitudinal anchorages.

In lieu of or in conjunction with expensive, full-scale vehicle tests on impact with highway guardrail systems, analytical simulations are often used. Because of its capability to model the geometric variables of the guardrail installation, an excellent computer algorithm for this purpose is the BARRIER VII program (1). However, it is necessary for inputs to this program that post, railing, and vehicle geometric and inertial properties be specified. The problem is not difficult for railing and vehicle properties but is quite complex for the properties of posts. For example, stiffnesses for elastic horizontal deflections and the deflections to failure must be specified for the posts in both the longitudinal and lateral directions at the railing height. Base moments and shear forces for failure must also be specified for the two directions. The failure mechanism of the post involves high rate impact loading and its effects on both the post material and the supporting soil. Because of these complexities, characterization of the post properties by analytical means is next to impossible to establish.

This paper describes a series of pendulum tests by which guardrail posts are characterized experimentally. Two of the commonly used post types were tested in five different general soil types. The results were then used as inputs for a series of BARRIER VII runs to establish the effects on guardrail performance. It will be shown that care must be exercised in the design of guardrails where soil conditions are of poor quality. This is particularly true for the shorter installations.

EXPERIMENTAL PROGRAM

To determine performance variations of posts as a function of soil conditions, an original pendulum test matrix was to consist of 80 tests as follows:

- Posts
  - W6 × 8.5 steel 1.83 m (6 ft) long with 1.12-m (44-in) embedment
  - 0.15 m × 0.20 m (6 in × 8 in) Douglas fir wood 1.60 m (5.25 ft) long with 0.89-m (35-in) embedment
- Axes
  - Major and minor
- Broad soil classifications
  - Sandy loam
  - Saturated clay
  - Stiff clay
  - Base material
  - Fixed support
- Repeatability
  - 4 tests of each configuration

Since previous tests had been run with a pendulum weight of 1814 kg (4000 lb) and an impact speed of 9.14 m/s (30 ft/s) (2, 3, 4, 5), these conditions were first used. However, unlike the previous tests, no pad was used in the impact area. On completion of the data reduction for the first 16 tests with a base material support, it was found that the rise portion of the force-time curve, which was of interest in determining the constants for BARRIER VII inputs, occurred much too fast (as low as 1 or 2 ms). Thus, the pendulum impact speed was reduced from 9.14 to 6.10 m/s (30 to 20 ft/s), and a 50.8-mm (2-in) plastic pad of Dow Ethafoam 600 was attached in the impact area of the post. This reduced the post inertia-peak effect and produced a rise time of about 15 to 20 ms, which is considered to be more realistic of actual field conditions where railing deformation and take-up of slack occurs in transmitting the impact loads to the posts. The final matrix of conducted tests, including the repeat tests for the base material and those of instrument malfunction, consisted of 102 tests.

Instrumentation for the pendulum tests consisted of a voice track, impact switch, speed trap, and two accelerometer channels recorded on magnetic tape at 1.52 m/s (60 in/s). The tapes were played back on visicorder traces at 0.81 m/s (32 in/s) for preliminary checks of the tests and then used for analog-digital reductions. Data were passed through a class 180 filter before digitizing. A sample rate of 16 000 Hz for four channels was used, and four records of 2048 words/record (0.5 s) were recorded on nine-track tape during the accelerometer calibration portion of the run. Sixteen records (2.0 s) were then taken for the speed trap, impact switch, and accelerometer test data. Data on the nine-track tape were then transmitted to a seven-track tape at the Institute's Hewlett-Packard computer facility.

As a backup program for the data reduction, high-speed photography was attempted. A Locam camera with a film speed of 500 frames/s was first tried without success. After reduction of the pendulum impact speed to 6.10 m/s, a Hycam camera was used at 1000 frames/s. Though every frame was recorded in the data reduction, the results were still not satisfactory. Thus, the analysis attempt was terminated and the Locam camera was used for documentary purposes only. In cases of accelerometer or instrument malfunction, the tests were simply repeated.

The method for determining the BARRIER VII inputs from the pendulum data is illustrated by the dashed line in Figure 1. Note that the inertia peak was ignored since post weights are placed at the railing node in BARRIER VII. At the peak force in the small circle of the figure, the corresponding time, displacement, and force were read from the associated output plots. These values were then used to prepare the pendulum test results shown typically in Table 1 for the wood posts and in Table 2 for the steel posts. Average values of the

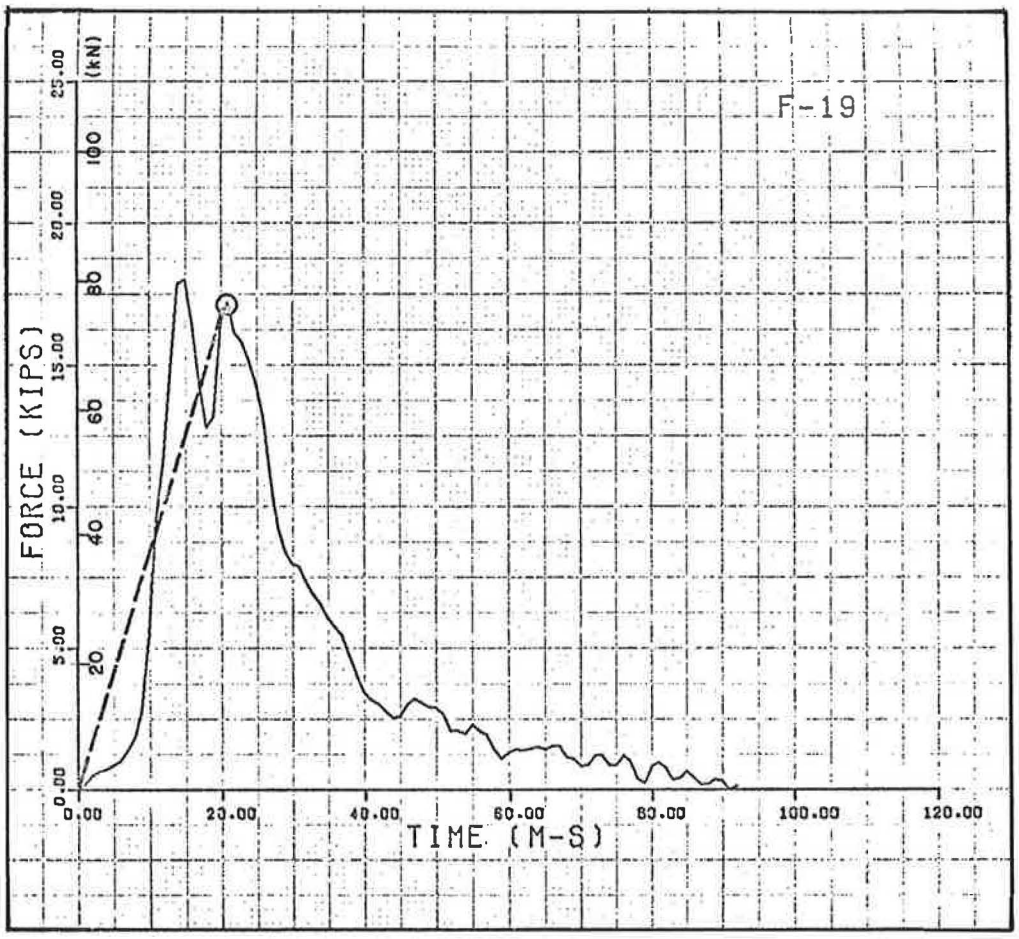

Figure 1. Method for determining BARRIER VII from pendulum data.

Table 1. Typical pendulum test results for 15.2 cm x 20.3 cm Douglas Fir posts (base material support).

Test No.	Maximum Force (kN)	Time (ms)	Distance (cm)	Remarks
Weak-axis tests				
F-83	49.8	22	13.2	Post fracture
F-87	28.9	19	11.5	Post fracture
F-91	35.6	22	13.5	Soil yield
F-96	49.4	16	9.7	Post fracture
Avg	40.9		12.0	k = 3.41 kN/cm
Strong-axis tests				
F-84	52.0	25	14.9	Soil yield
F-88A	28.5	24	14.6	Soil yield
F-92	32.5	19	11.8	Soil yield
F-95	32.0	20	12.1	Soil yield
Avg	36.5		13.4	k = 2.73 kN/cm

Note: 1 kN = 0.22 kip; 1 cm = 0.4 in.

Table 2. Typical pendulum test results for W6 x 8.5 steel posts (fixed support).

Test No.	Maximum Force (kN)	Time (ms)	Distance (cm)	Remarks
Weak-axis tests				
F-20	22.7	20	12.0	Post yield
F-24	23.6	21	12.7	Post yield
F-28	23.6	21	12.8	Post yield
F-31	20.9	21	13.2	Post yield
Avg	22.7		12.6	k = 1.79 kN/cm
Strong-axis tests				
F-19	77.0	21	12.6	Post yield
F-23	73.8	15	9.1	Post yield
F-27	73.4	20	11.9	Post yield
F-32	75.6	15	9.6	Post yield
Avg	74.7		10.8	k = 6.92 kN/cm

Note: 1 kN = 0.22 kip; 1 cm = 0.4 in.

maximum forces and distances were used to determine stiffnesses, and these values were finally used to prepare the BARRIER VII inputs shown in Table 3.

POST AND SOIL EFFECTS ON VEHICLE PERFORMANCE

The post properties from Table 3 were used as inputs for BARRIER VII runs to determine the effects on vehicle performance. As a first trial, the simulations were compared with Test 273 in Stoughton and others (6). This test had a short installation length of only 22.9 m (75 ft). Further, the test was quite severe; it used a 2250-kg (4960-lb) vehicle at a speed of 109.4 km/h (68 mph) and a 25° impact angle. However, the test site soil was extremely stiff, and the posts were driven into smaller predrilled pilot holes. The results of the tests, along with those of the simulations, are shown in Table 4. It can be seen that vehicle redirection is not predicted with the poorer soil types (negative velocity vectors). Using fixed support properties for the end posts does not improve the situation. The lesser severity and greater dynamic deflection with the fixed supports over the test were probably caused by the poorer quality wood used in the pendulum tests. Four static tests of the full-sized posts were conducted, and horizontal shear failures occurred at an average of 3.65-MPa (530-psi) shearing stress, compared with a 7.86-MPa (1140-psi) book value. Four static tests were then conducted on 0.05-m x 0.05-m (2-in x 2-in) specimens milled from the posts. These tests produced flexural failures with an average modulus of rupture of 58.8 MPa (8530 psi) compared with the 80.6-MPa (11 700-psi) book value.

Table 3. BARRIER VII post properties for various soil types.

Input Parameter	Soil and Post Types									
	Fixed Support		Base Material		Stiff Clay		Saturated Clay		Sandy Loam	
	Steel	Wood	Steel	Wood	Steel	Wood	Steel	Wood	Steel	Wood
k_A,[a] kN/cm	1.79	6.23	2.01	3.41	1.07	2.07	1.30	2.45	1.37	2.75
k_B,[a] kN/cm	6.92	7.97	4.31	2.73	2.03	2.49	1.98	2.14	3.40	2.24
M_{PA},[b] kN·m	39.9	38.4	26.1	19.5	14.2	12.3	8.1	8.3	15.7	12.1
M_{PB},[b] kN·m	12.1	28.0	10.9	21.8	8.1	11.6	6.4	8.8	8.3	13.5
F_{PA}, kN	22.7	52.5	20.5	40.9	15.1	21.8	12.0	16.5	15.6	25.4
F_{PB}, kN	74.7	72.1	48.9	36.5	26.7	23.1	15.1	15.6	29.4	22.7
δ_A, cm	12.6	8.4	10.1	12.0	14.1	10.6	9.3	6.7	11.4	9.2
δ_B, cm	10.8	9.0	11.4	13.4	13.1	9.3	7.6	7.3	8.6	10.1

Notes: 1 kN/cm = 0.56 kip/in; 1 kN·m = 8.84 in-kips; 1 kN = 0.22 kip; and 1 cm = 0.4 in. Customary units were required for program inputs.

[a] A = major axis; B = minor axis. [b] Moments based on height to center of railing = 0.53 m (21 in).

Table 4. Comparison of soil supports for 15.2 cm x 20.3 cm Douglas Fir posts.

Test or Simulation	50-ms Vehicle Acceleration (g)		Maximum Dynamic Deflection (m)	Exit Condition		Barrier Damage		Remarks
	Longitudinal	Lateral		Velocity Vector (°)	Vehicle Heading Angle (°)	Beam (m)	No. of Posts Damaged	
Test	6.75	6.95	1.13	-	-	11.4	3	Reported exit angle = 14°
Fixed supports	4.27	5.01	1.46	8.9	9.9	11.4	7	
Stiff clay support	2.31	2.32	2.38 at 0.30 s	-17.0	-8.5	-	10	Lateral failure of upstream anchor post
Sandy loam support	2.32	2.42	2.44 at 0.30 s	-17.1	-8.4	-	10	Lateral failure of upstream anchor post
Stiff clay with fixed end posts	2.31	3.40	5.53 at 0.65 s	-6.8	24.4	-	12	Lateral failure of downstream anchor post
Sandy loam with fixed end posts	2.32	3.18	5.24 at 0.62 s	-7.2	23.5	-	12	Lateral failure of downstream anchor post
Base material support	2.92	4.27	3.19 at 0.55 s	-2.0	13.3	-	12	Lateral failure of downstream anchor post
Saturated clay with fixed end posts	1.96	2.48	5.80 at 0.59 s	-10.0	19.2	-	12	Lateral failure of downstream anchor post

Note: 1 m = 3.3 ft.

Table 5. Comparison of soil supports for W6 x 8.5 steel posts.

Test or Simulation	50-ms Vehicle Acceleration (g)		Maximum Dynamic Deflection (m)	Exit Condition		Barrier Damage		Remarks
	Longitudinal	Lateral		Velocity Vector (°)	Vehicle Heading Angle (°)	Beam (m)	No. of Posts Damaged	
Test	4.0	6.7	1.23	-	-	7.6	5	Reported exit angle = 8°
Fixed supports	5.25	6.03	1.36	14.2	16.5	11.4	6	
Stiff clay support	3.41	2.87	6.76 at 0.80 s	-4.5	34.9	-	11	Lateral failure of downstream anchor post
Sandy loam support	3.61	3.02	6.36 at 0.79 s	-3.7	31.7	-	11	Lateral failure of downstream anchor post
Stiff clay with fixed end posts	3.41	6.32	2.11 at 0.44 s	8.3	5.6	-	13	No change—numerical instability at 0.57 s
Sandy loam with fixed end posts	3.61	6.32	2.19 at 0.45 s	7.9	5.3	-	13	No change—numerical instability at 0.56 s
Base material support	4.54	5.12	1.35	15.9	7.0	11.4	7	
Saturated clay with fixed end posts	3.04	5.60	6.12 at 0.80 s	5.3	46.7	-	18	Lateral failure of downstream anchor post

Note: 1 m = 3.3 ft.

Thus, the posts used in the pendulum tests were not of the best quality. Nonetheless, the results in Table 4 clearly indicate that such short installations can be expected to fail under severe impacts unless the posts are of good quality and are sufficiently anchored in the soil to cause the post strength to control the failure mechanism.

Table 5 shows the results for Test 120 from Michie and others (7). The test installation was longer at 34.3 m (112.5 ft) and had a less severe impact—a 1730-kg (3813-lb) vehicle at a speed of 91.4 km/h (56.8 mph) at a 28.4° impact angle. However, the impact point was so far down the guardrail that only the last two posts show unnoticeable permanent deformation in the test photographs. The table shows that again, with the poor clay and sand support, the vehicle is not predicted to redirect. However, by using the fixed support properties for the end posts, redirection is achieved before the lateral failures of the downstream anchor posts occur. Thus, if an installation of this length were to be constructed in poorer soils, a concrete footing should be used on the end posts so that the post strength will control the lateral failure.

A guardrail length of 45.7 m (150 ft) was finally used for a 2041-kg (4500-lb) vehicle at a speed of 96.5 km/h (60 mph) at a 25° impact angle to correspond with the accepted containment standard of Bronstad and Michie (8). The results are shown in Table 6. Note that fixed lateral post properties were again used on the three poorer soils. Vehicles were redirected in all cases (positive velocity vectors) but were not turned completely around with the three poor soils (negative heading angles).

Table 6. Post and soil effects on vehicle performance.

Condition	50-ms Vehicle Acceleration (g)		Maximum Dynamic Deflection (m)	Exit Condition		Barrier Damage	
	Longitudinal	Lateral		Velocity Vector (°)	Vehicle Heading Angle (°)	Beam (m)	No. of Posts Damaged
Douglas fir posts							
Fixed supports	4.32	5.95	1.37	13.8	10.8	11.4	6
Base material support	2.70	3.43	2.15	10.1	0.6	19.1	12
Stiff clay support[a]	1.97	2.82	2.91	2.2	-5.8	19.1	20
Saturated clay support[a]	1.81	2.39	3.08	8.0	-9.0	19.1	23
Sandy loam support[a]	2.06	2.95	2.66	2.5	-6.4	19.1	20
Steel posts							
Fixed supports	4.84	5.68	1.73	14.1	8.8	15.2	8
Base material support	3.29	4.33	1.91	11.7	0.5	19.1	9
Stiff clay support[a]	2.45	3.19	2.45	6.5	-1.5	19.1	15
Saturated clay support[a]	1.91	2.46	3.09	9.5	-7.5	19.1	23
Sandy loam support[a]	2.57	3.28	2.40	6.1	-1.6	19.1	15

Note: 1 m = 3.3 ft.

[a]Fixed support properties used for end posts.

CONCLUSIONS

Satisfactory full-scale vehicle guardrail or median barrier tests on installations of less than 45.7 m (150 ft) are usually achieved with exceptionally good post and soil conditions. The results discussed here, as established by BARRIER VII simulations with post properties determined by a series of pendulum tests, indicate that barrier failure problems can be expected for severe impacts on short installations with the poorer soil types. Thus, it is recommended that guardrail lengths be not less than 45.7 m unless precautions are taken to ensure the integrity of each post, particularly if the available space behind the barrier is limited. This can be accomplished by the use of concrete footings or greater embedment depths for the posts. For vehicle containment and redirection with barrier lengths of 45.7 m or greater, the end posts should be sufficiently anchored to develop the full strength of the post in the lateral direction, as well as the usual longitudinal anchorages.

ACKNOWLEDGMENTS

The work described here was conducted by the Division of Structural Research and Ocean Engineering, Southwest Research Institute (SwRI), San Antonio, Texas, for the Federal Highway Administration (FHWA). The opinions, findings, and conclusions expressed are ours and not necessarily those of the sponsor. For FHWA technical support of the program, special appreciation is expressed to Michael J. McDanold. SwRI personnel who made significant contributions to the program's development include R. E. Kirksey, G. W. Deel, and Jane E. Baker.

REFERENCES

1. G. H. Powell. BARRIER VII: A Computer Program for Evaluation of Automobile Barrier Systems. Federal Highway Administration, Rept. FHWA-RD-73-51, April 1973.
2. J. D. Michie. Response of Guardrail Posts During Impact. Southwest Research Institute, San Antonio, TX, Final Rept., Oct. 1970.
3. J. D. Michie and M. E. Bronstad. Impact Tests of Steel Barrier Posts Embedded in Soil. Southwest Research Institute, San Antonio, TX; United States Steel Corp., Final Rept., Sept. 1971.
4. M. E. Bronstad and G. K. Wolfe. Impact Tests of Formed Steel Barrier Posts. Southwest Research Institute, San Antonio, TX; Syro Steel Co., Final Rept., March 1974.
5. J. D. Michie and M. E. Bronstad. Dynamic Properties of Timber Guardrail Posts. Southwest Research Institute, San Antonio, TX, Technical Rept., Oct. 1970.
6. R. L. Stoughton, J. R. Stoker, and E. F. Nordlin. Dynamic Tests of Metal Beam Guardrail. TRB, Transportation Research Record 566, 1976, pp. 44-55.
7. J. D. Michie, L. R. Calcote, and M. E. Bronstad. Guardrail Performance and Design [NCHRP Project 15-1(2)]. Southwest Research Institute, San Antonio, TX, Jan. 1970.
8. M. E. Bronstad and J. D. Michie. Recommended Procedures for Vehicle Crash Testing of Highway Appurtenances. NCHRP, Rept. 153, 1974.

Abridgment

Development and Testing of a Breakaway Support Coupling for Light Poles

Arthur M. Dinitz, Transpo-Safety, Incorporated, New Rochelle, New York
Douglas B. Chisholm, Federal Highway Administration

Each year numerous injuries and fatalities occur as a result of vehicles hitting light poles adjacent to U.S. highways. Until recently the widely used transformer base has been considered "breakaway". The 1975 AASHTO Standard Specifications for Structural Supports for Highway Signs, Luminaires and Traffic Signals has tightened design standards by calling for an improvement in the performance of the breakaway feature. Satisfactory dynamic performance is indicated when the maximum change in momentum for a standard 1020-kg (2250-lb) vehicle, or its equivalent—striking a breakaway support at speeds from 32 to 97 km/h (20 to 60 mph)—does not exceed 4895 nt·s (1100 lb·s). A "preferable" maximum change of momentum of 3337 nt·s (750 lb·s) is also stated in the above specifications as a goal for the future.

POLE-SAFE BREAKAWAY SUPPORT COUPLING

The Pole-Safe breakaway support coupling (longitudinally grooved) is a frangible coupling designed for use on light poles so that they will break away under impact within these criteria. The coupling (Figure 1) is made from die-cast aluminum, roughly cylindrical in shape with a 2.54-cm (1-in) 8UNC threaded hole at one end and a 2.54-cm (1-in) 8UNC 304 stainless steel stud protruding from the other end. The coupling thus provides a breakaway spacer between an existing light pole and its foundation. It fits over the anchor bolt, and the stud protrudes through the pole base plate.

Technical features of this support coupling include the following:

1. It eliminates fatigue problems in tension and bending loads that would be present with circumferentially notched couplings, shear pins, notched bolts, and so forth.
2. Longitudinal notches provide high stress concentration for rapid fracture at relatively low impact force levels.
3. Ratio of service-load capacity to failure load is higher than existing designs due to unique geometry. Ratios up to 6:1 are possible.
4. Highest possible control of fracture mode ensures repeat impact performance for any design impact load.

The Pole-Safe breakaway coupling provides both a high tensile load capacity and a low breakaway force requirement (Figure 2). Under a tensile load, the longitudinal grooves do not become stress-risers since the stress field is parallel to the groove root. Under the loading induced by an impacting vehicle as shown in the previous force and moment diagram, the loads are perpendicular to the grooves. This efficiently concentrates the stresses at the groove root.

A 1020-kg (2250-lb) Vega impacting a 15-m (50-ft), 308-kg (680-lb) luminaire support at 32 km/h (20 mph) equipped with four Pole-Safe couplings experienced a peak deceleration of 8.0 *g* or 80 100 nt (18 000 lb). Since each coupling requires about 20 025 nt (4500 lb), i.e., $4 \times 20\,025 = 80\,100$ nt ($4 \times 4500 = 18\,000$ lb), it appears that there is a direct relationship between the peak fracture force of each coupling and the resultant vehicle deceleration. Every effort has been made to keep impact fracture loads low while maintaining the highest possible tensile load capacity.

Developmental Program

The new nature of the technology involved in the longitudinally grooved breakaway support coupling required an extensive developmental program:

1. To determine the physical changes to the coupling that would have an effect on the desired results;
2. To expand, clarify, and prove the theory by changing all of the variables to determine their effect on the system;
3. To determine the parameters of the variables for the optimization of the system; and
4. To apply this optimization to develop a breakaway support coupling for 2.54-cm (1-in) anchor bolts as well as other sizes as needed.

It was also noted that physical changes affecting desired results included coupling size, notch depth, notch sharpness, length and other characteristics of starter notch, type and surface finish of threaded stud, and imbedment of threaded stud.

Testing Procedure and Results

Many tests have been conducted on various prototypes manufactured during the development phases for the Pole-Safe coupling. The results presented in this report are those of the production batch from which couplings were used for the vehicle crash test. The following tests were conducted:

1. Bench-type load tests—axial pull load and shear load,
2. Corrosion tests followed by axial fatigue tests, and
3. Full-scale crash tests.

Bench-Type Load Tests

Numerous axial load tests have been conducted on a Tinius Olsen tensile testing machine located at Transpo-Safety's plant. The table below gives the results of the axial load tests done on the crash test

Figure 1. Pole-Safe breakaway support coupling.

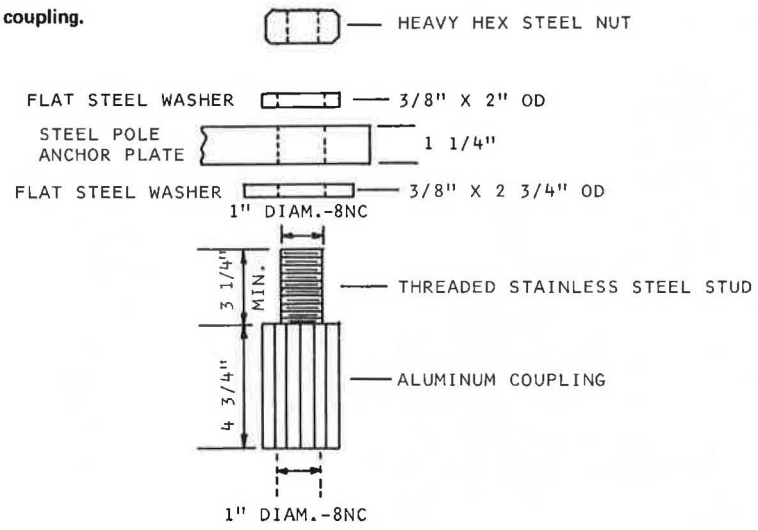

Figure 2. Diagram shows coupling's high tensile load capacity and low breakaway force requirement.

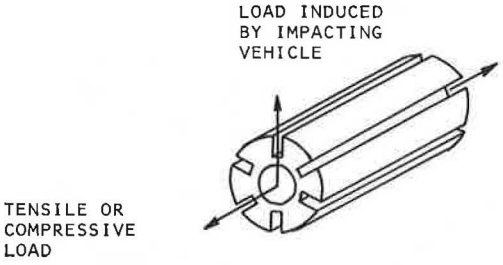

production lot [1 kg = 2.2 lb. Axial load—average, 27 420 lb; maximum, 30 650 lb; minimum, 26 000 lb].

Test Piece	Axial Load (lb)
CT 7-11-1	30 650
CT 7-11-2	26 000
CT 7-11-3	26 100
CT 7-12-3	26 900
CT 7-12-4	27 450

A jig for the shear load test was specially designed to fit into a Tinius Olsen tensile testing machine. The jig is two L-shaped structures positioned opposite each other with the couplings holding them together. The two structures are pulled apart laterally to simulate an impact shear load.

The shear load tests have been conducted on the same Tinius Olsen tensile testing machine as the axial load tests. The results of the shear load tests done on the crash test production lot appear in the following table [1 kg = 2.2 lb. Shear load—average, 4760 lb/coupling; maximum, 6300 lb/coupling; minimum, 3900 lb/coupling.]:

Test Piece	Shear Load (lb/coupling)
CT 7-11-4	6300
CT 7-11-5	3900
CT 7-11-6	5300
CT 7-12-1	3900
CT 7-12-2	4400

Corrosion Testing

Two couplings from the crash test production lot were subjected to a salt spray test for 336 hours at the Pittsburgh Testing Laboratory, Pittsburgh, Pennsylvania, in accordance with ASTM B117, which is basically exposure to 5 percent salt fog at 35°C (95°F).

The results showed a very slight pitting on the threaded stainless steel stud. However, no evidence of pitting or corrosion was noted anywhere on the aluminum coupling including the inside threaded area.

Fatigue Testing

The fatigue testing consisted of applying an oscillating force in tension along the axis of the threaded stud provided in the Pole-Safe coupling. The tensile load fluctuated between 227 kg (500 lb) and 4536 kg (10 000 lb) at a rate of 1800 cycles/min. Again, these test criteria are directly comparable to the Alco tests.

The first two tests were done on production lots manufactured in late May 1977. The results were no failures in 1 000 000 cycles applied in both sample 1 and sample 2.

The second two tests were done on one of the samples from the corrosion tests and one from the crash test production lot. The results were sample 1 from crash test production lot, 1.003×10^6 cycles applied, no failure; and sample 2 from crash test production lot, 1.003×10^6 cycles applied, no failure.

Vehicle Crash Testing

A full-scale vehicle crash test was conducted at the Texas Transportation Institute, College Station, Texas, on July 20, 1977, in basic conformance with NCHRP Report 153 and AASHTO specifications (Figures 3, 4, 5, 6). The test data and results were as follows:

1. Couplings: 4 production lot Pole-Safe couplings —2.54 cm (1-in) in diameter;
2. Pole: a steel 15-m (50-ft) mounting height pole with a 228-cm (7.5-ft) mast arm and a 34-kg (75-lb) weight simulating luminaire, total weight = 306 kg (676.8 lb);
3. Footing: reinforced concrete 76.2 cm dia.× 198 cm deep (30 in dia.× 78 in deep) with 34.2-cm (13.5-in) bolt circle with four 2.54-cm (1-in) anchor bolts extending 6.98 cm (2.75 in) above concrete footing;
4. Vehicle: Chevrolet Vega weighing 1020 kg (2290 lb);
5. Accelerometer data: approximate impact velocity, 33.1 km/h (20.6 mph);

Figure 3. Footing and base of Pole-Safe coupling in place for production lot test.

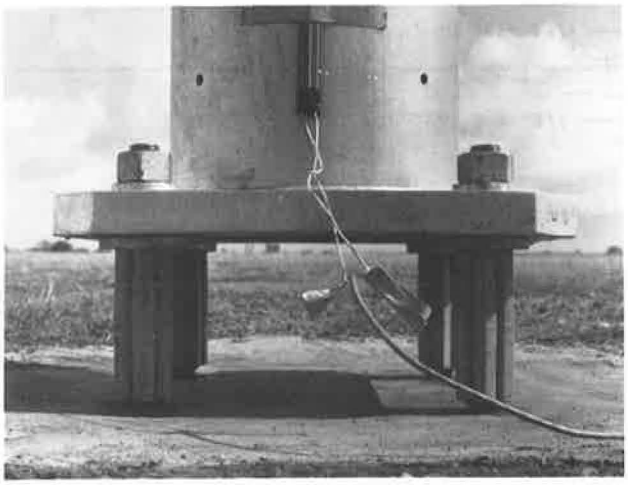

Figure 4. Pole-Safe coupling breaks away on vehicle impact.

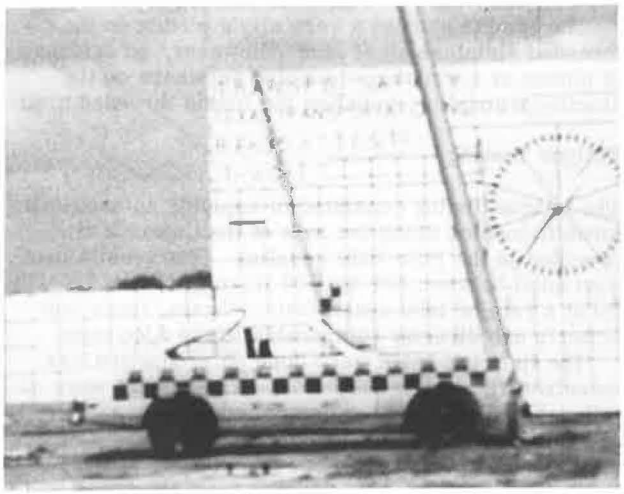

6. Peak deceleration: 8 g;
7. Average deceleration: 0.74 g; and
8. Change in momentum: 2403 nt·s (540 lb·s).

Pendulum Impact Testing

Three pendulum impact tests were conducted by Ensco, Incorpated, Springfield, Virginia, utilizing Pole-Safe 101 2.54-cm dia. (1-in dia.) couplings from the crash test production lot. In all of these tests, the 1020-kg (2250-lb) soft-nosed pendulum impacted the support at a height of 45.7 cm (18 in) and at a speed of approximately 32 km/h (20 mph).

Test 1 (604) utilized the couplings under a Hapco spun aluminum 15-m (50-ft) mounting height pole. Change of momentum produced was 2363 nt·s (531 lb·s).

Test 2 (605) had the Pole-Safe couplings mounted under a New York City aluminum transformer base. The momentum change was 3685 nt·s (828 lb·s).

Test 3 (606) has the Pole-Safe couplings mounted under a Pfaff and Kendall TB-2A cast aluminum transformer base. The change of momentum resulting was 2968 nt·s (667 lb·s). No damage to the pole or the anchor bolts occurred in any of these tests.

Figure 5. Coupling after breakaway.

Figure 6. Closeup of coupling after breakaway.

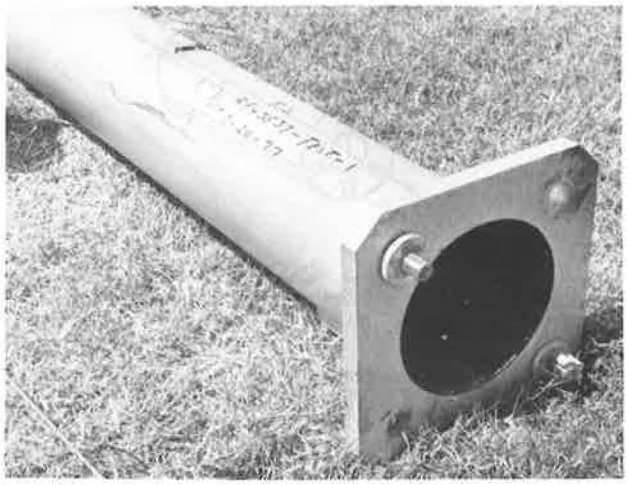

CONCLUSIONS

1. The Pole-Safe couplings meet the latest AASHTO and federal criteria for use as a breakaway light pole support system.
2. Since light poles and mast arms were not damaged in vehicle and pendulum crash tests, it is reasonable to believe that most poles installed with these couplings will be reusable after impact.
3. Since the anchor bolts in the vehicle and pendulum crash tests were not bent or damaged with the Pole-Safe couplings, it can be expected that highway use experience will be similar.

ACKNOWLEDGMENT

We wish to thank Gordon Samuelson of the Texas Transportation Institute and Jeffrey Bloom of Ensco, Incorporated, for their contributions to this report.

Notice: The Transportation Research Board does not endorse products or manufacturers. Trade and manufacturer's names appear in this report because they are considered essential to its object.

Dynamic Testing of Malleable Aluminum Transformer Bases for Highway Luminaires

John E. Haviland, New York State Department of Transportation
David J. Segal, Calspan Corporation, Buffalo, New York

The purpose of the reported test program was to develop modifications to existing malleable aluminum transformer bases for highway luminaires that could be performed in the field with minimal equipment and labor expenditure. The evaluation consisted of two phases; first, determining whether the modifications resulted in acceptable breakaway performance as indicated by the momentum change of the impacting vehicle, and, second, determining whether the modifications could result in a serious degradation of expected service life as indicated by results of a limited accelerated fatigue study. The dynamic tests were conducted in accordance with NCHRP Report 153 and used a 1020-kg (2250-lb) car impacting at 9 and 18 m/s (20 and 40 mph). Fatigue tests consisted of vibrating a horizontally mounted base and pole shaft at the resonant frequency of the pole until failure occurred. The tests indicated that a base saw cut, made horizontally to leave 76.2 mm by 4.76 mm (3 x $^3/_{16}$-in) thick metal on each side, would induce approximately 362 kg·s (800 lb·s) momentum transfer and 6 *g* 50 millisecond maximum average deceleration in the test vehicle. Terminating the saw cut in 38-mm (1½-in) diameter holes proved sufficient to induce fatigue failure in the unmodified pole instead of the base.

The highway appurtenances tested during the reported program were fabricated aluminum transformer bases and mercury luminaire aluminum lamp posts of the New York City type 8S. During the 1960s the transformer bases were fabricated by various manufacturers to New York City drawings J-3739 and J-3793. The bases were 457 mm (18 in) square at the bottom, 330 mm (13 in) square at the top, 660 mm (26 in) high, and were fabricated with a 3003-H14 aluminum skirt welded to 356T6 bolt rings top and bottom. The skirt was 4.76 mm ($^3/_{16}$ in) thick.

Three basic configurations, and derivations thereof, were tested. An unmodified transformer base provided a baseline with which to compare both impact and fatigue testing. The two modified configurations were produced by making horizontal saw cuts near the bottom of the bases. One configuration involved leaving uncut material on each flat side; the other, uncut material on each corner.

For the impact tests, the bases were mounted to a 25.4-mm (1-in) thick steel plate, drilled and tapped to accept four 25.4-mm (1-in) hex-head cap screws. The cap screws secured the transformer base to the mounting plate by means of cast aluminum washers and were tightened to 271 N·m (200 lb·ft) of torque. The steel plate was, in turn, mounted to the concrete test track with ten concrete anchors and bolts. The bases and poles were mounted in such a way that the luminaire arm was at a right angle to the center line of the test track, and the access door on the transformer base was on the opposite side of the point of impact.

Photographs of a typical installation are shown in Figure 1.

TEST CONDITIONS

Full-Scale Impact Tests

Five full-scale impact tests were conducted on the unmodified and modified aluminum transformer bases. All tests were conducted with small (compact or subcompact) vehicles with a nominal test weight of 1020 kg (2250 lb). The test conditions are summarized in Table 1.

The vehicles were prepared for testing by removing nonessential components (e.g., seats, gas tank) or by adding ballast to obtain a test weight of 1020 kg (2250 lb) ± 9 kg (20 lb). Instrumentation installed in the vehicles consisted of two triaxial accelerometer packages, one located on the drive shaft tunnel at the longitudinal center of gravity position and the other on the rear deck along the vehicle longitudinal center line. In addition to the acceleration transducers, signal conditioning and amplification equipment were installed in the vehicle trunk area. [See the complete report, Appendix A, for detailed descriptions of the data acquisition and reduction systems.]

Lateral guidance of the test vehicle was provided by the test track guide rail and a pair of large-diameter flanged aluminum wheels arranged so as to restrict vertical and lateral motion of the vehicle. It was noted in the first two tests (with the Pinto and a Vega) that the required mounting location of these guide wheels on the available vehicle substructure resulted in contact between the wheels and the transformer base. Consequently, a guide slipper that could be mounted further aft on the vehicle understructure and therefore avoid contamination for the test results was fabricated for the third and fifth tests. The guide wheels were used on the Maverick in the fourth test since they could be mounted sufficiently aft to avoid contact with the base. The tow cable was connected to the vehicles by means of a quick-release cable clamp. This clamp was located 229 mm (9 in) to the left of the vehicle center line so as to avoid cable rub on the transformer base.

Speed measurements were made at three locations for each test. The first location was the abort window station located at a distance ahead of the impact point as determined by the test speed. The vehicle speed at this location was automatically compared to preprogrammed limits and, if outside these limits, the test was aborted and the vehicle was stopped prior to impact. The second location determined vehicle speed at impact; the last location measured the vehicle speed at a predetermined distance after impact to obtain velocity (and therefore momentum) change.

Photographic documentation of the tests included 102 × 127-mm (4 × 5-in) black-and-white still photographs, standard-speed documentary motion pictures, and high-speed motion pictures. High-speed camera frame rates for each of the five tests are given in Table 2.

Fatigue Tests

In conjunction with the full-scale impact test program, accelerated fatigue tests were conducted on six base and pole assemblies in order to evaluate the extent of fatigue life degradation resulting from the base modifications. Tests were conducted on horizontally mounted trans-

Figure 1. Typical installation of pole and base for impact testing.

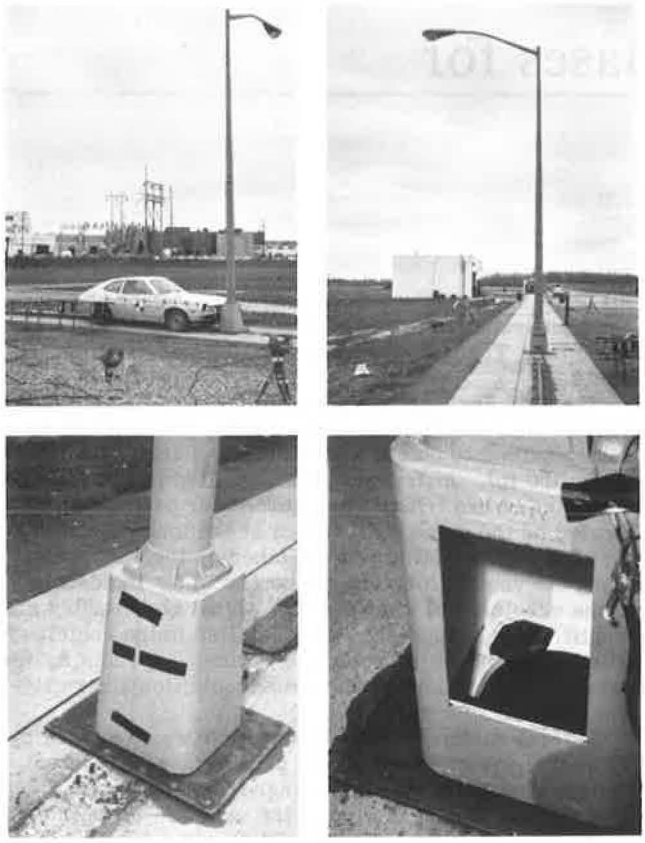

Table 1. Summary of full-scale impact test conditions.

Test No.	Target Impact Speed (m/s)	Vehicle	Vehicle Weight (kg)	Transformer Base Configuration
1	9	1971 Pinto	1020	Unmodified
2	9	1971 Vega	1020	Cut with 102 mm of wall material remaining
3	9	1971 Vega	1010	Cut with 76 mm of wall material remaining
4	18	1971 Maverick	1030	Cut with 76 mm of wall material remaining
5	9	1973 Vega	1020	Cut with 76 mm of wall remaining around base corners

Note: 1 m/s = 2.24 mph, 1 kg = 2.2 lb, 1 mm = 0.04 in.

former bases and pole assemblies with sinusoidal excitation provided by a rotating eccentric mass located at the approximate midpoint of the pole. Rotational speed of the eccentric mass was varied to excite the pole at its second natural frequency by means of a variable-speed electric motor. The mass weighed 1.18 kg (2.59 lb) and its eccentricity was 63.5 mm (2.49 in). The total weight of the vibratory assembly was 17.8 kg (39.3 lb).

The number of cycles to failure was determined by timing the duration of the test with a stop watch and measuring the vibration frequency with a General Radio Company Strobotac Type 1531-A. Although this method lacks a high degree of precision, it was deemed sufficiently accurate for comparative purposes.

It should be noted that only one sample of each configuration was tested using this procedure. Therefore, the possibility exists that these results would not be typical of the mean performance if a number of samples had been subjected to fatigue testing.

TEST RESULTS

Full-Scale Impact Tests

The first impact test was conducted on April 23, 1976, using a 1971 Ford Pinto to impact an unmodified transformer base and lamp post assembly. The car weight was 1020 kg (2250 lb), and the impact speed was 9 m/s (20.01 mph). Test data are summarized for this and all other impact tests in Table 3.

In this test, the unmodified transformer base did not break away during the impact. The maximum x component deceleration (positive forward) recorded at the tunnel was 32.8 g, and, at the rear deck, 23.75 g with an average of 28.3 g. The maximum average deceleration over a 50-ms time period was 16.8 g occurring between 55 and 105 ms at the rear deck location. Vehicle speed changes resulting from integration of the tunnel x acceleration and rear deck x acceleration were 11 and 10.6 m/s (24.5 and 23.75 mph) respectively. Analysis of the high-speed film coverage resulted in a speed change of 10.2 m/s (22.8 mph). The corresponding momentum changes were 1145, 1105, and 1060 kg·s (2513, 2436, and 2339 lb·s) respectively. Vehicle damage consisted of 495 mm (19.5 in) of frontal crush with a vehicle damage identification or impact code(VDI) of 12-FCEN-2. Damage to the transformer base consisted of a dented forward (struck) face and a cracked weld at the joint between the forward face and bottom.

In the second impact test, a 1971 Chevrolet Vega was used to impact a modified transformer base and lamp post assembly. The base was modified by saw cuts located 51 mm (2 in) above the bottom of the assembly and extending around each corner so that 102 mm (4 in) of panel material were left uncut on each of the four sides. The weight of the test vehicle was 1020 kg (2250 lb) and the impact speed was 9 m/s (19.96 mph). (See Table 3.)

The impact precipitated a breakaway of the transformer base resulting from an apparent combination shear and tensile failure of the uncut portion of the struck transformer base panel, a shear failure of the left panel, and tensile failure of the welds securing the right and rear panels to the base plate.

The peak x decelerations recorded at the tunnel and rear deck locations on-board the vehicle were 23.25 g and 20 g respectively, and the maximum average deceleration over 50 ms was 7.87 g occurring between 40 and 90 ms at the rear deck location. Vehicle speed changes resulting from integration of the tunnel and rear deck accelerations were 4.9 m/s (10.8 and 10.72 mph respectively). Analysis of high-speed film coverage indicated a speed change of 5.0 m/s (11 mph); speed trap measurement indicated a change of 4.6 m/s (10.2 mph) at a location 1.52 m (5 ft) beyond impact. The computed changes in momentum for these speed changes are 492, 487, 500, and 464 kg·s (1108, 1100, 1128, and 1046 lb·s) respectively. Damage to the vehicle consisted of frontal crush of 343 mm (13.5 in) with a VDI of 12-FCEN-2.

The third impact test was conducted on May 12, 1976, using a 1971 Chevrolet Vega weighing 1010 kg (2230 lb). The transformer base used in this test was modified with saw cuts located 51 mm (2 in) above the bottom of the assembly and extending around each corner so that 76 mm (3 in) of panel material were left uncut on each of the four sides. The vehicle impact speed was 9 m/s (19.78 mph). (See Table 3.) As a result of the impact, the transformer base broke away through failure of the 76 mm (3 in) of panel material remaining on the front and two sides and of the weld at the rear of the assembly.

The peak x decelerations recorded at the tunnel and rear deck locations on board the vehicle were 20 g and

14.5 *g* respectively, and the maximum average deceleration over 50 ms was 6.2 *g* occurring between 10 and 60 ms at the tunnel location. Vehicle speed changes resulting from integration of the tunnel and rear deck x accelerations were 3.4 and 3.50 m/s (7.6 and 7.8 mph) respectively. Analysis of high-speed film coverage indicated a speed change of 3.4 m/s (7.58 mph), and speed trap measurement indicated a change of 3.4 m/s (7.74 mph) at a location 1.52 m (5 ft) beyond impact. The computed changes in momentum for these speed changes are 350, 360, 350, and 357 kg·s (771, 793, 771, and 787 lb·s) respectively.

The front of the vehicle was crushed 381 mm (15 in), and the VDI for this test was 12-FCEN-2. Rotation of the pole after impact also resulted in contact with the vehicle roof on the driver's side and a cracked windshield.

The fourth impact test was conducted on June 10, 1976, using a 1970 Ford Maverick weighing 1030 kg (2270 lb). The transformer base used in this test was modified with saw cuts located 51 mm (2 in) above the bottom of the assembly and extending around each corner so that 76 mm (3 in) of panel material were left uncut on each of the four sides. The vehicle impact speed was 18 m/s (40.91 mph). (See Table 3.)

As a result of the impact, the transformer base broke away through failure of the 76 mm (3 in) of panel material remaining on the front and two sides and of the weld at the rear of the assembly.

The peak x decelerations recorded at the tunnel and rear deck locations on board the vehicle were 22.5 *g* and 17 *g* respectively, and the maximum average deceleration over 50 ms was 6 *g* occurring between 10 and 60 ms at the rear deck location. Vehicle speed changes resulting from integration of the tunnel and rear deck x accelerations were 3.22 and 3.33 m/s (7.2 and 7.44 mph) respectively. Analysis of high-speed film coverage indicated a speed change of 3.69 m/s (8.26 mph). The computed changes in momentum for these speed changes are 338, 349, and 388 kg·s (745, 770, and 855 lb·s).

An apparent malfunction in the speed trap measurement system, used to determine postimpact speed, resulted in an erroneous value of 6.7 m/s (14.94 mph).

Table 2. High-speed camera frame rates per second.

Camera Location	Test Number 1	2	3	4	5
South, wide	978	950	1001	925	880
South, medium	NA	NA	952	895	1100
East	1059	979	960	1034	860
Southeast, close	2820	2900	3480	2560	1100
Northeast, close	NTL	NTL	NTL	NTL	1300

Note: NA = not applicable, NTL = no timing light.

Therefore, no momentum transfer value is given in Table 3 for test 4.

The vehicle crush measured was 394 mm (15.5 in) and the VDI for this impact was 12-FCEN-2. Pole kinematics after impact resulted in contact with the vehicle roof causing a dent of about 76-102 mm (3-4 in) in depth.

The fifth impact test was conducted on September 8, 1976, using a 1973 Chevrolet Vega weighing 1020 kg (2260 lb). The transformer base used in this test was modified with saw cuts on each of the four sides 95 mm ($3\frac{3}{4}$ in) above the bottom of the assembly. The cuts were terminated with 25-mm (1-in) diameter stress relief holes so that 76 mm (3 in) of uncut material remained at each of the four corners. The vehicle speed at impact was 9 m/s (20.16 mph). (See Table 3.) As a result of the impact, the transformer base broke away through failure of the material remaining at the corners.

The peak decelerations recorded at the tunnel and rear deck locations on board the vehicle were 16 and 13.5 *g* respectively, and the maximum average deceleration over 50 ms was 5.86 *g* occurring between 20 and 70 ms at the tunnel location. Vehicle speed changes resulting from integration of the tunnel and rear deck x acceleration components were 4.3 and 4.0 m/s (9.68 and 8.96 mph) respectively. Analysis of high-speed film coverage indicated a speed change of 4.1 m/s (9.28 mph). Speed trap measurements at impact and 2.44 m (8 ft) after impact resulted in a speed change of 4.8 m/s (10.85 mph).

Examination of the computerized data for this test disclosed that the 50-ms maximum average deceleration, speed change, and the momentum transfer values were not consistent with data from tests 2, 3, and 4 in that momentum transfer appeared about 91 kg·s (200 lb·s) high, and speed change appeared 0.9-1.3 m/s (2-3 mph) high as shown below for the tunnel "X" accelerometer (1 m/s = 2.24 mph, 1 kg = 2.2 lb, and 1 mm = 0.04 in).

Item	Test Number 2	3	4	5
Maximum 50-ms avg deceleration, *g*	7.9	7.6	6.0	5.9
Speed change, m/s	4.8	3.5	3.2	4.3
Speed change time, m/s	75	70	50	100
Tunnel momentum change, kg·s	504	351	338	452
Metal remaining, mm	102	76	76	76
Test speed, m/s	9	9	18	9

Review of the high-speed photography disclosed that the left front wheel rose several centimeters off the ground shortly after impact. Inspection of the lower portion of the transformer base disclosed that there were two secondary impacts that were caused by the towing attachment and the guide slipper used to maintain lateral placement. As shown here, a comparison of the velocity change plots indicated that test 5 extended at least 20 ms

Table 3. Summary of test results.

Test No.	Maximum 50-ms Avg Deceleration (*g*)	Peak Deceleration (*g*)	Speed Trap Measurement: Speed Change (m/s)	Speed Trap Measurement: Momentum Change (kg·s)	Integration of Tunnel Acceleration: Speed Change (m/s)	Integration of Tunnel Acceleration: Momentum Change (kg·s)	Integration of Rear-Deck Acceleration: Speed Change (m/s)	Integration of Rear-Deck Acceleration: Momentum Change (kg·s)	High-Speed Film Analysis: Speed Change (m/s)	High-Speed Film Analysis: Momentum Change (kg·s)	Vehicle Damage: VDI	Vehicle Damage: Permanent Deformation (mm)
1	16.8	32.8	NM	NM	10.9	1145	10.6	1105	10.2	1060	12-FCEN-2	495
2	7.9	23.25	4.6	485	4.8	504	4.8	499	4.8	499	12-FCEN-2	343
3	6.2	20.0	3.45	358	3.50	351	3.48	360	3.48	350	12-FCEN-2	381
4	6.0	22.5	-	-	3.2	338	3.3	349	3.7	388	12-FCEN-2	394
5	5.86	16	4.8	506	4.3	457	4.0	418	4.1	457	12-FCEN-2	343

Notes: 1 m/s = 2.24 mph, 1 kg = 2.2 lb, 1 mm = 0.04 in.
NM = not measured for this test.

Table 4. Summary of accelerated fatigue test data.

Test No.	Base Configuration	No. of Cycles to Failure
1	Unmodified	15 060
2	Saw cut 45 mm up from bottom with 76 mm of material remaining uncut on each side; saw cuts terminated with 6-mm stress relief holes	930
3	Saw cut 91 mm up from bottom with 76 mm of material remaining uncut around each corner; saw cuts terminated with 13-mm stress relief holes	1 350
4	Saw cut 95 mm up from bottom with 76 mm of material remaining uncut around each corner; saw cuts terminated with 25-mm stress relief holes	1 840
5	Saw cut 111 mm up from bottom with 76 mm of material remaining uncut around each corner; saw cuts terminated with 38-mm stress relief holes	6 900
6	Saw cut 64 mm up from bottom with two 38-mm sections of uncut material left on each side; saw cuts terminated with 38-mm stress relief holes	11 650

Note: 1 mm = 0.04 in.

longer than the other tests. Since the maximum average 50-ms deceleration values of tests 3, 4, and 5 are approximately equal and consistent with the value of test 2—where the only difference was an additional 25 mm (1 in) of metal on each side—we believe that the computed momentum transfer value for test 5 is excessive by approximately 91 kg•s (200 lb•s) because of the extended velocity change time.

The computed momentum changes from these speed changes are 457, 418, 457, and 506 kg•s (997, 923, 956, and 1118 lb•s) respectively. Film analysis also indicated a secondary impact between pole and car prior to the second speed trap, which accounts for the higher speed change obtained by that method.

The vehicle crush was 343 mm (13.5 in). The VDI for this impact was 12-FCEN-2.

Fatigue Tests

The accelerated fatigue test series consisted of six tests involving five modified bases and one unmodified base with which comparisons of the relative fatigue life (in terms of cycles to failure) could be made. The excitation was provided by a rotating eccentric weight located at approximately the midpoint of the horizontally mounted pole as discussed in an earlier section of this paper. The excitation frequency corresponded to the second natural frequency of the pole as determined by visual observation and was 6.9 Hz. The resulting sinusoidal excitation force due to the rotating eccentric weight had a magnitude of 17.8 kg (39.3 lb).

The fatigue test results are summarized in Table 4. The first test of the unmodified transformer base and pole provided a baseline configuration. This lasted approximately 15 060 cycles before a failure appeared on the pole immediately above the pole-mounting flange weld.

The second test was conducted on a base that was modified by making saw cuts located 45 mm (1⅞ in) up from the bottom and extending around the corners so that 76 mm (3 in) of uncut material were left on each side. All cuts were terminated with 6-mm (¼-in) stress relief holes. This configuration failed due to propagation of cracks from the end of the saw cuts after approximately 930 cycles.

For the third test, the base was modified by cutting the sides—91 mm (3⅝ in) up from the bottom—and leaving 76 mm (3 in) of uncut material at each corner. Saw cuts were terminated with 13-mm (½-in) stress relief holes. Failure resulted from the initiation of cracks from the saw cuts after 1350 cycles. These cracks followed the heat-affected zone surrounding the weldment of the corner stiffener.

The base used in the fourth fatigue test was similar to the third, except that 25-mm (1-in) stress relief holes were used to terminate the saw cuts. Again, failure resulted from crack propagation from the stress relief holes after approximately 1840 cycles. These cracks followed the heat-affected zone surrounding the weldment of the corner stiffener.

Modifications to the bases used for the fifth and sixth tests were intended to move the areas of stress concentration away from the zones of metal that were affected by the welding process during assembly. The fifth base was similar to those in the third and fourth tests, but the saw cut was elevated to 111 mm (4⅜ in) above the bottom and terminated by 38-mm (1½-in) stress relief holes. Failure again resulted from propagation of cracks from the stress relief holes but the fatigue was increased to approximately 6900 cycles. Although the increased height of the saw cuts removed most of the influence of heat-affected metal, there is still some evidence of it. New York state engineers believe, therefore, that this modification would provide satisfactory performance in the absence of the weldment.

The last base modification tested consisted of saw cuts located 64 mm (2½ in) above the bottom of the base extending around each corner and of a separate cut on each side, so that two 38-mm (1½-in) sections were left uncut on each side outboard near the corners. Failure of this configuration occurred due to propagation of a crack immediately above the pole-mounting flange weld, the same location of the failure in the first vibration test after approximately 11 650 cycles. The failure of the pole at a lower number of cycles than in the first test was not expected since this pole had been used in previous fatigue tests. However, this base modification did not result in failure of the base, thus indicating that the in-field expected service life should approach that of the unmodified base and pole combination.

EVALUATION OF TRANSFORMER BASES

A comparative evaluation of the performance of the transformer bases tested under the reported program is contained in this section. The performance evaluation appraisal is based on three factors: (a) structural adequacy, (b) impact severity, and (c) vehicle trajectory hazard.

Structural Adequacy

Of the five impact tests performed, only the first with the unmodified transformer base proved inadequate in this category. At the nominal impact speed of 9 m/s (20 mph), this base failed to break away indicating an undesirable highway appurtenance. The remaining four tests, all employing modified bases, indicated adequate structural performance in that breakaway occurred. The final locations of the poles and mast arms for these four tests are inconclusive because the abort brake discussed in Appendix A of the complete report prevented the vehicles from clearing the pole-mounting site and drop zone at postimpact speed.

No firm conclusions can be drawn from the accelerated fatigue tests performed under this program because there are no data that relate performance under the employed test conditions to in-field service life expectancy and because testing was performed on only one sample of each modification. Implications drawn from the results are that the modification employed for the sixth fatigue test should approach the in-field service

life expectancy of the unmodified configuration and that the modification used in the fifth fatigue test may approximate that of the unmodified base in the absence of weldments in or near the plane of saw cuts.

Impact Severity

The primary criterion for evaluation of breakaway supports is a maximum vehicle momentum change of 500 kg•s (1100 lb•s) with a desirable limit of 350 kg•s (750 lb•s). The momentum changes occurring in the five tests conducted are summarized below (1 kg•s = 2.2 lb•s):

Item	Test Number 1	2	3	4	5
Speed trap measurement	–	485	358	–	506
Integration of acceleration					
Tunnel	1145	504	351	338	457
Rear deck	1105	499	360	349	418
High-speed film reduction	1060	512	350	388	457

In test 1, there was no penetration in the speed trap measurement, and in test 4 the measurement was erroneous. Test 5 was biased due to secondary impacts.

As indicated in the above summary, the momentum change, resulting from test 2 with a modified transformer base cut so that 102 mm (4 in) of material remained on each side panel, comes close to meeting the maximum allowed momentum change at an impact speed of 9 m/s (20 mph) with a 1020-kg (2250-lb) vehicle.

The third and fourth tests employed a modified transformer base cut with 76 mm (3 in) of material remaining on each panel, and succeeded in nearly meeting the desirable momentum change limit of 350 kg•s (750 lb•s). These tests were conducted with nominal 1020-kg (2250-lb) vehicles at speeds of 9 and 18 m/s (20 and 40 mph) respectively.

The fifth impact test employed a transformer base cut so that 76 mm (3 in) of material remained at each corner. This further modification was made in an attempt to increase the fatigue life of the base and, in a 9-m/s (20-mph) impact with a 1020-kg (2250-lb) vehicle, successfully limited the momentum change to below 500 kg•s (1100 lb•s). However, as discussed in the complete report, the momentum transfer is believed to be approximately 91 kg•s (200 lb•s) too high as a result of secondary impacts with the base by both the towing attachment and the guide slipper.

The maximum 50-ms average deceleration computed for the five tests are as follows: Test 1, 16.8 *g*; test 2, 7.9 *g*; test 3, 6.2 *g*; test 4, 6.0 *g*; and test 5, 5.9 *g*.

Vehicle Trajectory Hazard

No substantial vehicle trajectory hazard exists with roadside appurtenances tested since they are not redirective devices. However, as noted previously, pole kinematics after impact could not be adequately defined because of the influence of the abort brake that did not allow the vehicle to clear the pole drop zone at exit velocity.

ACKNOWLEDGMENTS

This project was jointly funded by the Federal Highway Administration and New York State Department of Transportation with all testing performed under their joint supervision by Calspan Corporation, Buffalo, New York; the complete report is available to the public through the National Technical Information Service, Springfield, VA 22161.

The contents of this report reflect our views, and we are responsible for the facts and the accuracy of the data presented herein. The contents do not necessarily reflect the official views or policies of the New York State Department of Transportation or of the Federal Highway Administration. This report does not constitute a standard, specification, or regulation.

Pendulum Tests of Breakaway Wood Sign Supports Using Crushable Bumpers

C. E. Kimball and J. D. Michie, Southwest Research Institute, San Antonio, Texas

Ten pendulum impact tests of breakaway wood sign supports were conducted to evaluate safety performance. Two sizes of timber supports were tested per AASHTO impact conditions, i.e., 1020 kg (2250 lb) mass and 32 km/h (20 mph). Two crushable pendulum nose designs were also used to evaluate relative performance. The findings indicate that both support sizes can be modified by drilled holes to effect structures that safely break away with a pendulum mass momentum change of less than 3.36 kN·s (750 lb·s). The findings also indicate that the crushable nose design has an important effect on the breakaway performance. Sequential photographs illustrate that the fracture mechanism is similar for the ten tests.

Two sizes of timber sign supports were impact-tested at the Southwest Research Institute's (SwRI) pendulum facility to evaluate their performance as breakaway roadside structures. A total of eight tests were conducted on 100 × 150-mm (4 × 6-in) and 150 × 200-mm (6 × 8-in) timber sign supports with and without holes near grade level with a crushable pendulum nose design (1). Two additional tests were conducted with a recently developed crushable pendulum nose design (2). Details of the program, test procedures, results, and conclusions are summarized in the following sections.

BACKGROUND

Evaluation Criterion

Patrick (3) and Blamey (4) concluded that head and chest impact injuries occur among vehicle occupants when the head velocity, measured relative to the vehicle, exceeds 18 km/h (11 mph). Edwards (5) stated that if the vehicle velocity change exceeds 10 km/h (6 mph), there is a possibility of minor passenger injury; velocity changes larger than 19 km/h (12 mph) should be avoided. Since vehicle velocity change imparted by a specific breakaway structure is an inverse function of the impacting vehicle mass, a more definitive performance criterion was established by coupling a 910-kg (2000-lb) vehicle with the 19-km/h (12-mph) velocity change to produce a 4.93-kN·s (1100-lb·s) impulse or change in momentum (9). For this same impulse and an 1820-kg (4010-lb) automobile, the velocity change is 10 km/h (6 mph) and, hence, the impact is less hazardous to vehicle occupants. In 1975, AASHTO (6) indicated that while the 4.93-kN·s (1100-lb·s) impulse is acceptable, a maximum 3.36 kN·s (750 lb·s) is preferred. Procedures for conducting vehicle crash tests of breakaway of yielding supports are described in NCHRP Report 153 (7).

Pendulum Test

Because of variation in crush characteristics of automobiles and the relative high cost for staging full-scale tests, effort has been devoted by the Federal Highway Administration (FHWA) (8) and others (2) to develop an "equivalent" nonautomobile test. In 1970, FHWA (9) permitted the use, with certain exceptions, of ballistic pendulum tests as a substitute for full-scale vehicle testing to determine acceptability of breakaway characteristics of luminaire supports. An interim acceptance level of a 1.79-kN·s (400-lb·s) change in momentum of the impacting mass was established when tested with a 910-kg (2000-lb) pendulum mass, a 32.2-km/h (20-mph) impact speed, and 0.51-m (20-in) striking height. This procedure implied that a pole that produced a 4.93-kN·s (1100-lb·s) change in vehicle momentum in a full-scale test would produce a 1.79-kN·s (400-lb·s) momentum change in the rigid-nose pendulum mass. The difference in momentum change was attributed to vehicle crush characteristics and other factors. Unfortunately, it has been shown that pole breakaway performance cannot be

Figure 1. Sign configuration for test specimen.

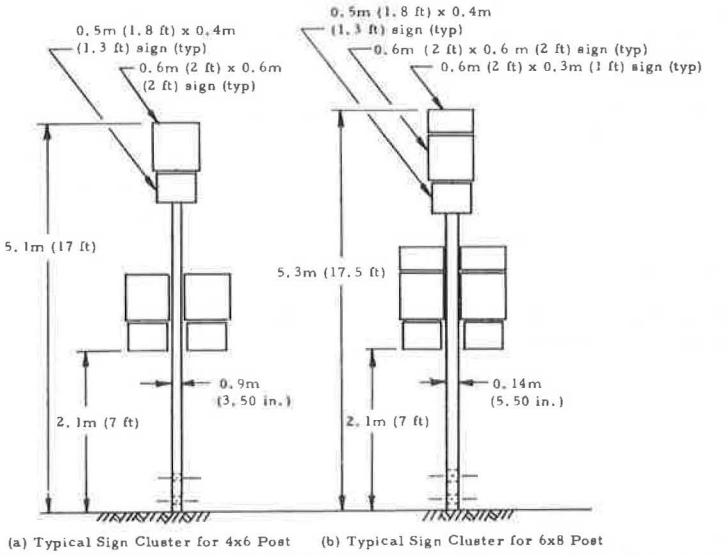

(a) Typical Sign Cluster for 4x6 Post (b) Typical Sign Cluster for 6x8 Post

Figure 2. Specimen breakaway designs.

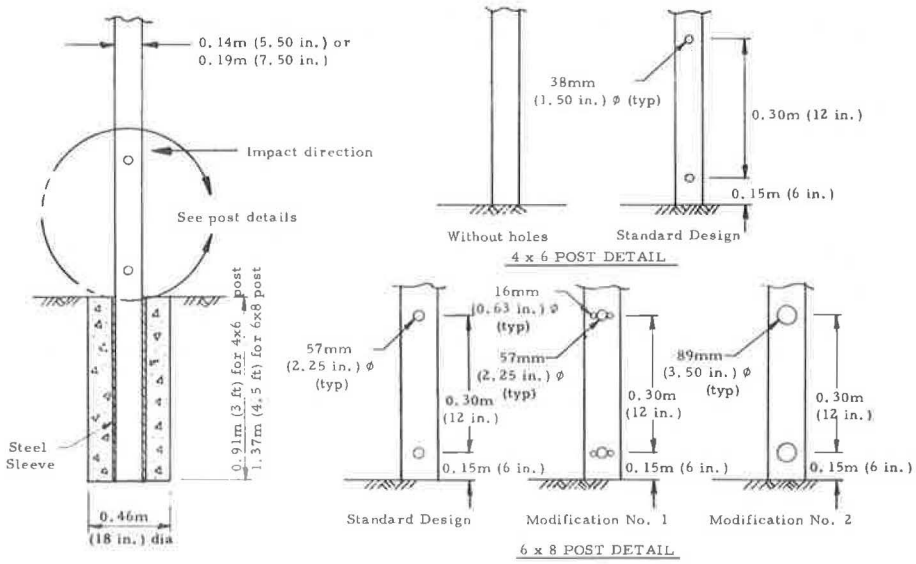

Figure 3. Crushable nose configurations.

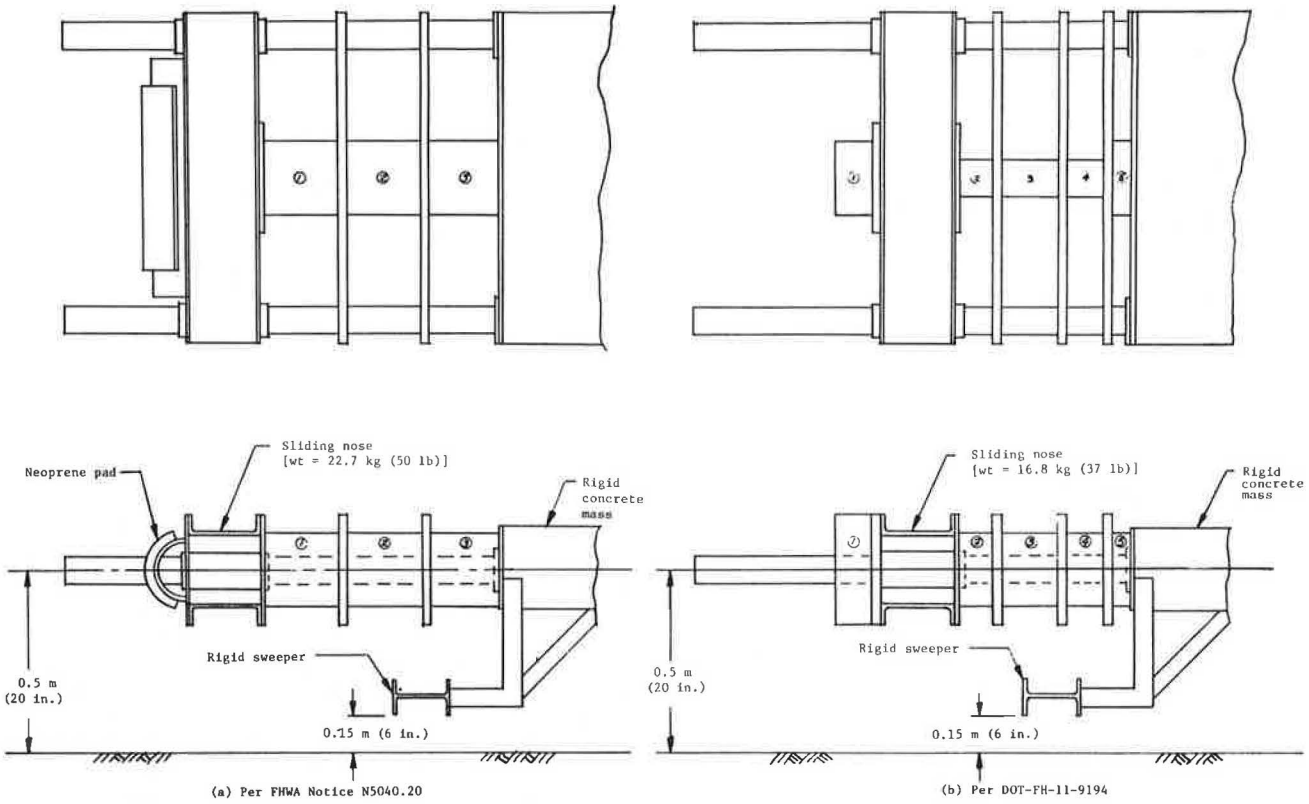

Figure 4. Photographs of test setup.

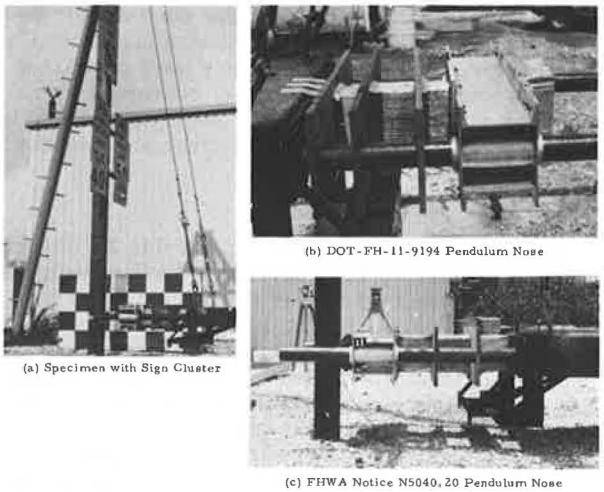

Table 1. Details of honeycomb configurations.

Nose Design	Stage No.	Height (m)	Width (m)	Thickness[a] (m)	Static Strength (kN)
FHWA Notice N5040.20	1	0.20	0.20	0.20	21
	2	0.20	0.20	0.20	37
	3	0.20	0.20	0.20	65
DOT-FH-11-9194	1	0.30	0.20	0.10	32
	2	0.20	0.10	0.10	11
	3	0.20	0.10	0.15	19
	4	0.20	0.10	0.10	33
	5	0.20	0.20	0.05	65

Note: 1 m = 3.3 ft and 1 kN = 0.225 kip.
[a]Thickness before 6.4-mm (0.25-in) precrush.

reliably projected from rigid-nose pendulum test results (8).

Crushable Pendulum Nose

In 1976, FHWA (1) presented details for a crushable nose for pendulum and bogies and stated that nonautomobile test procedures are considered equivalent for some types of hardware—luminaire supports, slip-base and load-concentrating sign supports, and, with a bogie only, single-post timber and base-bending sign supports. However, testing by FHWA in the fall of 1976 revealed that the pendulum tests using this nose setup failed to produce results correlating with full-scale test results obtained at the Texas Transportation Institute for certain support types. In particular, steel slip-base luminaire supports were severely deformed by the pendulum impact and, in some cases, momentum changes over 5.38 kN•s (1200 lb•s) were recorded. Full-scale test results for a subcompact vehicle striking a slip-base luminaire support at 32.2 km/h (20 mph) were in the 2.24-kN•s (500-lb•s) range.

A second-generation crushable pendulum nose has recently been developed by FHWA and Ensco (2). The nose has been configured to develop crush characteristics of a pre-1974 Chevrolet Vega. This vehicle was chosen because it is a typical 1020-kg (2250-lb) automobile. Although this nose design has not been endorsed by FHWA engineering as a replacement for design presented in FHWA Notice N5040.20, preliminary findings indicate the pendulum results compare favorably with full-scale crash test results (2).

Although the objective of the program reported here was to evaluate breakaway characteristics of timber sign supports with the pendulum nose presented in FHWA Notice N5040.20, two additional tests were performed using the second-generation crushable nose to provide

Table 2. Test matrix and data summary.

Test No.	Specimen Dimensions (m)	Breakaway Design[a]	Pendulum Nose Configuration[b]	Impact Velocity (m/s)	Pulse Duration (m/s)	Velocity Change (m/s)	Peak Force (kN)	Impulse (kN·s)	Energy (kJ)		
									Total Kinetic[c]	Nose Crush[d]	Specimen Fracture[e]
M1	0.10 x 0.15	Standard	A	9.03	50	0.73	34.7	0.75	6.46	0.40	6.06
M2	0.10 x 0.15	Standard	A	9.17	53	0.73	35.1	0.75	6.60	0.67	5.93
M3	0.10 x 0.15	Standard	B	9.10	84	1.77	60.5	1.81	14.84	8.39	6.45
M4	0.10 x 0.15	Without holes	A	8.90	30	0.62	34.7	0.63	5.44	1.24	4.20
M11	0.15 x 0.20	Standard	A	9.17	100	5.68	82.7	5.80	36.69	18.43	18.26
M12	0.15 x 0.20	Standard	A	8.96	95	3.13	64.1	3.19	23.62	10.59	13.03
M13	0.15 x 0.20	Mod. 1	A	8.96	55	1.23	35.6	1.26	10.48	6.92	3.56
M14	0.15 x 0.20	Mod. 1	A	8.96	40	0.91	45.4	0.93	7.90	2.79	5.11
M15	0.15 x 0.20	Mod. 2	A	9.24	42	1.21	49.8	1.23	10.66	4.01	6.65
M16	0.15 x 0.20	Mod. 1	B	8.84	77	2.39	81.0	2.44	18.56	9.92	8.73

Note: 1 m = 3.3 ft, 1 m/s = 3.28 ft/s, 1 kN = 0.225 kip, 1 kN·s = 223.1 lb·s, 1 kJ = 0.738 ft-kip.

[a]See Figure 2 for details.
[b]A, per FHWA Notice N5040.20; B, per DOT Contract FH-11-9194.
[c]$KE = 0.5\ m\ (V_f^2 - V_o^2)$.
[d]See Table 2.
[e]Specimen fracture energy = total KE - nose crush energy.

Table 3. Pendulum nose deformation and crush energy.

Test No.	Stage No.	Average Thickness (mm)			Compressive Strength (kN)	Crush Energy (kJ)
		Initial	Final	Crush		
M1	1	197	178	19	21	0.40
	2	197	197	0	37	0.00
	3	197	197	0	65	0.00
M2	1	197	165	32	21	0.67
	2	197	197	0	37	0.00
	3	197	197	0	65	0.00
M3	1	95	13	82	32	2.62
	2	95	13	82	11	0.90
	3	146	24	122	19	2.32
	4	95	20	75	33	2.48
	5	44	43	1	65	0.07
M4	1	197	133	159	21	1.24
	2	197	197	0	37	0.00
	3	197	197	0	65	0.00
M11	1	197	29	168	21	3.53
	2	197	35	162	37	5.99
	3	197	60	137	65	8.91
M12	1	197	37	160	21	3.36
	2	197	35	162	37	5.99
	3	197	178	19	65	1.24
M13	1	197	35	162	21	3.40
	2	197	102	95	37	3.52
	3	197	197	0	65	0.00
M14	1	197	64	133	21	2.79
	2	197	197	0	37	0.00
	3	197	197	0	65	0.00
M15	1	197	38	159	21	3.34
	2	197	179	18	37	0.67
	3	197	197	0	65	0.00
M16	1	95	25	70	32	2.24
	2	95	11	84	11	0.92
	3	146	18	128	19	2.43
	4	95	19	76	33	2.51
	5	44	16	28	65	1.82

Note: 1 mm = 0.039 in, 1 kN = 0.225 kip, 1 kJ = 0.738 ft-kip.

comparison and insight to their relative performance.

Test Specimens

Timber test specimens and signing hardware were supplied by the Michigan Department of State Highways and Transportation (MDSHT). The timber supports were Southern yellow pine with pentachlorophenol preservative. The test articles were assembled and erected according to MDSHT drawings S3.30, S9.20, and engineering sketches. Arrangement of signing is shown in Figure 1.

Test Procedures

The timber specimens were modified as shown in Figure 2 and inserted into a 0.46-m (18-in) round concrete footing that had been constructed with a sheet metal sleeve. Wood shims were used to ensure that the specimen was tightly fitted in the sleeve. Soil, specified and consolidated per recommendations of NCHRP Report 153, represented a relatively stiff support for the concrete footing.

A 1020-kg (2250-lb) reinforced concrete mass with a swing radius of 7.9 m (26 ft) impacted each specimen 0.5 m (20 in) above grade. The front of the 0.9 × 1.8 × 0.2-m (3 × 6 × 0.75-ft) mass was fitted with a crushable aluminum honeycomb nose to simulate vehicle crush or deformation. Details of the two types of nose configuration are shown in Figures 3 and 4 and Table 1.

To initiate a test, the pendulum mass was elevated to a predetermined height and released. Actual impact speed was determined from a photocell-operated speed trap.

Signals from an accelerometer, mounted at the rear of the concrete pendulum mass, were continuously recorded throughout the impact events by a high-speed magnetic tape recorder. These were later processed through an SAE J211 Class 60 filter, converted from analog to digital format, and subsequently processed by digital computer for kinematic and dynamic parameters.

FINDINGS

A summary of test results appears in Table 2. Velocity change and impulse are key parameters when evaluating performance of the break-away mechanism. Because nose crush energy is reflected in the impulse values and two different nose designs were used, fracture energy of the specimens was determined by subtracting the nose crush energy (i.e., honeycomb deformation × compressive strength) from the change in pendulum kinetic energy. A summary of nose crush findings is presented in Table 3. Typical impact sequence photographs are shown in Figure 5.

ANALYSIS OF TEST RESULTS

Performance

Of the ten tests, only test M11, the standard 150 × 200-mm (6 × 8-in) support, failed to pass the acceptable maximum 4.93-kN·s (1100-lb·s) or preferred maximum 3.36-kN·s (750-lb·s) change in momentum criteria. All other specimens broke away within the preferred maximum impulse limits. From these tests, it appears that all single support designs except that evaluated in test M11 should be accepted for in-service use, provided the designs satisfy environmental loadings.

Figure 5. Sequence photographs of fracture mechanism.

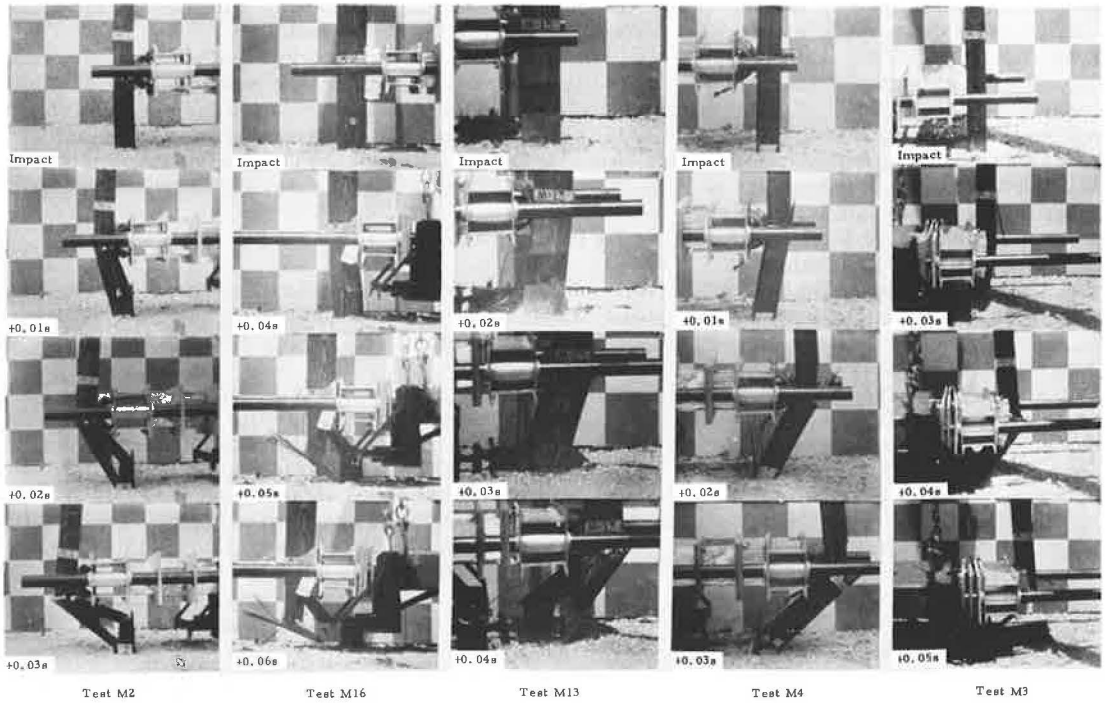

Stages of Support Fracture

Four stages of support fracture are shown in Figure 5 for tests M2, M3, M4, M13, and M16. These illustrations are also typical for tests M1, M11, M12, M14, and M16:

1. Stage 1. The first photograph in each test shows the support at instant of impact. No deformation of support or crushing of pendulum nose has occurred.
2. Stage 2. Between stages 1 and 2, practically all pendulum nose crush has occurred. A plastic hinge is forming in the support at the point of pendulum contact and a second hinge is forming at grade. The portion of the support above the pendulum remains essentially vertical. Peak resisting force of the support occurs at or about the time of this stage.
3. Stage 3. A vertical split in the support forms from grade up to the pendulum contact. The forward (away from the pendulum contact) segment of the partially severed support breaks in flexure at grade level and at the pendulum plane. For the rear segment, the break occurs at the lower hole pattern and at the pendulum plane. For test M4, no vertical fracture is evident; the support fractures at grade and at the pendulum plane.
4. Stage 4. Fracture of the support is completed.

Foundation

All tests were performed with the support mounted in a 0.46-m (18-in) diameter concrete footing. The footing minimized movement of the support during impact, although some movement was observed in high-speed cine for tests M11 and M12. The effect of this small movement is unknown but it is surmised to have caused a slight increase in momentum change. The soil is specified by NCHRP Report 153 and provides a high level of lateral support to the concrete foundation and specimen. Installation procedures for the sign supports should include guidelines that will assure a densely compacted soil around the concrete footing.

Michigan's standard practice is to cast the footing in place after making the hole with an auger. This could result in a more rigid foundation depending on soil conditions in the field. It follows, therefore, that actual field conditions could result in less momentum change than the laboratory tests indicate.

An important aspect of the concrete footing is the rigid flexure line or stress riser at grade level. All specimens were observed to ultimately break at this juncture. Without this stress riser, it is conjectured that a tougher, less brittle failure would occur at or below grade. Hence, to effect field performance corresponding to these test results, the concrete footing is required.

Crushable Nose Designs

Two crushable nose designs were used in the program. Although the eight tests with configuration A and two tests with configuration B are too few to draw statistically valid conclusions, the following observations are presented.

First, the two nose designs do not give similar results and therefore are not interchangeble. More of the pendulum kinetic energy is absorbed in crushing the softer nose. For example, 0.53-kJ (0.4-ft·kip) average energy was absorbed by the nose in tests M1 and M2 as opposed to 8.39-kJ (6.2-ft·kip) energy absorbed by the soft configuration B nose in test M3. Since essentially all nose crushing occurs prior to fracture of the support, the change in momentum attributed to the nose crush is calculated to be 0.061 kN·s (13.6 lb·s) for configuration A (average of M1 and M2) and 0.972 kN·s (217 lb·s) for configuration B in test M3. Similarly, more energy and momentum change is caused by configuration B in test M16 than for configuration A in tests M13 and M14.

A second consideration is that the contact force between the pendulum mass and the wood support builds up

more slowly for the soft-nose configuration B designs. Thus, the more sudden onset rate of loading for the harder nose design, which promotes a more brittle fracture of the wood, is attenuated. This action results in the specimen exhibiting tougher strength characteristics for the softer nose pendulum.

It is noted that configuration B is patterned to match the crush properties of a pre-1974 Chevrolet Vega. After 1974, a stiffer bumper and front end were produced to meet new U.S. Department of Transportation safety regulations. Hence, by using configuration B, the more conservative crushable nose is utilized in evaluating roadside appurtenances. At some time in the future, when most pre-1974 vehicles are no longer in service, a more rigid pendulum nose should be used.

To date, no full-scale vehicle tests have been performed on the Michigan sign support designs. Hence, a comparison between full-scale crash tests and pendulum test results cannot be made.

CONCLUSIONS

A number of conclusions can be made from the findings:

1. With the exception of test M11 on the 150 × 200-mm (6 × 8-in) support standard, all configurations produced less than the maximum preferred momentum change specified by FHWA (1). Although test M12, a replication of test M11, did produce less than the preferred momentum change, it would seem prudent to use modifications 1 or 2 to achieve a higher degree of safety performance.
2. The two crushable nose designs are not equivalent based on momentum change of the pendulum and fracture energy of the support. A major part of the difference is due to the energy absorbed in the nose crush. In addition, it appears the slower buildup of force in the soft nose tests may attenuate the tendency for low-energy brittle fracture of the wood and thereby produce a tougher breakaway phenomenon.
3. The fracture mechanisms of the modified supports were generally consistent with (a) a shear failure occurring between the upper hole, through the lower hole, and to grade, and (b) flexure fractures occurring at the upper hole, at the lower hole, and at grade. Knots or other wood discontinuities located in these failure planes would probably affect the results.
4. Since all specimens were tested with a concrete footing, any operational design based on these findings should include a similar foundation. We believe that a less rigid foundation and stress riser at grade level would increase the toughness of the fracture mechanism, thereby effecting a less conservative breakaway support.

REFERENCES

1. AASHTO Standard Specifications for Highway Signs, Luminaires and Traffic Signals. Federal Highway Administration, FHWA Notice N5040.20, July 14, 1976.
2. J. Bloom. Refinement of Pendulum Test Procedure for Improving Correlation With Full-Scale Impacts. ENSCO, Inc., Interim Progress Rept., FHWA Contract No. DOT-FH-11-9194, April 1977.
3. L. M. Patrick, H. J. Mertz, and C. K. Kroll. Knee, Chest, and Head Impact Loads. Proc., 11th Stapp Car Crash Conference, Oct. 10-11, 1967, Anaheim, CA, p. 116.
4. C. Blamey. Results From Impact Tests on Telegraph Poles. Highway and Bridges, Vol. 32, No. 1576, 1964, pp. 7-8.
5. T. C. Edwards, J. E. Martinez, W. F. McFarland, and H. E. Ross. Development of Design Criteria for Safer Luminaire Supports. NCHRP, Rept. 77, 1969.
6. Standard Specifications for Structural Supports for Highway Signs, Luminaires and Traffic Signals. American Association of State Highway and Transportation Officials, Washington, DC, 1975.
7. M. E. Bronstad and J. D. Michie. Recommended Procedures for Vehicle Crash Testing of Highway Appurtenances. NCHRP, Rept. 153, 1974.
8. D. B. Chisholm and J. G. Viner. Dynamic Testing of Luminaire Supports. Federal Highway Administration, Office of Research and Development, Rept. FHWA-RD-73-55, 1973.
9. Application of Highway Safety Measures—Breakaway Luminaire Supports. Federal Highway Administration, FHWA Notice TO-20, Nov. 16, 1970.

Abridgment

Breakaway Sign Testing, Phase 1

J. C. Powers, W. M. Szalaj, and R. L. Hollinger, Bureau of Operations Research, Division of Research and Development, New Jersey Department of Transportation

Because of the damage to people and vehicles when an errant vehicle hits a fixed object, the state of New Jersey developed a breakaway system for large ground-mounted sign supports. Testing was conducted under various controlled conditions and indicated that the system met the appropriate criteria for a breakaway support. Subsequent to the testing, some modifications were made to the system, including the components used to restrain the breakaway section of the post to the fixed post segment.

After several years of experience it was found that the system was not performing as desired, although no injuries or deaths were reported as a result of hitting the breakaway structures. Frequently, the restraint components failed, permitting the struck post to separate completely from the remaining post. Other components also were found to fail on occasion, although the system continued to function sufficiently to prevent any reported injuries.

At this time a detailed review of the breakaway system, including the results of investigations of actual sign impacts, became appropriate. Personnel from the state transportation department's research, design, construction, and inspection units studied the system, suggested necessary modification, and assisted in de-

Figure 1. Breakaway sign structure.

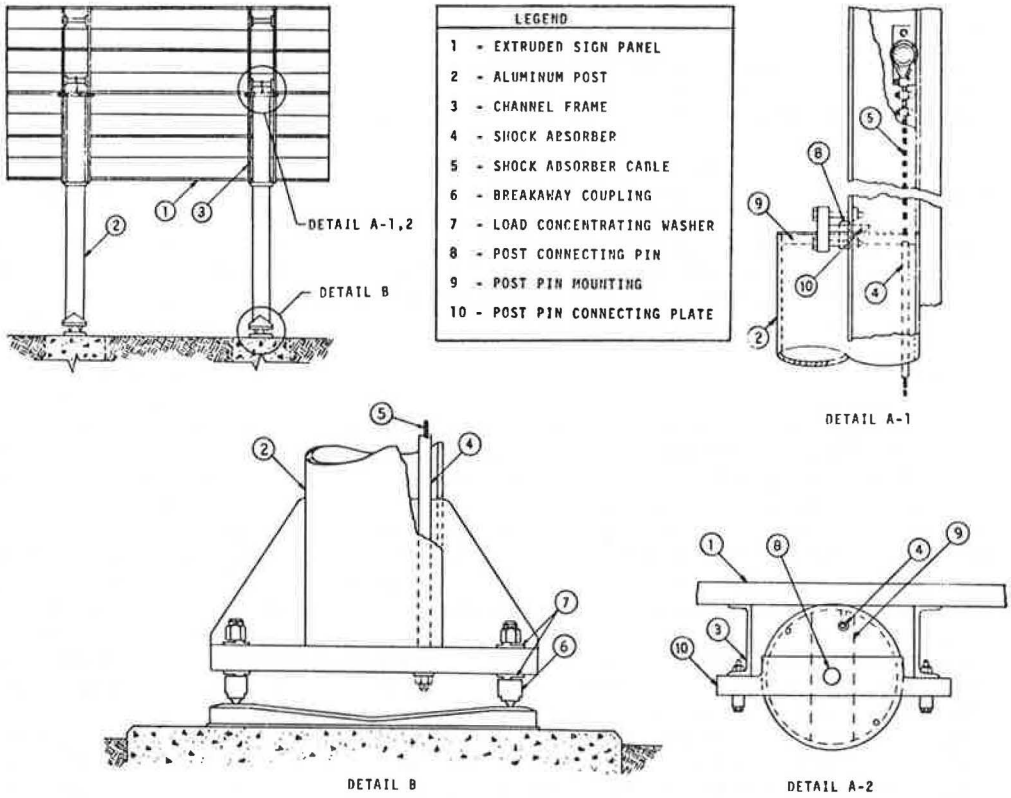

Table 1. Summary of breakaway test results.

Test	Test Conditions	Panel-to-Frame Attachments: Frame Slip (m)	Panel-to-Frame Attachments: Panel Dip (m)	Post-to-Frame Connection	Shock Absorber
0	Basic sign design	0	0.3	Post pin jammed	No action
1	Maximum sign clips	0.2	0.3	Post pin jammed	Minimal action
2	Maximum sign clips, modified shock absorber	0.75	0.3	Post pin jammed	Minimal action
3	Sign panel bolted, spherical post pin, modified shock absorber, cable slack	0	1.2	Post separated successfully	Substantial action
4	Sign panel, conical post pin, modified shock absorber, cable slack	0	1.4	Post separated successfully	Substantial action

Note: 1 m = 3.3 ft.

veloping a work plan for future research and testing. From the analysis of impacts and group discussion, several minor modifications were implemented immediately. It was also agreed that controlled testing of the system was necessary to further isolate any problems and to verify proper functioning of the modified design.

Although actual vehicle crash tests would be necessary to measure momentum change and to test the reaction of the system under real life conditions, the cost of such tests limited their number. A system using a heavy truck and a steel cable was developed for use in the problem determination phase, although differences in the test conditions, such as lack of vehicle crush and the resulting longer impact duration, precluded measuring momentum change in a definable manner. However, it was felt that the conditions would be adequate to show actual sign-structure performance well enough to define any improperly functioning components. To record the data, photographs were taken by normal-speed still and high-speed movie cameras. A videotape was also used to permit immediate playback of the tests.

It was decided to test the unmodified design initially to show the reaction of existing structures to impacts. Additional tests would be done to show the effects of various modifications, including sign-panel attachment methods and the post restraint system. Other modifications would be made based on observations of component performance during the tests.

BREAKAWAY SIGN SUPPORT

The New Jersey breakaway system consists of three basic parts other than the panel itself and the posts (Figure 1). The base of each post is connected to the anchor bolts with metal couplings and washers that break under vehicle impact but resist wind loads applied to the sign panel. The sign panel sits over a pin on the top of the post with the lower edge of the panel held to the post by a clamp. On impact the lower clamp breaks, and the post and attached pin are to drop free of the panel and rotate upward and away from the panel. Meanwhile, the post is still attached to the panel by a wire rope and aluminum tube (shock absorber) that extrudes and reduces the force applied to the panel during restraint of the free post. The system uses the panel as a part of the restraint system.

Problem Definition

Investigation of the field impacts showed consistent problems with release of the post from the sign panel and with the shock-absorbing system. Frequently, the panel mounting assembly slipped through clips used to hold the panel to the mounting assembly while little or no operation of the shock absorber was found.

Test Structure

A breakaway sign structure with a 1.8 × 3.6-m (6 × 12-ft) extruded sign panel was identified as the critical size for the tests. This structure is the smallest capable of accepting the heavier of two post restraint designs. The extruded sign panel can handle up to 3 sign clips/m (1 sign clip/ft) of vertical panel size, more than other panel types. Additionally, this panel is the smallest used for breakaway signs and, consequently, also represents a lower limit for sign clip locations. Tests were designed to permit the independent analysis of modification (see Table 1.)

FINDINGS

Shock-absorber performance was a source of major concern during testing. The shock-absorber connecting cable affects the operation of the breakaway system in two ways. First, acting as a hinge where post separation occurs, it rotates the post up and away from the impacting vehicle. Second, it transmits the impact energy to the sign panel. During initial tests, the hinge point jammed where post separation should occur. Separation eventually occurred at the expense of connecting hardware. Similar jamming results were noted when several field impacts were reviewed. It was suggested that the shock-absorber cable was having a negative effect on post separation. Pretensioning the cable is a procedure currently specified by New Jersey Department of Transportation standards (3). It was decided to test the effect of leaving this cable loose. It was hoped that it would free the connection where the post separation should occur, preventing jamming. However, post separation occurred only after destruction of the connecting hardware. It was decided that the connecting pin design was also a factor in the jamming. In standard installations this connection is accomplished by letting the weight of the sign rest on a round pin. During impact, several events must occur in order for the sign to function properly. The timing of events is critical. When the post rotates too far before the pin is freed of the weight of the sign, the mechanism will jam. Subsequent post performance is then negatively affected. It was felt that the system being used consistently did not allow enough post rotation. The design had been predicated on the theory that the post weight would pull the pin free before it could rotate far enough to jam. Apparently just allowing slack in the shock cable would not by itself ensure enough post drop to free the pin.

A modified pin was developed by simply rounding the top of the pin. In addition to using this modified pin, it was decided that a generous amount of slack should be put into the shock-absorber cable. When these conditions were tested, post separation occurred smoothly. Further, the shock-absorber slack was drawn taut with sufficient impulse to start the energy-absorbing action.

At this point, two things had been confirmed. First, the breakaway system with a vertical shock absorber can be effective, even on small sign sizes. Second, we could not depend only on post weight to effect post release. Indeed, the rounded post pin had prevented jamming since the post did not drop at all.

It was apparent after reviewing high-speed films of current tests that the impulse provided to the shock absorber was instrumental in initiating the proper action of the device. However, the breakaway design had evolved around a taut connecting cable in order to ensure that the panel would not separate from the pin unless impacted. Modifications to the pin connection were needed to allow a slack cable to be incorporated into the design. Trading off advantages of the rounded pin against the horizontal resistance to wind forces provided by an unrounded pin resulted in a cone-shaped pin. The conical design is believed to provide an adequate area of horizontal contact so that wind forces alone will not cause the post to separate. A test run with the conical pin and slack in the shock-absorber cable performed satisfactorily. After impact, the cable was again drawn taut with enough impulse to initiate shock-absorber action. The system performed without any damage to the connecting hardware. This absence of hardware damage in successive tests where the sign performance was satisfactory led us to believe that testing further structural design modifications would not be necessary.

A second area of concern was the panel slippage. It had been observed from field impacts that a frame to which the sign panel is attached does not always remain attached to the panel during impact. Initially, the use of as many sign clips as possible was tested. Frame slipping initiated by the drag of the separated post continued to occur. As a result, during later tests the panel was secured to the frame with bolts. In these tests there was no frame slippage recorded; but, as a trade-off, the sign panel was pulled downward a greater amount during impact. It is a concern that the panel may dip low enough to hit the top of a vehicle passing under the sign.

Analysis of the latter tests led to the conclusion that bolting improves the performance of the shock absorber. Kinetic energy expended during frame slippage when clips are used is instead expended by the shock absorber when the panel is bolted. It was decided to observe the panel action related to the vehicle clearance during full-scale impacts with both bolted and clipped panels before a final judgment is made.

RECOMMENDATIONS

Full-scale crash testing in accordance with the Recommended Procedures for Vehicular Crash Testing of Highway Appurtenances (4) is recommended to identify how the breakaway sign structure, with the proposed modifications, will function during an actual vehicle impact situation. [Since 1974, minor changes have occurred in these procedures (5).]

Testing is to be organized with two initial tests on the same size sign structure that was used during simulated impact testing. First, a maximum number of sign clips should be used and then bolts should be used to secure the sign panel.

An analysis of the panel dip causing secondary impacts with the vehicle under these conditions will be one indication of whether it is desirable to continue to consider bolting or friction clipping the sign panel. Further tests should then be run to provide heavy-vehicle impact data and should include an angle impact of about 15° as well as impacts with a larger sign size.

Full-scale tests are to include the conical pin and generous slack in the shock-absorber cable.

It is also recommended that the breakaway sign structure as modified should be installed in locations where it will be subjected to high winds. Its performance under field conditions should be observed for at least 1 year prior to recommending that existing specifications be changed.

ACKNOWLEDGMENTS

The contents of this report reflect our views, and we are responsible for the facts and the accuracy of the data presented herein. The contents do not necessarily

reflect the official views or policies of the Federal Highway Administration. This report does not constitute a standard, specification, or regulation. This report was prepared in cooperation with the U.S. Department of Transportation, Federal Highway Administration.

REFERENCES

1. N. E. Shoemaker. Full Scale Dynamic Testing of the N. J. Breakaway Sign Structure. Cornell Aeronautical Laboratory, Inc., Sept. 1970.
2. F. C. Turner. Application of Highway Safety Measures—Breakaway Luminaire Supports. Circular Memorandum to Regional Federal Highway Administrators and Division Engineers, June 5, 1968.
3. Standard Details. New Jersey Department of Transportation, July 1976.
4. Recommended Procedures for Vehicle Crash Testing of Highway Appurtenances. NCHRP, Rept. 153, 1974.
5. Recommended Procedures for Vehicle Crash Testing of Highway Appurtenances. TRB, Transportation Research Circular 191, Feb. 1978.

Evaluation of Bolted-Base Steel Channel Signpost

Hayes E. Ross, Jr., and Michael J. Effenberger, Texas Transportation Institute, Texas A&M University, College Station
Lawrence J. Sweeney, Franklin Steel Company, Franklin, Pennsylvania

A recent survey has shown that the steel flanged channel post, or U-post, is the most widely used type of sign support in the United States. In the past, it has been common practice to drive the full-length U-post into the ground. To facilitate its installation, a simple stub-signpost support system has been developed. Initially, a relatively short stub post is driven into the ground. Then the signpost, with sign panel attached, is bolted to the stub. A retainer-spacer strap in the bolted connection serves to provide a snug fit between the signpost-to-stub connection and to help control the impact trajectory of the sign panel and the signpost. Static load tests and full-scale vehicle crash tests were conducted to evaluate the stub-signpost system. Crash tests of both single- and multiple-post sign configurations were conducted in accordance with current standards and guidelines. The stub-signpost system satisfied current safety criteria in all cases. This paper describes these tests and their results.

A recent survey (1) found that there are more than 10 million roadway signs on the 50 state highway systems. Millions more are used on city streets and county roads. This same survey also found that the steel U-post is the most widely used type of sign support.

It has been common practice to drive the full-length U-post into the ground to the desired embedment depth. Driving the post in this manner can be awkward and hazardous to the installation crew since the post may be up to 4.88 m (16 ft) in length or possibly longer. Equipment, such as a ladder or a lift truck, is necessary to drive the post from such heights. Installation may also be accomplished by inserting the pole in a drilled hole and backfilling with excavated soil. However, this method is usually more costly than driving the post.

To simplify the installation procedure for the U-post, the Franklin Steel Company developed the Eze-Erect system. Initially, a stub post, about 0.91 m (3 ft) in length, is driven into the ground. Then the signpost with sign panel attached for single-post installations is attached to the stub post with the Eze-Erect bolted connection. A retainer-spacer strap is used in the connection primarily to provide a close fit at the post-to-stub connection during normal loading conditions. It also helps control the impact trajectory of the signpost resulting from a vehicle collision, especially for low-speed impacts.

Static load tests and full-scale vehicle crash tests were conducted to evaluate the Eze-Erect system. The crash tests were conducted in accordance with current standards and guidelines (2, 3). This paper summarizes these tests and their results. Full details of the tests are presented in two research reports (4, 5).

EZE-ERECT SYSTEM

Figure 1 shows the general details of the first-generation design of the Eze-Erect system. Further details of the first-generation retainer-spacer strap and the connection are shown in Figure 2. Offset in the strap was established as a result of static load tests of various bolted connections. These tests took place in February 1976 at Standard Pressed Steel Laboratories, Jenkintown, Pennsylvania. As shown, the top connector bolt was 1.3 cm (0.50 in) from the top of the stub post, and the connector bolts were on 12.7-cm (5-in) centers. Overlap dimension was 15.2 cm (6 in). Hardware consisted of four bolts, each bolt having two heavy-gauge plain washers, a lock washer, and a hex nut. The two connector bolts were 3.8 cm (1.5 in) long. All bolts were $\frac{5}{16}$-18 UNC, Grade 5. As discussed in this paper, both static and dynamic tests were conducted on the first-generation assembly at the Texas Transportation Institute (TTI) in March 1977.

Subsequent to the tests on the first-generation assembly, modifications were made as shown in Figure 3. The location of the top connector bolt was changed from 1.3 cm to 2.5 cm (0.5 to 1 in) from the top of the stub post. Also, the hardware was reduced to four bolts and four nuts. All bolts were $\frac{5}{16}$-18 UNC × 3.8 cm (1.5 in) long, Grade 5. The bolt and nut are of the integral flange type to eliminate plain washers. The hex nut is a prevailing torque type to eliminate the lock washer. This assembly will be referred to hereafter as the second-generation assembly. Static and dynamic testing conducted on the second-generation assembly are discussed in subsequent sections of this paper.

It is noted that other bolted overlap configurations have been used with U-posts, without the retainer-spacer strap. However, to achieve the required wind resis-

Figure 1. Eze-Erect signpost assembly.

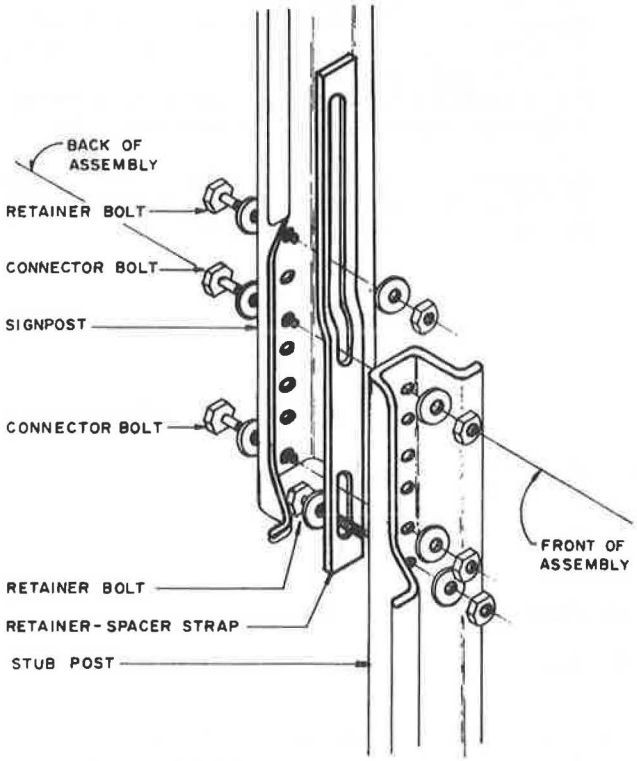

tance, overlaps from 30.5 cm (12 in) to 152.4 cm (60 in) are required. The impact performance of such configurations has not been determined.

STATIC TESTS

Tests were conducted to determine the static load capacity of the first- and second-generation Eze-Erect assemblies. The signpost-stub assembly was loaded in a cantilevered test arrangement in the static tests.

Table 1 contains details and results of the tests. Note that in test 2, failure was due to fracture in the web section of the stub post. Failure occurred at the top connector bolt hole. A similar failure occurred in the full-scale crash test of the first-generation assembly. Distance from the top of the stub post to the top connector bolt hole was increased from 1.3 to 2.5 cm (0.5 to 1 in) to correct this problem (see Figure 3). Tests of the 3-kg/m (2-lb/ft) and the 4.5-kg/m (3-lb/ft) sign post (tests 1 and 2) were not repeated with the second-generation assembly. However, reductions in the moment capacity of the second-generation assembly due to a reduction in the connector bolt spacing from 12.7 to 10.2 cm (5 to 4 in) should be offset to a large extent by the increase in the distance of the top connector bolt hole from the top of the stub from 1.3 to 2.5 cm.

Direction of loading for the data in Table 1 was normal to the front of the assembly (see Figure 1 for front of assembly). Each assembly was also loaded in a direction normal to the rear of the assembly, and the results were similar to those shown.

Figure 2. First-generation retainer-spacer strap.

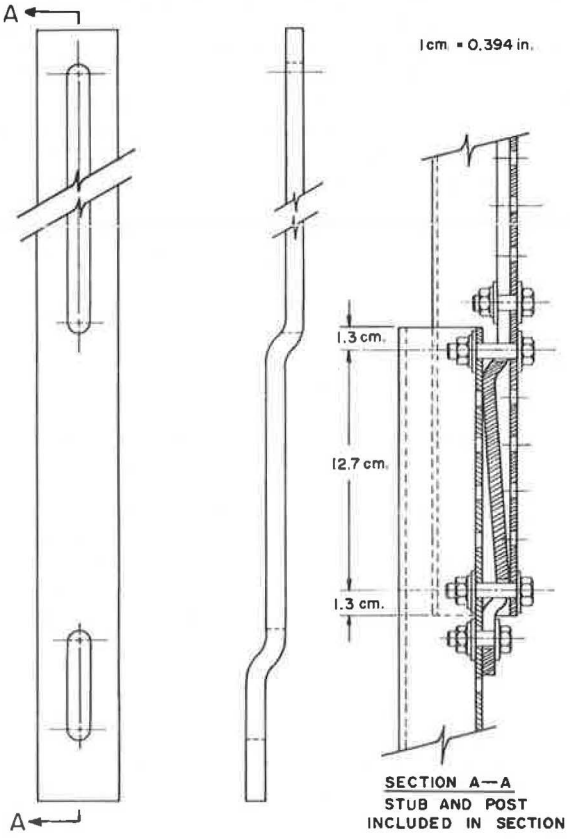

Figure 3. Second-generation retainer-spacer strap.

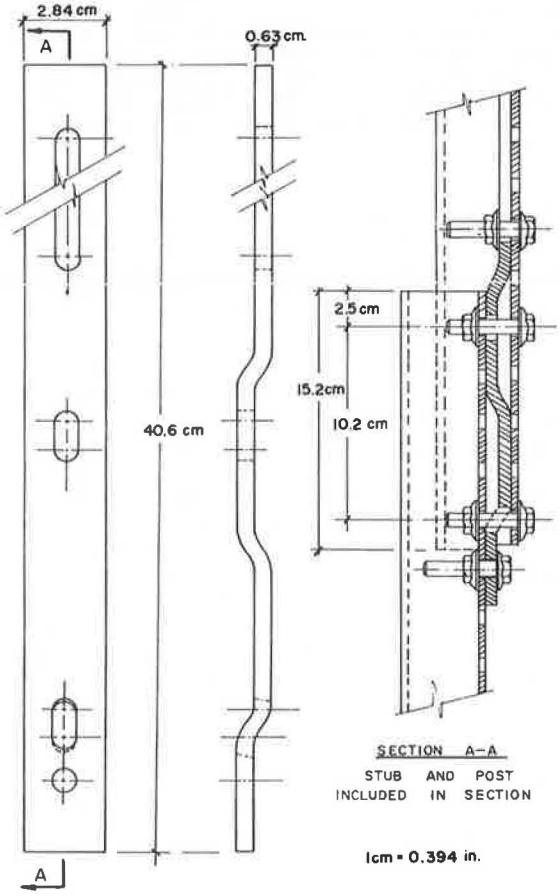

Table 1. Static test data.

Test No.	Eze-Erect Assembly Generation	Signpost Size[a] (kg/m)	Stubpost Size[a] (kg/m)	Load at Failure[b] (N)	Bending Moment at Failure (N·m)	Cause of Failure
1	First	3.0	4.1	1250	3048	Excessive deflection
2	First	4.5	4.5	1637	3743	Web of base post split
3	Second	6.0	6.0	1370	4380	Bolt fractured

Note: 1 kg/m = 0.67 lb/ft; 1 N = 0.225 lbf; 1 N·m = 0.737 lbf·ft.
[a]Signposts and stubposts were Franklin Steel Company U-posts, rolled from rail steel.
[b]Direction of load was normal to front of assembly (normal to front of sign panel that would be mounted on post).

Table 2. Failure moment of Eze-Erect assembly versus failure moment of signpost.

Signpost Size (kg/m)	Elastic Section Modulus[a] (cm^3)	Plastic Section Modulus[a] (cm^3)	Moment at Initial Yielding[b,c] (N·m)	Fully Plastic Moment[b] (N·m)	Eze-Erect Failure Moment (N·m)
3.0	3.77	4.59	1559	1898	3048
4.5	6.88	8.85	2848	3661	3743
6.0	9.18	11.64	3797	4814	4179

Note: 1 kg/m = 0.67 lb/ft; 1 cm^3 = 0.061 in^3; 1 N·m = 0.737 lbf·ft.
[a]Values furnished by Franklin Steel Company.
[b]Based on minimum yield of 413.4 MPa (59.9 kips/in^2) for rail steel.
[c]Moment at which flexure stress equals 413.4 MPa in extreme fibers.

Figure 4. Single-post sign installation.

For comparative purposes, consider the failure moment of the Eze-Erect assembly versus the predicted failure moment of the individual signpost, as given in Table 2. In all cases, the Eze-Erect assembly transmitted a moment greater than the "elastic" moment of the individual post. In fact, in two of the three tests, the Eze-Erect assembly transmitted a moment greater than the fully plastic moment of the individual post. It is noted that the ultimate strength of rail steel normally exceeds 758 MPa (110 kips/in^2).

FULL-SCALE CRASH TESTS

Six full-scale crash tests were conducted on the Eze-Erect system. Initially, four single-post installations were tested with the first-generation Eze-Erect assembly. Subsequently, two tests on three-post installations were made in which the second-generation Eze-Erect

Figure 5. Close-up of Eze-Erect assembly.

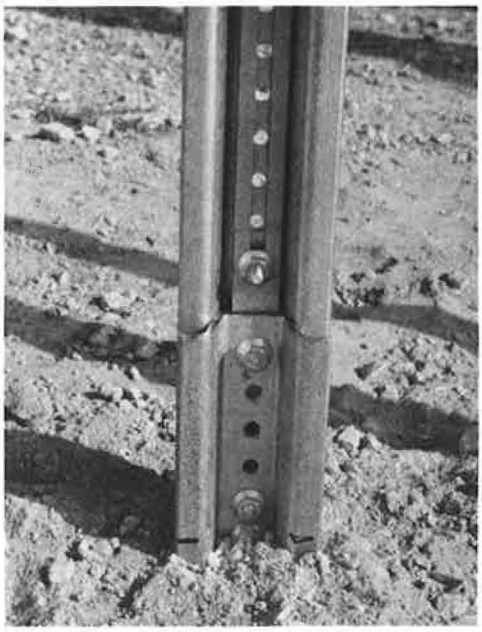

Figure 6. Single-post installation details.

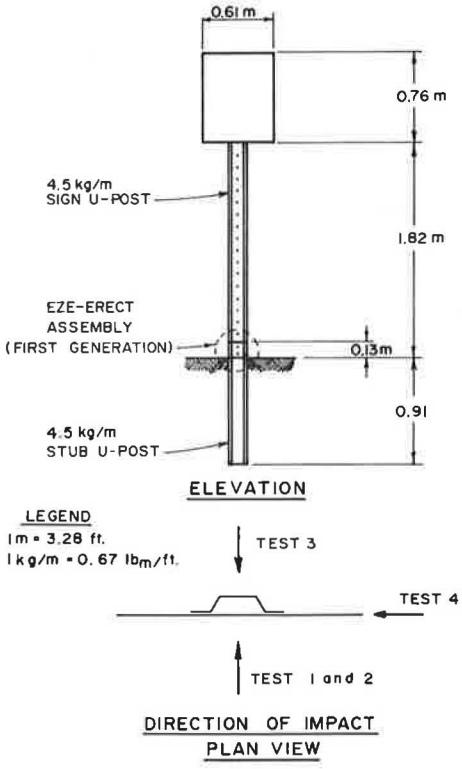

Figure 7. Three-post sign installation.

Table 3. Test conditions.

Test No.	Type of Installation	No. of Post Impacted	Eze-Erect Assembly Generation	Impact Speed (km/h)	Direction of Impact
1	Single-post	1	First	36.5	
2	Single-post	1	First	95.9	
3	Single-post	1	First	27.7	
4	Single-post	1	First	26.7	
5	Three-post	3	Second	29.9	
6	Three-post	2	Second	30.1	

Note: 1 km/h = 0.62 mph.

assembly was used. The single-post installation and the Eze-Erect assembly are shown in Figures 4 and 5. Details of the installation appear in Figure 6. The three-post installation is shown in Figures 7 and 8.

The tests were conducted in accordance with the recommended guidelines in NCHRP Report 153 (2). Soil at the test site also met the criteria outlined in NCHRP Report 153. Table 3 gives other details of the tests.

The test vehicles were 1971-1973 Chevrolet Vegas; each weighed 1034 kg (2280 lb). Electronic instrumen-

Figure 8. Three-post installation details.

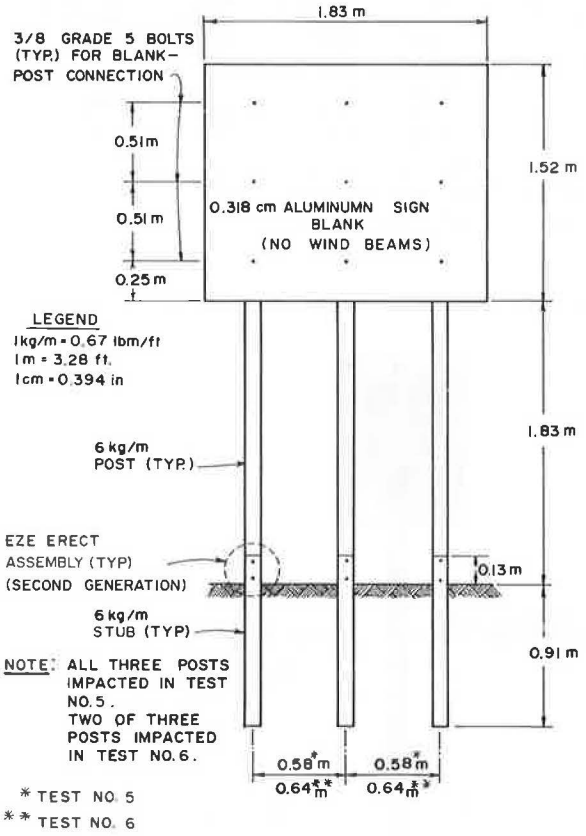

Table 4. Summary of test results.

Test No.	Type of Impact	Impact Speed (km/h)	Change in Momentum (N·s)*	Penetration of Passenger Compartment by Test Article	Vehicle Damage Classification TAD	Vehicle Damage Classification SAE	Refurbishment Required on Sign Installation
1	Single-post, head-on	36.5	846	No	FL-1	12FLEN1	Both stub and signpost would have to be replaced; sign panel could be reused; web of stub fractured at top connector bolt hole
2	Single-post, head-on	95.9	797	No	FR-1	12FREN1	Complete installation would have to be replaced
3	Single-post, rear hit	27.7	1638	No	FL-1	12FLEN1	Stub post would have to be replaced; signpost could probably be straightened and reused; sign panel would need to be rescreened
4	Single-post, side hit	26.7	1593	No	FR-2	12FREN1	Complete installation would have to be replaced
5	Three of three-post hit, head-on	29.9	2884	No	FD-2	Unavailable	All signposts would have to be replaced; all stub posts and the sign panel were reusable
6	Two of three-post hit, head-on	30.1	2056	No	FD-2	Unavailable	Two signposts would have to be replaced; third signpost and sign panel were bent but could possibly have been straightened; all stub posts were reusable

Note: 1 km/h = 0.62 mph; 1 N·s = 0.22 lb-s.

*Based on accelerometer data; change in momentum computed according to guidelines in section 7, part 2, of NCHRP Report 153 (2).

Figure 9. Stub after test 1.

Figure 10. Stub after test 2.

tation consisted of two longitudinal accelerometers. High-speed cameras were used to record vehicle time-displacement data.

Table 4 summarizes the results of the four single-post tests and the two multiple-post tests. In all tests, the change in momentum values was below the desirable limit of 3338 N•s (750 lb•s) and well below the upper limit of 4895 N•s (1100 lb•s) as recommended by the American Association of State Highway and Transportation Officials (AASHTO) (3). In no test did the test article penetrate the passenger compartment; in fact, the windshield was not broken in any of the tests. Damage to the vehicle was minor, and the vehicle was operable after each test.

After completion of tests 1 and 2, it was ascertained that low-speed impacts are more critical for this type of installation than high-speed impacts. In other words, impacts at speeds of approximately 16.1 km/h (10 mph) to 48.3 km/h (30 mph) cause higher changes in momentum than do impacts at higher speeds. This is due to the impact behavior of rail steel—it tends to fracture,

Figure 11. Stubs after test 5.

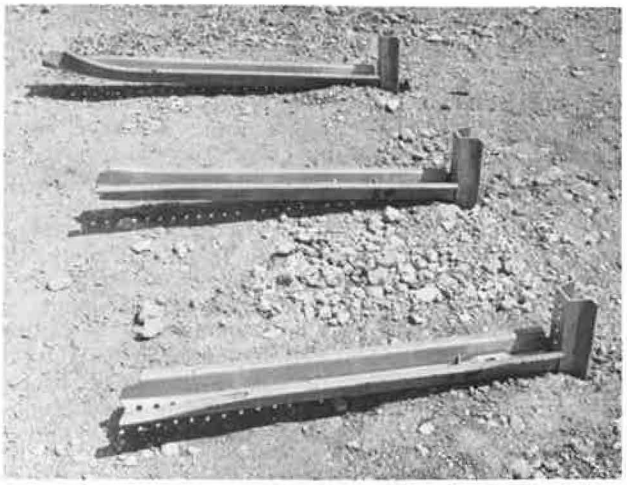

Figure 12. Stubs after test 6.

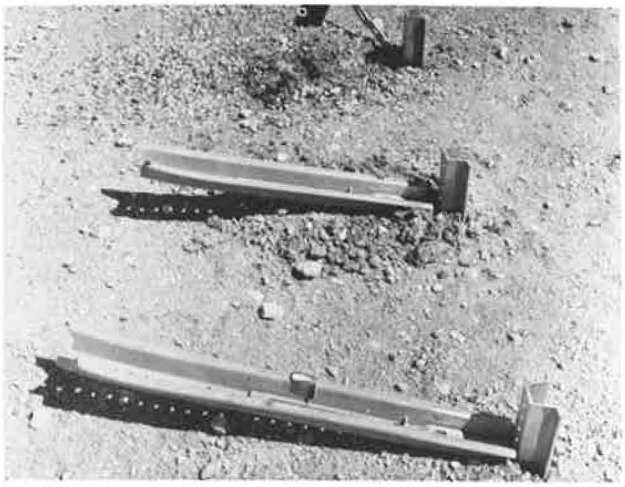

rather than yield, especially at the higher speeds, and thus offers lower resistance to impact. Such behavior is a desirable characteristic for a signpost. As a result, the remainder of the test program was conducted at low speeds.

Considerable improvements were observed in the dynamic behavior of the second-generation Eze-Erect assembly (tests 5 and 6) over that of the first-generation assembly (tests 1 through 4). Figures 9 and 10 show the assembly damage after tests 1 and 2. Note the tear in the top of the stub post. Figures 11 and 12 show the assembly after tests 5 and 6. In tests 5 and 6 there was no damage to the stub, and with minor soil retamping the stub would be reusable.

CONCLUSIONS

The Eze-Erect assembly (a bolted stub-signpost connection) provides a simple but effective device for installing a steel U-post sign support system. Use of the bolted stud-signpost connection will reduce the hazard associated with driving full-length posts. Special equipment such as a lift truck or other devices needed to obtain the required heights for driving will not be required since the stub can be driven from ground level. Another desirable feature of the system is that the sign panel can be mounted to the signpost prior to erection of the post.

Results from a limited number of static load tests indicate that the Eze-Erect assembly does not compromise the elastic strength of the installation. In other words, the bolted connection was shown to have the bending moment capacity of the individual signpost itself.

Full-scale vehicle crash tests were conducted to evaluate the impact performance of the Eze-Erect assembly for a full range of impact speeds and impact angles. Both single-post and multiple-post installations were crash tested. The tests were conducted in accordance with current guidelines (2). Soil at the test site met the recommended criteria (2). In all tests, the change in momentum values was below the desirable limit of 3338 N·s (750 lb·s) and well below the upper limit of 4895 N·s (1100 lb·s) as recommended by AASHTO (3). In no test did the test article penetrate the passenger compartment; in fact, the windshield was not broken in any of the tests. Damage to the vehicle was minor, and the vehicle was operable after each test.

REFERENCES

1. H. E. Ross, Jr., J. L. Buffington, G. D. Weaver, and D. L. Schafer. State of the Practice in Supports for Small Highway Signs. Texas Transportation Institute, Texas A&M Univ., Research Rept. 3254-1, Interim Rept. on Contract DOT-FH-11-8821, June 1977.
2. M. E. Bronstad and J. D. Michie. Recommended Procedures for Vehicle Crash Testing of Highway Appurtenances. NCHRP, Rept. 153, 1974.
3. Standard Specifications for Structural Supports for Highway Signs, Luminaires and Traffic Signals. American Association of State Highway and Transportation Officials, Washington, DC, 1975.
4. M. J. Effenberger and H. E. Ross, Jr. Report on the Static and Dynamic Testing of Franklin's U-Post and Eze-Erect Connection. Texas Transportation Institute, Texas A&M Univ., Research Rept. 3491-1F, June 1977.
5. H. E. Ross, Jr., and K. Walker. Static and Dynamic Testing of Modified Eze-Erect System. Texas Transportation Institute, Texas A&M Univ., Research Rept. 3636-1F, Feb. 1978.